

Thesis for the degree  
of Candidata Scientiarum

**Sissel Håvåg**

**Qualitative and quantitative  
determination of naphthenic  
acids in Heidrun crude oil**

**DEPARTMENT OF CHEMISTRY  
FACULTY OF MATHEMATICS  
AND NATURAL SCIENCES  
UNIVERSITY OF OSLO 09/2006**



Life is like a box of chocolate,  
You never know what you are gonna get.

(Forest Gump)

# CONTENTS

PREFACE .....	4
ABSTRACT .....	5
KEYWORDS .....	5
ABBREVIATIONS .....	6
1. Introduction .....	8
1.1 Crude oil.....	8
1.2 Naphthenic acids .....	10
1.3 Naphthenic acid corrosion.....	12
1.4 Biodegradation of naphthenic acids in aquatic environments.....	13
1.5 Toxicity of naphthenic acids.....	14
1.6 Use of naphthenic acids.....	15
1.7.1 The naphthenate deposition problem .....	16
1.7.2 Characterization of ARN.....	17
1.7.3 NAs in wastewaters.....	19
1.7.4 Extraction of NAs from water.....	20
1.7.5 NAs in crude oil.....	20
1.7.6 Extraction of NAs from crude oil.....	21
1.7.7 The Acid IER method.....	21
1.7.8 Characterization of NAs.....	22
1.7.9 MS detection methods.....	23
1.8 Aim of study.....	26
2. Experimental .....	28
2.1 Materials and reagents.....	28
2.1.1 Materials and reagents used in the GPC HPLC systems.....	28
2.1.2 Materials and reagents used for extraction of ARN from A-22 oil.....	29
2.1.3 Materials and reagents used in the direct infusion negative ESI TOF MS .....	29

2.1.4	Materials and reagents used in the $\mu$ LC MS analysis .....	30
2.2	Considerations made for solvents and samples.....	31
2.3	Samples obtained from Statoil.....	31
2.4	Spiking and extraction of A-22 oil .....	33
2.5	Column packing.....	34
2.6	Accurate mass determination of Statoil f 9.....	35
3.	Results and discussion.....	36
3.1	Fractionating the A1 polar.....	36
3.1.1	Comparing Waters Styragel HR2 and Ultrastyrigel columns.....	36
3.1.2	GPC fractionating and identification of ARN in A1 polar.....	37
3.1.3	GPC fractionation of A1 polar.....	38
3.2	Identification of ARN with negative ESI TOF MS.....	39
3.3	Accurate mass determination of Statoil f 9.....	42
3.4	Development of the mobile phase gradient used in the $\mu$ LC MS analysis.....	43
3.5	$\mu$ LC MS detection.....	44
3.6	Extraction of ARN from A1 polar spiked crude oil.....	53
3.7	Determination of ARN in spiked crude oil.....	54
3.8	Quantitative determination of ARN using MeOH extraction and $\mu$ LC MS.....	61
3.9	Attempts on quantitative determination of ARN using an internal standard.....	72
4.	Conclusion .....	76
5.	References .....	77
6.	Appendix.....	81

## **PREFACE**

This graduate study has been carried out at the University of Oslo, Faculty of Mathematics and Natural Science, Department of Chemistry, in the period of January 2003 to September 2006. My supervisors have been Elsa Lundanes and Tyge Greibrokk.

I would like to thank my supervisors at UiO, Elsa Lundanes and Tyge Greibrokk for always being helpful and supportive and for creating an academic environment that is both fun and inspiring.

I would also like to thank Heidi Mediaas, Torbjørn Vegard Løkken and Hege Kummernes from Statoil for an interesting and challenging project and excellent guidance during this study. You have provided me with inspiration during struggling moments.

I would also like to thank all of my fellow students for a good social environment and discussions of various topics.

Thanks to Hege Lynne and Hanne Røberg-Larsen, at the analytical course laboratory for their help with everything I have asked for and for making me feel welcome, you have made my life so much easier. Thanks to John Vedde who performed an accurate molecular weight determination of my sample using a FTICR MS and a QTOF MS.

Finally I would like to thank my husband Joachim, and my family, for their patience with me through this time, and Andreas, my lovely son, which was born in the middle of the practical work of this thesis.

Oslo, Norway, September 2006

Sissel Håvåg.

## **ABSTRACT**

The main aim for the work on this thesis was to find a fast and sensitive method for qualitative and quantitative determination of the naphthenic acids (NAs) called the ARN acid family in crude oil. As there are three main components in the ARN acid family with quite similar molecular mass, separation of the acids with respect to the hydrophobicity, was essential to obtain reliable determination of all three acids. The sample preparation developed in this work consisted of liquid-liquid extraction of 10 mL crude oil with 20 mL methanol (MeOH):triethyl amine (TEA) (99.9:0.1). 500 nl of the MeOH phase was loaded on a 0.3 mm I.D. x 10 cm 3.5  $\mu\text{m}$  Kromasil C18, 100  $\text{\AA}$  column at a flow rate of 5  $\mu\text{L}/\text{min}$ . A water- MeOH mobile phase (MP) gradient containing 0.1 % TEA was also developed and used during the entire work on this thesis. The time for one injection, including reconditioning of the column was 35 min. The ARN acids were separated and detected down to 4.36 ppm with negative electrospray (ESI) on a time of flight mass spectrometer (TOF MS). However more work is needed to get control of the method, as the validation work with an internal standard gave poor results.

## **KEYWORDS**

Naphthenic acids, naphthenate deposition,  $\mu\text{LC}$  MS, MeOH extraction.

## ABBREVIATIONS

$\mu$ LC	micro liquid chromatography
$^{13}\text{C}$ NMR	carbon-13 nuclear magnetic resonance
A1 Polar	020103003.03 A1 Polar (isol: 08.04.02)
A-22 oil	030123002 A-22 oil Heidrun
AcN	acetonitrile
APCI	atmospheric pressure chemical ionization
CI	chemical ionization
DCM	dichloromethane
EI	electron ionization
EIC	extracted ion current
ELSD	evaporative light scattering detector
Eq.	equation
ESI	electrospray ionization
FAB	fast atom bombardment
FAIMS	high-field asymmetric waveform ion mobility spectrometry
FICIMS	fluoride ion chemical ionization mass spectrometry
FTICR	fourier transform ion cyclotron resonance
FTIR	fourier transform infrared
GC	gas chromatography
GPC	gel permeation chromatography
HPLC	high performance liquid chromatography
HTGC	high temperature gas chromatography
I.D.	inner diameter
LC	liquid chromatography
$m/z$	mass to charge ratio
MeOH	methanol
MS	mass spectrometer
NA	naphthenic acid
O.D.	outer diameter
SFE	supercritical fluid extraction
SPE	solid phase extraction
TAN	total acid number

TEA	triethylamine
TIC	total ion current
TLC	thin layer chromatography
TOF	time of flight
VPO	vapor pressure osmometry



# 1. Introduction

## 1.1 Crude oil

Crude oil is the term for unprocessed oil, and it is a very complex mixture that varies much in composition, viscosity, density, and flammability. They can be found in a continuous range from highly flammable, light liquids (similar to gas condensate), to highly viscous and heavy tar-like materials. Crude oil is not a uniform material with a simple molecular formula; it is a mixture of gaseous, liquid, and solid hydrocarbon compounds, occurring in sedimentary rock deposits throughout the world. Organic compounds range from methane to extremely heavy hydrocarbon molecules with up to 80 carbon atoms [1]. The smallest hydrocarbons are gaseous at room temperature, the larger hydrocarbons are liquids and the largest are solids. In crude oil these compounds are dissolved in each other [2]. The composition of the oil mixture depends on its location. Two neighboring wells may produce quite different crude oils and even within a well the composition may vary extensively with dept. The variation from one source to another is also significant, and many of the compounds are unstable at the conditions in the sediments. Heating under certain conditions or the presence of process catalysis can cause them to break into smaller components or combine with other constituents. Table 1 shows some of the constituents in typical crude oils [3], and Table 2 shows the elemental composition of crude oil [4].

Table 1: Major constituents in crude oil [3].

Hydrocarbon compounds	Paraffin hydrocarbons (alkanes) Cycloparaffins (naphthenes, cycloalkanes) Aromatic hydrocarbons Asphaltenes
Sulfur compounds	Elemental sulfur and H <sub>2</sub> S Mercaptans Sulfides Disulfides Polysulfides Thiophenes
Nitrogen compounds	Pyridines Quinolines and isoquinolines Acridines Pyroles Indoles Carbazols Porphyrin
Oxygen compounds	Carboxylic acids Phenols Cresols Naphthenic acids

Table 2: Elemental composition of crude oil [3, 4].

Element	Percentage range (wt %)
C	80-87
H	10-14
N	0.2-3
O	0.05-1.5
S	0.05-6

Even though at first these variations may seem small, the different crude oils are quite different; no two batches of crude oil are chemically identical. The high fractions of C and H suggest that crude oil consists of hydrocarbons, which certainly has been proven to be the case [4, 5]. From thorough analysis it appears that the larger part of crude oil consists of alkanes, cycloalkanes (naphthenes), and aromatics, with smaller amounts of polycyclic aromatics, sulphur-containing compounds, nitrogen-containing compounds, oxygen-containing compounds, and more. Both linear and branched alkanes are present [5]. Crude oil is categorized based on the molecular weight distribution of their constituents, and distinctions are made between light, medium, and heavy crude oil, as seen e.g. in Table 3, [1, 6, 7]. In gasoline applications the linear alkanes are much less valuable than the branched alkanes, whereas in diesel fuel the linear alkanes are desirable [4].

Table 3: Names, fraction of the total, and approximate molecular size of crude oil fractions from a Crude Oil [6, 7].

Fraction	No.carbons	b.p.	%
Gases	1-4	<0	2
Light Naphtha	5-7	27-93	34
Heavy Naphtha	6-10	93-177	
Kerosene	10-15	177-293	11
Light Gas Oil	13-18	204-343	21
Heavy Gas Oil	16-40	315-565	31
Residuum	>40	>565	

## 1.2 Naphthenic acids

The term “naphthenic acid” is commonly used to account for all carboxylic acids present in hydrocarbon deposits (oil sands, bitumen, and crude oil), including acyclic acids, this is not entirely correct, a more correct description is that carboxylic acids include NAs [8].

NAs are natural ingredients of crude oil and are known to be produced during the in reservoir biodegradation of crude oil hydrocarbons [8, 9], and they are considered to be a class of biological markers, closely linked to the maturity and the biodegradation level of the oil fields [10]. NAs are found in crude oil because either the deposit has not undergone sufficient catagenesis (the cracking process in which organic kerogens are broken down into hydrocarbons) or bacteria biodegradation [8]. Heavy crudes from geologically young formations have the highest acid content, and paraffinic crudes usually have low acid content [11].

NAs are classified as carboxylic acids containing one or more alkyl-substituted acyclic rings (naphthenes) [12], with minor amounts of aliphatic carboxylic acids, the general formula is  $C_nH_{2n+z}O_2$  [8, 13, 14]. The acyclic components are highly branched. Z is a zero or negative even number that specifies the different ring numbers in the acids [8]. The absolute value of Z divided by 2 gives the number of rings in the compounds; the rings may be fused or bridged. NAs are  $C_{10}$ - $C_{50}$  compounds with 0-6 fused saturated rings and with the carboxylic acid group apparently attached to a ring with a short side chain [13]. Examples of structures that may be found in crude oils are given in Figure 1 [13, 15, 16]. The distribution of carbon number and ring content varies with crude oil source and distillate fraction. NAs with similar total acid number (TAN) and average molecular weight can have significantly different profiles, as referred to by Havre [10].

The polarity and nonvolatility of NAs increase with MW, giving individual compounds within the NA group varying physical, chemical and toxicological properties [17]. Because of the complexity of these NA mixtures, the complete separation, quantification and identification of individual compounds have not been achieved [8]. They are completely soluble in organic solvents and have water solubilities that are pH dependent. Typical pKa values for NA components are 4.9 [18].

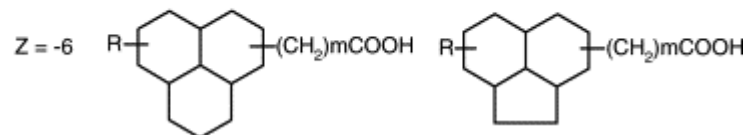
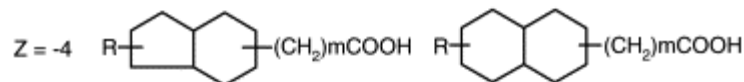
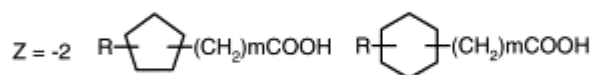
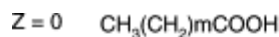


Figure 1: Examples of structures of NAs for various Z-families. R represents an alkyl group,  $m$  represents the number of  $\text{CH}_2$  units, and the Z series correspond to different ring numbers in the acids [8, 13, 15, 16].

The NAs are a varied group of carboxylic acids that can account for as much as 4-8 % of raw petroleum (v/v) (varies between the different crudes), and represent an important component of the waste generated during petroleum processing [10, 19].

One example of the complexity of NA mixtures can be seen by considering the single formula  $\text{C}_{10}\text{H}_{18}\text{O}_2$  ( $Z = -2$ ) and specifying that the ring contains six carbon atoms, 37 carboxylic acid isomers that meet these criteria can be drawn [8].

The total amount of NAs in crude oil samples are normally expressed as the TAN. But the TAN is not a reliable measure for the amount of NAs. TAN is the number expressed in milligrams (mg) of potassium hydroxide needed to neutralize the acid in one gram of oil [3, 20]. The test is used to indicate the amount of oxidation that the fluid has undergone. The TAN increases as the fluid undergoes increased amounts of oxidation [21]. Crude oil with high acid numbers may contain only a small amount of NAs, this is because the TAN value measures total acidity, that is, not just the NAs, but also other acidic components (up to 40 % [22]) such as terpenoid dicarboxylic acids, phenylic acids, mercaptanic acids, naphtheno aromatic acids and fatty acids [20, 22-24].

NA concentrations and composition vary widely in commercial sources and crude oil deposits. Results from studies indicate significant differences especially in the C22+ fractions (i.e. compounds containing more than 22 carbons) [13].

### 1.3 Naphthenic acid corrosion

When NA containing crude oils are processed in refineries, corrosion may occur, this type of attack is called “naphthenic acid corrosion” [25]. This type of corrosion is a well known problem and a major concern in crude oil processing. NAs present in crude oils are considered only to be a part of the problem and simple measures of corrosivity based on the TAN are insufficient [16, 22]. The fundamental problem is the complexity of the factors affecting corrosiveness. The role of crude oil composition, temperature, fluid velocity, turbulence, physical state (vapor or liquid), pressure and materials of construction may also contribute to the extent of oxidation [8, 20].

Steel alloys that are resistant to corrosion by sulphide-containing compounds can be corroded by NAs. This “naphthenic acid corrosion” involves the reversible binding of the metal ion by the carboxylate with the formation of hydrogen gas (chelation). High throughput rates and operating temperatures between 220 and 400 °C favor corrosion. Temperatures above 400 °C decompose NAs, forming a film of coke that protects the alloy [3]. The nature and extent of corrosion can also be influenced by sulphur species and chlorides, but unlike naphthenic corrosion, sulphuric corrosion increase in severity with increasing temperature [3, 8, 16, 24]. NA corrosion is associated with TAN, temperature, and fluid rate. When the crude oil has a TAN of more than 0.5, the NA corrosion is generally high, but the TAN value is a poor quantitative measure of the severity of the corrosive behavior of the oil [3]. It has been observed that the corrosive behavior of oils with fairly low TANs was comparable to others with high TANs, whereas other oils with high TANs have been observed to be less corrosive than their TANs might indicate [16, 22].

The extent of corrosion by NAs does not only depend on NA content, but also on the chemical structure of the NA, the availability of the carboxylic acid group to adsorb on the metal surface and to form metal complexes. It is well known that an increase in the number of  $(CH_2)_n$  groups in C chains, up to  $n = 3$  to 4, increases the adsorbability in a given reaction series of organic compounds. After that, the steric hindrance between organic molecules causes a decrease in adsorbability [24].

The sulphur content in a crude oil is an important factor in NA corrosion, mainly due to a competition between the two kinds of processes, naphthenic attack and hydrogen sulphide attack according to the following equations: [16].



Equation Eq. (1) illustrates the NAs direct attack iron (carbon steel). Here the NAs are transported towards the metal surface which adsorbs the NA molecules. Active sites on the metal surface react with the NAs and generate corrosion products [26]. Eq. (2) illustrates the corrosion by hydrogen sulphide [20]. The difference lies in the corrosion product, iron naphthenate, which is very soluble in oil, and iron sulphide, which tends to form a protective film on the metal [24]. Eq. (3) illustrates the reaction between hydrogen sulphide and the soluble iron naphthenate that produces iron sulphide, precipitated in the oil [16]. By this reaction the NAs are regenerated. Crude oils with 2-3 % sulphur content form a protective layer, whose stability is dependent on flow, particularly wall shear stress, and temperature [20, 25]. This is why a crude oil with a high NA content and low sulphur content seems to be more corrosive at high temperatures than a crude oil with the same NA content and high sulphur content [25].

## 1.4 Biodegradation of naphthenic acids in aquatic environments.

Biodegradation is the decomposition of organic material by microorganisms. The different types of hydrocarbons and heteroatomic components in the crude oil determine the rate and degree of the biodegradation [27]. Linear and carboxylic acids of lower molecular weight are removed more rapidly than the corresponding hydrocarbons by biodegradation and water washing [28-30]. The biodegradation potential is reduced by methyl substitutions on the cycloalkane ring, although these compounds can be degraded with the addition of mineral nutrients. Microbial activity is both nitrogen- and phosphorus- limited [31, 32].

Biodegradation of NAs also occurs within oil reservoirs that remain below 75 °C, and as the crude matures it causes the oil to gradually increase in density. Over geologic time, the microorganisms remove alkanes, branched alkanes, and cycloalkanes, and may also attack aromatics, in the order of ring number. During the progress of biodegradation there is an increase in nitrogen-containing compounds related to the organisms themselves, and not simply the reduction in specific compound types [22].

Because NAs are relatively soluble in water (as naphthenates) and have neutral or alkaline pH, they are relatively mobile in petroleum contaminated water and easily available to micro-organisms for the degradation processes [8]. Given the right conditions, both aerobic and anaerobic cultures of original microbial communities from oil sand tailings water are capable of degrading NA mixtures in aquatic systems. (Oil sands tailings are a byproduct of the bitumen extraction process, and are composed of water, sands, slit, clay and residual bitumen. In northern Alberta, Canada, every barrel (1000 liters) of oil extracted produces 3000 liters of fluid tailings

[13, 33]). The unsubstituted parent cycloalkanes resistance to microbial attack has been explained by the deficiency of exposed terminal methyl groups for the initial oxidation; while resistance of shorter chain n-alkyl substituted cycloalkanes to microbial attack has been explained as the failure of the short chains to be the sole source of carbon and energy, for the growth of the microorganism [27]. Bacterial cultures enriched from oil sands tailings were found to be able to use both a commercial mixture of NAs and a mixture of organic acids extracted from oil sand tailings as their sole carbon source [28, 34].

The storage of tailings pond water in shallow, well aerated pits, results in a major improvement in water quality by removal of NAs and residual bitumen. After 1-2 years, the tailings pond water will be comparable to the natural, unpolluted water in the same area [35]. For substantial biodegradation to occur, the deposit must come in contact with surface water [22].

Temperature also has a large effect on microbial degradation kinetics with a significant increase in first-order rate constant between 10 and 30 °C [28, 29, 36]. The structure of the NAs also affects the kinetic as a more closed geometry of the NAs corresponds to lower bioavailability. Hence, e.g. complex high molecular weight compounds will be degraded at a lower rate compared to a lower molecular weight compound [17, 28, 36].

Microbial activity will mineralize parts of the organic carbon present in an extracted organic acids mixture, although there is no indication of a reduction in any gas chromatographic peaks with biodegradation in some studies [17], but in other studies there are some reduction in the chromatographic peaks of the lighter acids [28]. Aerobic degradation of the organic acids mixture reduces acute toxicity to approximately one half of the original level [28]. Respirometric measurements of microbial activity within oil sands tailings that contain microorganisms are used to provide further evidence that the indigenous microbial community could biodegrade NAs and components within the extracted organic acids mixture [17, 34].

NAs stored at 4 °C are considered stable, showing no signs of change in concentration over a 10 month period [37].

## 1.5 Toxicity of naphthenic acids

NAs of low molecular weight have been identified as the main component responsible for the acute toxicity to aquatic organisms, including bacterial populations, aquatic algae, fish, and mammals, in refinery wastewaters and in oil sand tailings [19, 29, 31]. But since there are found hundreds of these compounds in crude oil materials, it is not established which specific NA that are the most toxic. Toxicity does not automatically correlate directly to the NA concentration, it

is more a function of the NA structure content and the complexity of the mixture [8, 23, 29, 38, 39].

Mammalian toxicological studies indicate that while acute toxicity in wild mammals is unlikely under worst case exposure conditions, repeated exposure may have harmful health effects [19]. Further evaluation of the effects of NAs on mammals (including rats, dogs, and rabbits [19, 31]) have indicated increased vascular permeability in capillaries, notable effects on the formation of red and white blood cells and blood particles involved in clotting. Tests with Wistar rats indicate that the liver is the target organ in both acute and sub-chronic dosing experiments [19]. In tests with rainbow trout, all NA compounds and mixtures tested were cytotoxic (prevents cell division) to varying degrees in four rainbow trout cell lines [17, 19, 31, 40].

Acute toxicity tests revealed a complete absence of detectable toxicity following biodegradation of NAs, i.e. biodegradation decreases the concentration and toxicity of NAs [30].

There are also many industrial uses for NAs, so they are released to the environment from many activities. The concentrations of inorganic constituents, such as trace metals, major ions and nutrients, do not appear to be high enough to produce the toxic effects observed [8, 35].

## 1.6 Use of naphthenic acids

Originally the NAs were recovered from crude oil distillates to minimize refinery equipment corrosion, but they have now found a wide use as commercial articles. However, not all crudes contain enough usable acids to make recovery an economic process [11].

NAs, NA esters and NA metal salts are a highly marketable product because they have many areas of application; they are used as emulsifiers, textile and wood preservatives, paint driers, surfactants, and adhesion promoters in tire manufacture. They improve water resistance and adhesion of concrete; increase high pressure resistance of drilling oils; prevent foaming in jet fuel; prevent fungus growth in wood; preserve and act as a flame retardant in fabric; increase insecticide solubility by acting as emulsifier; catalyze rubber vulcanization; stabilize vinyl resins; and catalyze production of alkyl and polyester resins. The use of copper and zinc naphthenates has replaced creosote as a wood preservative [8, 23, 28].

NAs that are commercially derived from crude oil are a complex mixture. The NA product quality is determined by the refining process and the crude oil source used [11]. This makes large compositional variations among commercial supplies of NAs. Traditionally the TAN number has been used as an indicator of the product quality. Since the TAN value also



measures other acid components in the oil, such as several compound classes of carboxylic acids, naphtheno aromatic acids and fatty acids, some supplies with high enough TAN values contain only small amounts of NAs [23, 41].

### 1.7.1 The naphthenate deposition problem

Calcium naphthenate deposition is a complicated problem for high production stability for oilfields where acidic crudes are produced, especially since increasing shares of the oilfields around the world are relatively acidic, i.e. they have high TAN values, as referred to in [42, 43]. At the Statoil operated Heidrun field in the Norwegian Sea, naphthenate deposits were first observed in 1996 [44]. Naphthenate deposit has always been thought to be a mixture of oil, water, sand, and calcium salts of NAs in the crude oil [44]. Particles and sand following the well stream was held up by the naphthenate, increasing the density of the phase until lumps would drop through the water phase to the separator bottom [44]. The NAs, which are a liquid at separator conditions, solidifies rapidly to an almost rocklike hardness after being cooled. Due to this density the naphthenate deposits have a tendency to clog virtually all parts of the liquid systems at oil platforms, and they are neither soluble in water nor oil. This causes operational problems, including long enough shutdown periods for the process equipment to cool below the naphthenate solidification temperature [42].

To avoid this problem, different chemicals are added to the crude oil to keep the NAs in solution. This causes pollution of the jet water from the separator, both from the added chemicals and from increase in the oil and NA content in the effluent water, which again causes pollution of the Norwegian Sea [44].

After closer analysis it has been found that the acids in the deposit do not resemble the acids in the crude oil, and it only takes a few ppm of naphthenate inhibitor to suppress the naphthenate deposition from oil and water containing 2 wt % NAs and 0.1 wt % calcium, respectively. This indicates that some selection criteria decide which of the NAs that are a part of the naphthenate deposition process [42].

Characterization of calcium naphthenate deposits from the Heidrun field suggests that a family of 4-protic acids with molecular weight in the range 1227 – 1235 g/mol, called the ARN acid family, is the main ingredient of the naphthenate deposit from oilfields offshore Norway, Great Britain, China, and West Africa [42, 43].

## 1.7.2 Characterization of ARN

The NAs called the ARN acid family has a molecular weight of 1227 – 1235 g/mol, which correspond to the homologous series with empirical formula of  $C_{80}H_{138}O_8$ ,  $C_{80}H_{140}O_8$ ,  $C_{80}H_{142}O_8$ ,  $C_{80}H_{144}O_8$  and  $C_{80}H_{146}O_8$ , with Z numbers ranging from 12 to 8 indicating 8 to 4 rings in the hydrocarbon skeleton [45].

Brandal and co-workers [46] used electrospray ionization Fourier transform ion cyclotron resonance mass spectrometry (FTICR MS) in the negative mode to characterize naphthenate deposition from ARN. The main peak had  $m/z = 1230.0627$ , which corresponds with the ion  $[C_{80}H_{141}O_8]^-$ , and the parent compound  $C_{80}H_{142}O_8$ . The compound has 6 saturated rings [42, 43, 46].

Lutnaes and co-workers [45] subjected the naphthenate deposition from ARN to an extensive nuclear magnetic resonance (NMR) spectroscopy study. This research pointed to a C80 compound of dimeric nature. The obtained correlations between proton and carbon resonances allowed the determination of the C14 structural units A and B, and the central C24 unit C, as shown in Figure 2.

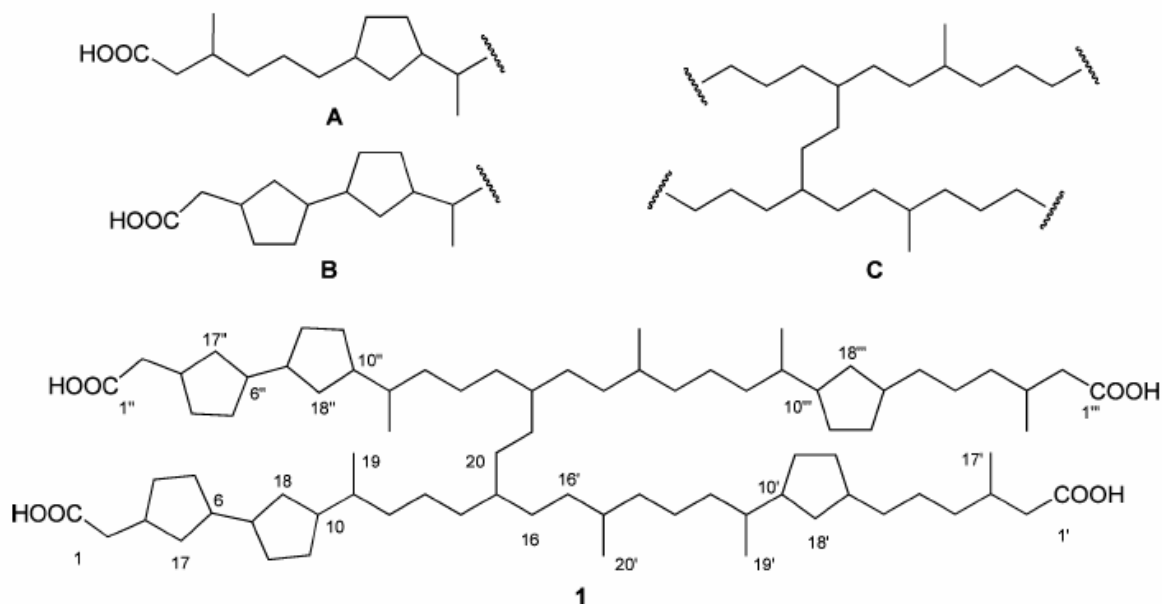


Figure 2: Structures of molecular fragments A, B and C, and (6:17,10:18,10:18,6:17,10:18,10:18)-hexacyclo-20-bis-16,16-biphytane-1,1,1,1-tetracarboxylic acid (1), one of four possible regioisomers of the tetraacid with six rings, as determined by NMR spectroscopy [45].

Lutnaes and co-workers [45] assumed that the stereochemistry according to the Cahn-Ingold-Prelog sequence rules of each individual phytane parts would be as shown in Figure 3. (Cahn-Ingold-Prelog Sequence Rules: The letters used to assign absolute stereochemistry based on the 'Cahn, Ingold, Prelog' 'Sequence Rules'. After assigning priorities to the substituents around an asymmetric centre the molecule is viewed such that the bond from the asymmetric centre to the substituent of lowest priority is going away from the viewer, or into the page [47]).

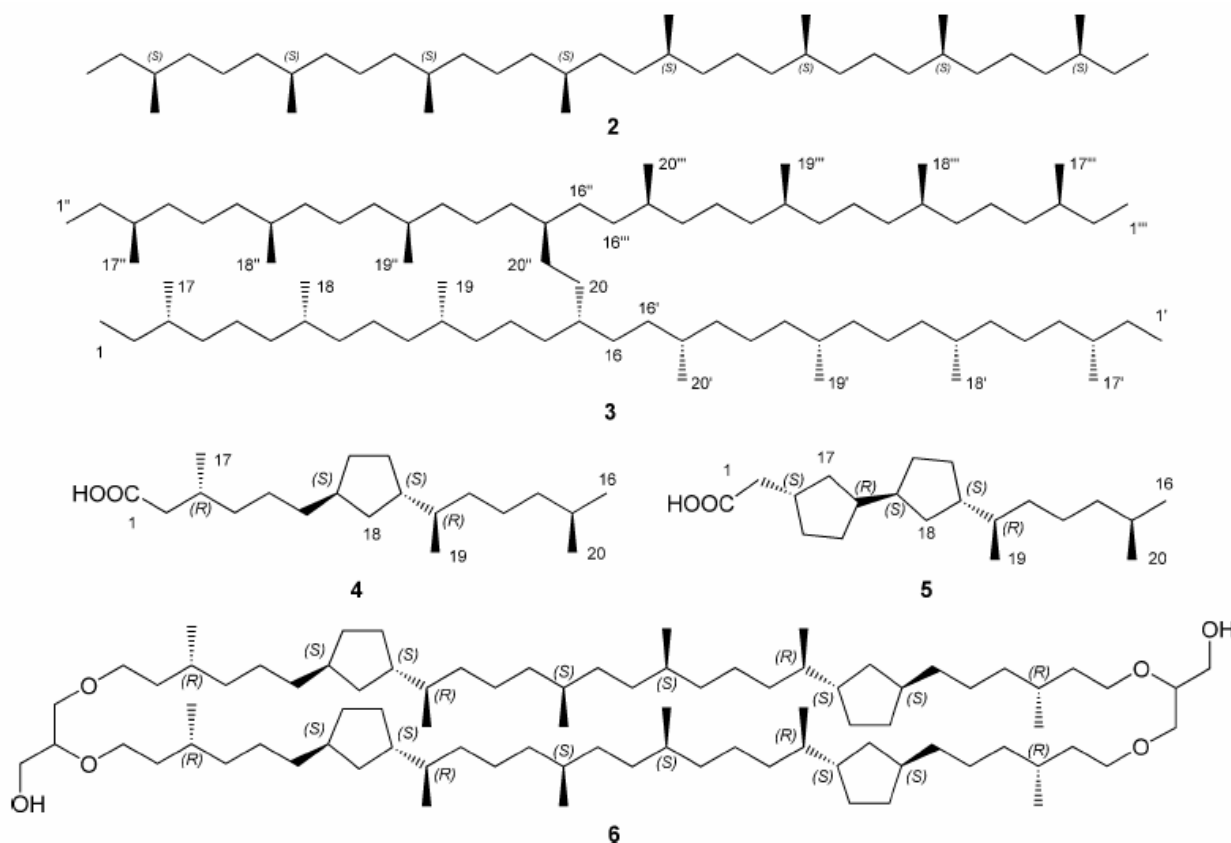


Figure 3: Structures of 16,16-biphytane (2), 20-bis-16,16-biphytane (3), phytanic acid moieties 4 and 5 with stereochemistry according to the Cahn- Ingold- Prelog sequence rules indicated, and tetracyclic glycerol dibiphytanyl glycerol tetraether (GDGT-4, 6) [45].

Conformational studies also made by Lutnaes and co-workers [45] might aid in understanding the chemical properties of these tetraacids. Some results are shown as an example for one of the stereoisomers of 1 (Figure 2) where the absolute stereochemistry has been kept identical to the corresponding stereocenters in 3–5 (Figure 3). Five different conformations are shown in Figure 4. Four of them (1a–d) can be organized in planar arrangements with increasing van der Waals interactions. One particular conformation, 1b on the anionic form, is an excellent candidate as a building block for a naphthenate deposition from ARN with calcium ions. Conformation 1d might have trans-membrane properties as well. Finally the fifth conformer, 1e

has the lowest free energy, is internally solvated and stabilized through extensive van der Waals interactions and might be a form found in organic solvents [45].

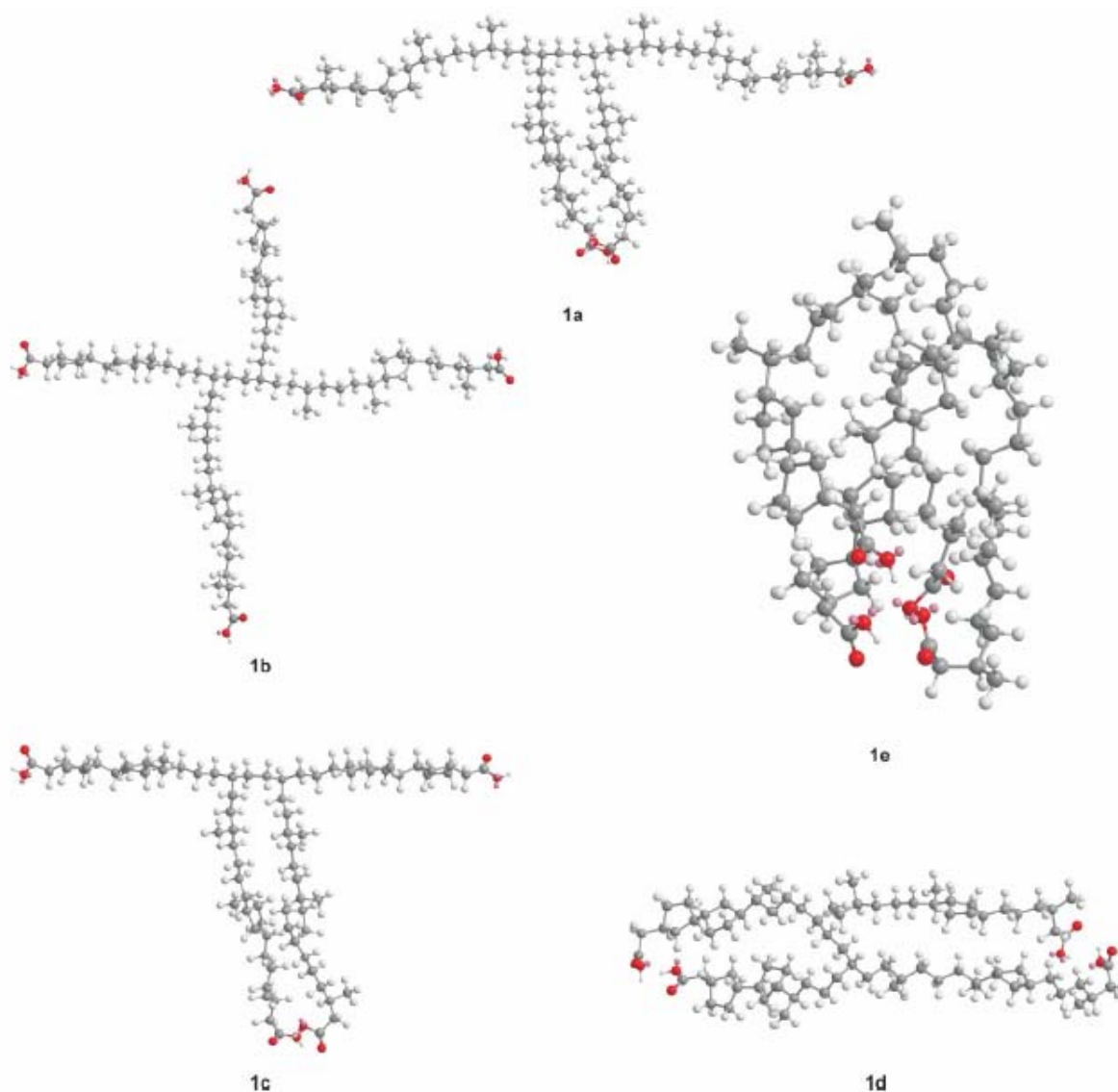


Figure 4: Conformations calculated for (6:17,10:18,10<sup>o</sup>:18<sup>o</sup>,6<sup>o</sup>:17<sup>o</sup>,10<sup>o</sup>:18<sup>o</sup>,10<sup>o</sup>:18<sup>o</sup>)-hexacyclo-20-bis-16,16'-biphytane-1,1',1'',1'''-tetracarboxylic acid (**1**), with stereochemistry preserved from 20-bis-16,16'-biphytane (**3**) [45].

### 1.7.3 NAs in wastewaters

NAs are released into tailings pond waters through extraction of bitumen from the Athabasca oil sands deposit in northern Alberta, Canada. This is a unique process of surface mining used to obtain oil sands ores that contain bitumen [8]. The main environmental receiver is water. NAs enter surface water systems mainly through tailing water, but also through ground water mixing

and erosion of riverbank oil deposits. In northern Alberta, Canada the Athabasca Oil Sands contain on average 200 mg NAs per kg of ore and tailing pond water may contain 20-120 mg/ L NA [8, 30]. Syncrude processes about 500 000 ton of ore each day so there is a potential to release 100 ton of NAs from the ore each day [8, 29]. Extensive exposure of NAs to water over time causes accumulation in sediments [29].

NAs in crude oil consist of a large group of saturated aliphatic and alicyclic carboxylic acids. Since NAs have similar structure and behavior as naturally occurring dissolved organic carbon components in surface water, and have significant complexity dependent on oil source and geological factors, they are an analytical challenge. The lack of suitable separation and identification methods for NAs has hindered many studies to determine specific information on toxicity, corrosiveness, structural relationships, environmental reactivity, and degradation pathways in the environment [29].

#### 1.7.4 Extraction of NAs from water

The most frequently used method for NA recovery from water is acidifying and dichloromethane extraction: Water samples are acidified with  $H_2SO_4$  to pH 2-2.5, extracted with dichloromethane and then taken to dryness [13, 30, 37, 40]. Sometimes the basic and neutral organic compounds are removed by adjusting the water sample to pH 12 with NaOH and extraction with dichloromethane before the acidification and extraction step mentioned above [48].

SPE (solid phase extraction) with a divinyl benzene supported sorbent can be used for NA extraction from water. Here the SPE column is pre washed with MeOH and water, the water sample with NAs are loaded on the column, and the column is washed with more water and dried. The sorbed NAs are eluted with acetonitrile [49].

NAs in water can also be adsorbed onto granular activated carbon from water samples, and extracted from the activated carbon with supercritical fluid extraction [40].

#### 1.7.5 NAs in crude oil

NAs are minor constituents in crude oils, but have long been of interest for refining because of the corrosion problems and deactivation of heterogeneous catalysts during refining, their surfactant properties, their geochemical significance and their commercial application [11, 22,

50, 51]. Knowledge of the detailed chemical composition of the acids responsible for corrosion can assist identification of problem crude oils and potentially lead to improved processing options for corrosive oils [22]. There still remain many challenges in characterization of the actual molecular structure and type of NAs [12]. The ring type and carbon number distribution is of special interest because corrosivity and toxicity are dependent on the sizes and structures [14, 52]. Geochemical studies also have an interest in NA characterization with regard to migration, biodegradation and as biological markers [14, 53].

### 1.7.6 Extraction of NAs from crude oil

The most frequently used methods for NA recovery from crude oil are:

Extraction by supercritical fluid [54].

Liquid-liquid extraction by a potassium alcoholic solution. This technique often causes the formation of an emulsion, which makes the quantitative recovery of the acids difficult [30, 37].

Extraction on an ion-exchanging resin in an aqueous medium, using cyclohexane as the sample solvent. The cyclohexane makes the asphaltene precipitate on the functional groups of the resin, causing a loss of acids with the interfering compounds [55].

Extraction on an ion-exchanging resin in a nonaqueous medium, which is a method for routine and rapid analysis of carboxylic acids in crude oils. However, the conditioning of the resin by the hexane does not allow elimination of the Cl<sup>-</sup> (original counterion), which makes the exchange between the carboxylic acids and the resin functional groups very difficult [9, 50].

Extraction on activated silica gel by a potassium alcoholic solution, but this method requires a long time (~72 h) and a high quantity of extraction solvent [56].

### 1.7.7 The acid IER-Method

Statoil isolates NAs from Heidrun crude oil using the Acid-IER Method, a method for selective isolation of carboxylic acids (herein lies the NAs including the ARN acid family) from crude oils and other organic solvents [57]. The selectivity of the method has been demonstrated to be >98 mol %.

Sugar (poly-1, 6-glucose) based QAE Sephadex A-25 ion exchange resin (Acid IER) was used. This cross linked resin is a strong ion exchanger with diethyl-(2-hydroxy-propyl) aminoethyl as the ion exchange group. The fact that it is sugar based makes the IER hydrophilic, and therefore, more selective towards carboxylic acids than hydrophobic IER's.

This method is time consuming, with hours of stirrings at several occasions, and will isolate all of the carboxylic acids in crude oil, and not just ARN [57]. The carboxylic acid fraction is called A1 polar by Statoil.

### 1.7.8 Characterization of NAs

Characterization of the NA structures is a difficult problem because these polar compounds suffer from thermal instability, low volatility, and ineffective ionization by traditional ionization methods [11, 14, 55]. In addition to this, typical analytical tools lack the chromatographic and mass resolving power for identification of individual compounds. Mass spectrometry (MS) techniques, including gas chromatography (GC) MS [30, 50], electrospray ionization Fourier transform ion cyclotron resonance mass spectrometry (ESI FTICR MS) [58], and high resolution mass spectrometry [22] has with varying degrees of success managed to characterize some NAs.

When GC is used to analyze NA mixtures, extensive sample preparation, including derivatization, is required [17, 23, 30, 50]. HPLC methods often do not require derivatization, but tedious sample preparation is often necessary to simplify the matrix. Even with extensive sample preparation HPLC is unable to separate all the NAs in a natural sample [59].

Many isomers in the NA group of petroleum can still not be resolved by current MS methods, nor can the mixture be fully separated using GC [8, 23, 30] or high performance liquid chromatography (HPLC) [59, 60]. However, it is possible to catalogue the mixture into groups of isomers with specific carbon number and Z number. This is possible since the formula for NAs ( $C_nH_{2n+z}O_2$ ) dictates specific molecular weights for each combination of n and Z. This allows further characterization of the mixture into relative groups of 1-, 2-, 3-, etc. ring structures [8, 37]. Because toxicity, degradability and other characteristics may be related to structure, Z family characterization may be one important means of establishing these correlations and are therefore often determined for samples of isolated NAs [8, 23, 38, 39].

There is a lot more work done on lighter NAs than on the heavier NAs, this can occur from a number of reasons. NAs with carbon number  $n \leq 21$  contribute most of the toxicity, this makes the lighter NAs more interesting when they are analyzed [19, 28, 29, 31, 61]. Average scans are often made between  $m/z$  50- 500 or lower [12, 14, 23, 38, 49], while others define NAs

as a group of relatively low molecular weight acids (<500 g/mol) [30] and commercial NAs tend to have carbon number  $n$  between 7 and 17 [28]. This may be a reason why there is a lack of work done on heavier acids.

Using commercially available model NA mixtures, MS protocols can be developed, by means of the fragment ions that are characteristic of the NAs molecular structures. These protocols can be used for the characterization and differentiation of NA mixtures [15]. Well-ordered patterns are often observed for NAs of  $Z = 0$  and  $-2$  which correspond to acyclic acids and monocyclic acids, respectively. For NAs of  $Z = -4, -6,$  and  $-8$ , specific zones are observed which can allow pattern recognition of unknown NA samples obtained from different origins. But something that complicate this procedure is that commercial products can consist of thousands of NAs and fatty acids which all elute together, resulting in large humps with very few resolvable peaks [15, 23].

The elemental composition is used to predict the structure based on common understanding of possible configurations. This approach does not provide conclusive information on molecular structures, particularly for highly complex mixtures where different structures may be associated with the same elemental composition [8]. Separation of these components combined with tandem mass spectrometry of separated ions could provide further characterization of complex mixtures [8].

### 1.7.9 MS detection methods

Due to the lack of articles written in English about NAs detected with other detectors than MS, only MS ionization and detection methods are mentioned here.

#### Electron ionization (EI) MS

EI MS was used in the first semiquantitative determination of the carboxylic (naphthenic) acids in a fraction of crude oil. Carboxylic acids were isolated from a crude oil and fractionated by ion exchange chromatography and TLC. Samples were placed directly on a probe that was heated during the analysis. EI of free carboxylic acids caused excessive molecular fragmentation, confounding interpretation of the mass spectra. Derivatization of the acids to their 1,1,7-trihydroperfluoroheptyl esters gave higher molecular weight products with stronger molecular ions, thereby simplifying the interpretation of the spectra. The TLC fraction contained about 1500 compounds, and many of them belonged to homologous series [41]. This method is not in



use anymore because of the extensive developments in the chromatographic and mass spectrometric areas.

### Electrospray ionization mass spectrometry (ESI MS)

ESI is by far the most popular and most widespread ionization technique in on-line liquid chromatography (LC) MS. It is both a simple and an elegant method; it can handle small and large molecules, operates at atmospheric pressure and relatively low temperatures, and provides soft molecule ionization [62].

MS with negative ion ESI has been used to determine NA concentration in aqueous samples. Since ESI MS is a soft ionization technique it is capable to analyze NA mixtures, although complete resolution of components of complicated mixtures such as those associated with petroleum is still difficult [37].

Negative ion ESI MS has been used to characterize NAs in an extract from oil sands tailings water [48]. Negative ion ESI is easily influenced by signal suppression by matrix compounds. Without pH adjustments the NAs will be in neutral form in several mobile phases (acetonitrile, MeOH, acetone, etc), which will give weak signal intensities in negative ion ESI. This problem can be solved by adding to the mobile phase a basic molecule to the mobile phase (e.g. triethylamine TEA) which induces the formation of  $\text{RCOO}^-$  ions by removing a proton from the acid molecule, resulting in enhanced  $(\text{M}-1)^-$  signal [37, 38]. With negative ion ESI it is possible to determine molecular distribution of acids without derivatization. When using the standard addition method, the absolute concentrations can be obtained semiquantitatively [63].

The ions obtained with ESI MS correspond to the molecular weight of ions of specific NA isomers, allowing the identification of carbon number and Z series. Peak height can be used to determine relative concentrations, using NA standards. ESI MS can also provide overall concentration of NAs in stock solutions [37, 49].

ESI MS also holds a great potential for online LC MS to separate acids by HPLC followed by mass spectrometric characterization of NAs.

### Atmospheric pressure chemical ionization (APCI)

Negative-ion atmospheric pressure chemical ionization using acetonitrile as a solvent and mobile phase appears to give relatively clean mass spectra for the characterization of NAs, without discrimination of heavier ions and formation of fragment and cluster ions. Z series types and carbon number distribution of NAs without derivatization can be found with APCI. APCI, similar to ESI MS, also holds a great potential for online LC MS to separate acids by high performance liquid chromatography (HPLC) followed by mass spectrometric characterization of NAs [63],[14]

## Fluoride ion chemical ionization mass spectrometry (FICIMS)

NAs from crude oils and refinery wastewater can be determined by FICIMS using fluoride ions ( $F^-$ ) to abstract protons (H) from the carboxylic acids ( $RCOOH$ ) to form carboxylate ions ( $RCOO^-$ ) [64]. Hydrocarbons and other nonacidic matrix molecules cannot be ionized by  $F^-$ , and will not interfere with the analysis. The samples are distilled off a probe by increasing the temperature from 70 to 300 °C. Quantitative determination of the NAs are calculated from relative distribution of NAs by carbon number within a given Z series, and the relative mole percentages of each Z series within the total sample [64].

## Negative ion fast atom bombardment (FAB) MS

Negative ion FAB using triethanolamine in the matrix has been used to characterize NAs from a commercial preparation and from a crude oil. FAB analysis detects all of the NAs, including those with high molecular weight. Ion exchange chromatography was used to isolate the NAs from the crude oil. Each crude oil analyzed with this method showed a distinct distribution of acids based on carbon and Z numbers [16, 38].

## FTICR MS

Negative ion mode nanospray ionization with Fourier transform ion cyclotron resonance MS has high mass accuracy, ultrahigh resolution, and selective observation of deprotonated NAs and can therefore be used to analyze NAs from crude oils dissolved in acetonitrile. An overview of the Z series distribution of NAs present in the crude oil samples can be obtained [39, 45].

## Negative ion electrospray ionization with high-field asymmetric waveform ion mobility spectrometry (ESI FAIMS)

ESI FAIMS can be coupled to either a quadrupole or a time of flight MS. This fast separation mechanism is dependent more on the ion structure (including ion dipole moment and ion polarisability), than on the ion size, and therefore, ions of the same  $m/z$  (i.e., the same elemental composition) can be separated [65, 66]. With this method it is possible to analyze NA mixtures from different sources directly without extensive sample preparation. Sample dilution with MeOH is sufficient to eliminate suppression effects and to obtain quantitatively reliable mass and isomer distributions of NA components in 3 min. The FAIMS separation is proved to be acritical in determination of elemental composition and in simplifying dissociation spectra to allow for better identification of examined compounds. Tandem mass spectrometry of NA ions

separated by FAIMS indicates that it is possible to obtain substantially more information than is available now in the field of NA analysis [52].

## 1.8 Aim of study

At Statoil in Trondheim they have found that the ARN acid content is the only limiting factor for naphthenate deposition [42, 43]. As it appears that the ARN acid family is the source to the naphthenate deposits, this may be a valuable starting point for designing an environmental friendly naphthenate deposit inhibitor. Another opportunity is that quantitative analysis of ARN will give a prediction of the amount of calcium naphthenate deposition one oil well potentially can produce, this may have importance for the process facility design [42]. Statoils work on the naphthenate deposition problem and the ARN acid family is presented by Baugh, Vinstad and Mediaas [42-44, 57]. The molecular structure and the interface behavior are looked at by Lutnaes and Brandal [45, 46].

The prefractionation step used at Statoil is either directly from the naphthenate deposit, which is a faster but less selective method, or the tedious Acid- IER method [42]. The efficiency and selectivity of the Acid- IER method with regard to carboxylic acids have been demonstrated to be >98 mol %, which is good, but the downside is that it takes more than 24 hours to isolate the carboxylic acids in a crude oil sample with this method [57]. After the prefractionation step the NAs are converted to methyl or benzyl esters for HTGC MS (high temperature GC MS) or LC MS analysis respectively. <sup>13</sup>C MNR, FTICR MS and Vapor Pressure Osmometry (VPO) have been used to look at the structure and to determine the exact molecular weight of ARN [42].

The main aim for this thesis was to develop a method where ARN can be detected and quantified in a crude oil without tedious prefractionation and derivatization steps. But the concentration of ARN is only about 2ppm (2µg/g) in Heidrun oil [67], thus a prefractionation step may be necessary to be able to determine ARN in the concentrations of 4 ppm to 0.5 ppm. A simple methanol extraction would be quicker and more unproblematic than the Acid- IER.

When it comes to the separation of the ARN acids in the ARN acid family, microcolumn liquid chromatography was chosen. This is a complementary technique to conventional sized LC. The most significant advantages of microcolumn LC are the ability to work with minute sample sizes, small volumetric flow-rates, and the improved detection performance with the use of concentration sensitive detection devices due to reduced chromatographic dilution and easier connection to the MS [68, 69]. Decreasing the column volume puts requirements on the

instrumentation applied in microcolumn LC. All volumetric extracolumn dispersion sources have to be scaled down according to the volume of the separation column. This is particularly important for the injection and detection volume [68, 69].

When it comes to detection, the ESI interface can be operated at extremely low mobile flowrates that are typically used with microcolumn LC ( $\mu$ LC), resulting in extremely low mass sensitivity limits of detection. Micro LC ESI MS interfaces also have a near-linear relationship upon the concentration of the analyte, making it an important tool in quantitative analysis [62, 68, 69].

## 2. Experimental

### 2.1 Materials and reagents

#### 2.1.1 Materials and reagents used in the GPC HPLC systems

The gel permeation chromatography (GPC) HPLC system consisted of a model 6000 pump from Waters (Waters Associates, Milford MA, USA) and a Varex MK III light scattering detector detector (ELSD) from Alltec, (Deerfield, USA), the drift tube temperature and nebulizer gas flow rate selection for the evaporator tubing in the ELSD was based on instructions in the operation manual [70]. The data processing program was TotalChrom from Perkin Elmer Instruments LLC (Connecticut USA). Polystyrene standards with different molecular weights, (760 g/mol and 4000 g/mol) and (760 g/mol and 2000 g/mol), from Fluka AG (Buchs, Switzerland) were used.

The nebulization gas in the ELSD was N<sub>2</sub> (99.996 %) from AGA (Oslo, Norway). Two columns were used, one Waters Styragel HR2 (7.8 (i.d.) x 300 mm) was tested and rejected, and one Waters 100 Å  $\mu$ Styragel GPC column (7.8 x 300 mm), with an effective molecular weight separation area of 50-1500 g/mol was used in the GPC fractionation step. HPLC grade Toluene from Rathburn, (Walkerburn, UK), was used as mobile phase with 1 ml/min isocratic flow rate. The injection volume was 66  $\mu$ l, using a Rheodyne (California, USA) Model 7010 six port valve injector. A schematic drawing of the system used is presented in Figure 5.

To be able to see where the ARN acids eluted in the chosen system, four different fractions were collected (see Table 4) and analyzed with negative electrospray TOF MS.

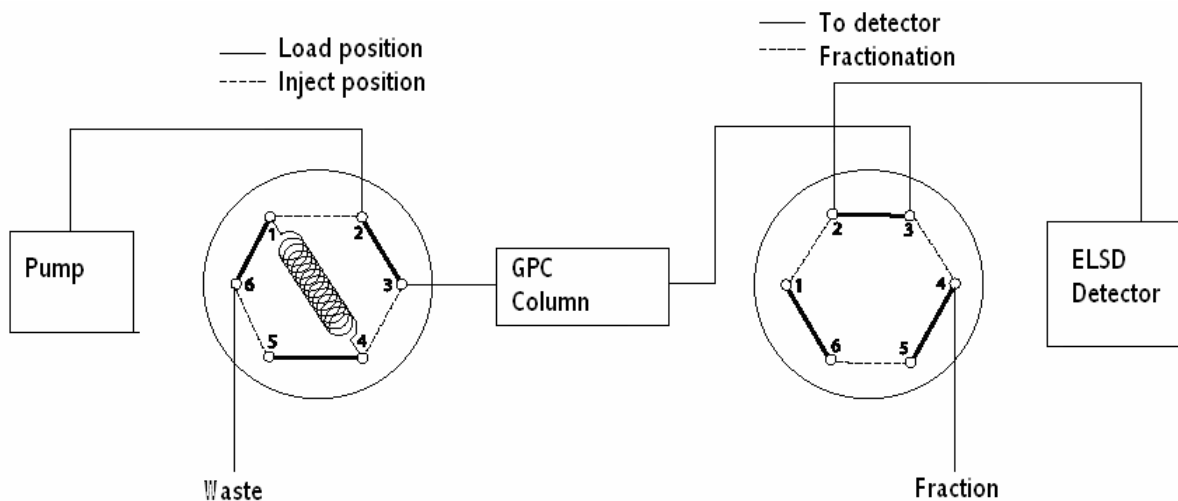


Figure 5: Sketch of the GPC HPLC system.

### 2.1.2 Materials and reagents used for extraction of ARN from A-22 oil

The extraction of ARN from A-22 oil was performed with four different solvents, to see which gave the best recovery. HPLC grade MeOH, from BDH Laboratory supplies, (Dorset, UK), acetonitrile (AcN) from Rathburn, acetone from Merck (Darmstadt, Germany), and toluene from Rathburn. A Banson (Danbury USA) 5500 type ultrasonic bath, was used to optimize the extraction recovery and Sterlitech Teflon syringe filters (0.2  $\mu\text{m}$  and 0.4  $\mu\text{m}$ ) made of naturally hydrophobic Teflon (Teflon®), from Alltec were used to filter the solvent phase before the TOF MS analysis. Figure 7 illustrates a flow chart of the work done with the A1 polar, and Figure 8 illustrates a flow chart of the work done with the extraction of ARN from A-22 oil.

Water free MeOH (obtained by drying HPLC grade MeOH, from BDH Laboratory supplies, with molecularsieb from Merck) was also used at a later time in the extraction procedure, to see if this made any difference in the recovery of ARN.

### 2.1.3 Materials and reagents used in the direct infusion negative ESI TOF MS

The outlet of a direct infusion pump from a 74900 Series Cole Parmer (Instrument Co., Vernon Hills, IL, USA) was connected to a Micromass (Manchester, UK) LCT TOF MS. The TOF MS was equipped with a Z-spray atmospheric pressure ionization source for ESI, which was

modified to handle flow rates in the low  $\mu\text{l}/\text{min}$  range. Ionization was performed in negative mode, and ARN was observed as  $[\text{M}-\text{H}]^-$ . The following voltages were used: -3200V on the capillary, -50V on the sample cone and -5V extraction cone. In order to obtain a stable spray performance and aid solvent vaporization, nebulizer gas and desolvation gas were applied at 50 l/hour and 200 l/hour, respectively. The TOF MS instrument was controlled by Mass Lynx v3.5 software, later the software was upgraded to Mass Lynx v 4.0, and mass spectra were acquired in the  $m/z$  range 100-1300.

The four different samples extracted with four different solvents were injected into the direct infusion TOF MS system both with and without TEA from Fluka AG.

#### 2.1.4 Materials and reagents used in the $\mu\text{LC}$ MS analysis

Negative electrospray MS analysis was performed on the LCT TOF MS from Micromass, with MassLynx 3.5 and 4.0 software. An Agilent (Palo Alto, CA, USA) 1100 series gradient pump was used. The mobile phase gradient as described in Table 6 was used and contained MeOH (HPLC grade, BDH Laboratory supplies), TEA (Fluka) and grade 1 water which was obtained from a Milli-Q ultrapure water purification system (Millipore, Bedford, MA, USA), the flow rate was 5  $\mu\text{l}/\text{min}$  and a six ports Valco injector (Valco Instruments Co. Houston, TX, USA) with a injection volume of 500 nl was utilized. Three Kromasil C 18 columns with 3.5  $\mu\text{m}$  particles, 0.32 mm inner diameter and 100 mm length were used, one was made in house by a procedure described in section 2.5, and the other two were purchased from G&T Sepatech (Kolbotn, Norway).

The outlet of the analytical column was connected to the LCT TOF MS (Micromass). The TOF MS was equipped with a Z-spray atmospheric pressure ionization source for ESI, which was modified to handle flow rates in the low  $\mu\text{l}/\text{min}$  range. Ionization was performed in negative mode, and ARN was observed as  $[\text{M}-\text{H}]^-$ . The following voltages were used: -3200V on the capillary, -50V on the sample cone and -5V extraction cone. In order to obtain a stable spray performance and aid solvent vaporization, nebulizer gas and desolvation gas were applied at 50 l/hour and 200 l/hour, respectively. Mass spectra were acquired in the  $m/z$  range 100-1300, with a scan rate of 1 scan/min. A schematic drawing of the system used is presented in Figure 6.

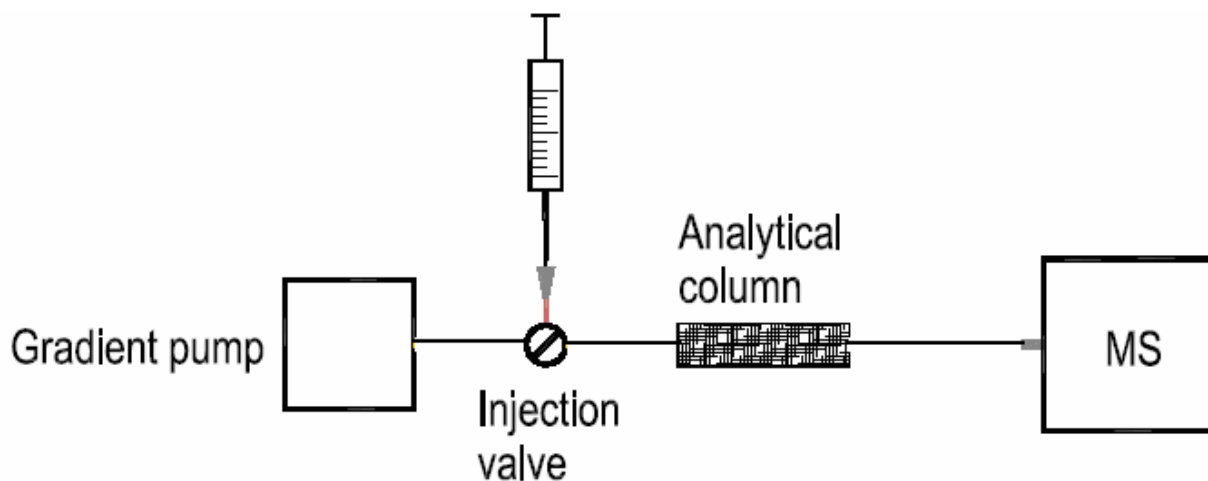


Figure 6: Sketch of the  $\mu$ LC MS system.

## 2.2 Considerations made for solvents and samples

All contact surfaces for solutions containing toluene were glass or teflon, to avoid dissolution of organic contaminants. Samples containing ARN (NAs) were stored at 4-6 °C to avoid degradation. Microliter automated pipets were always used to deliver microliter volumes. Since ARN precipitates in water, the lab equipment was dried before use, and molecularsieb from Merck was used to get 100 % water free MeOH.

## 2.3 Samples obtained from Statoil

A-22 crude oil (oil Heidrun, 030123002 (centrifuged) without ARN), and 5 glass vials with carboxylic acids (including approximately 3.30 % ARN) dissolved in isopropanol and toluene which had been isolated with the Acid IER-Method (020103003.03), called A1 polar was obtained from Statoil, Trondheim, see Table A1 in Appendix.



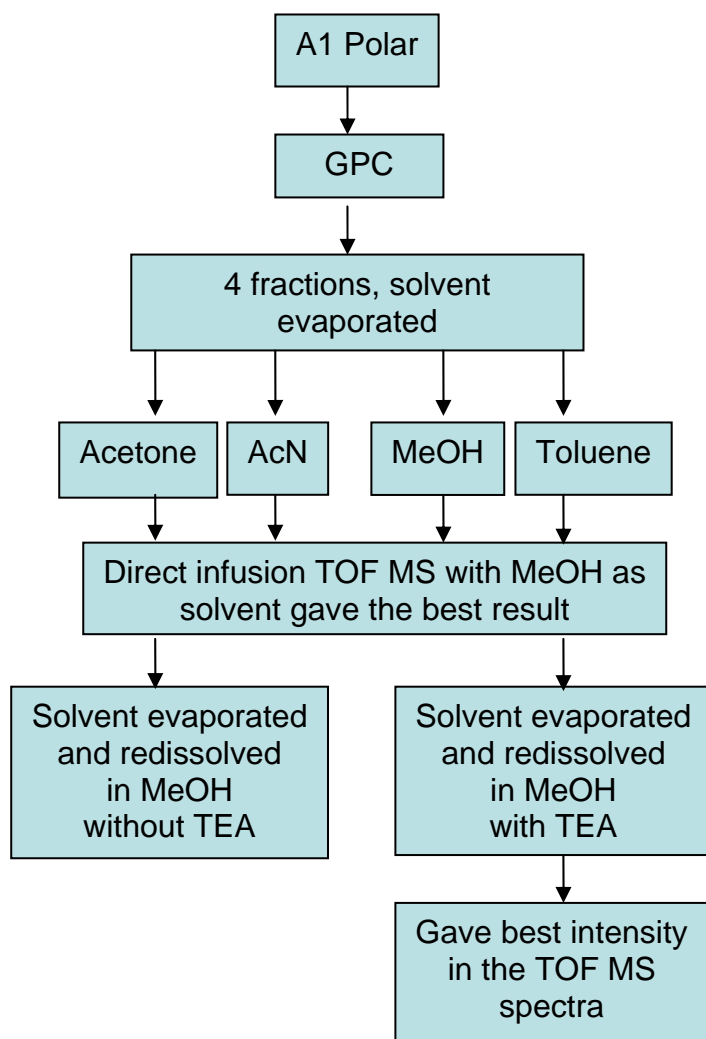


Figure 7: Flow chart of the work done with the A1 polar.

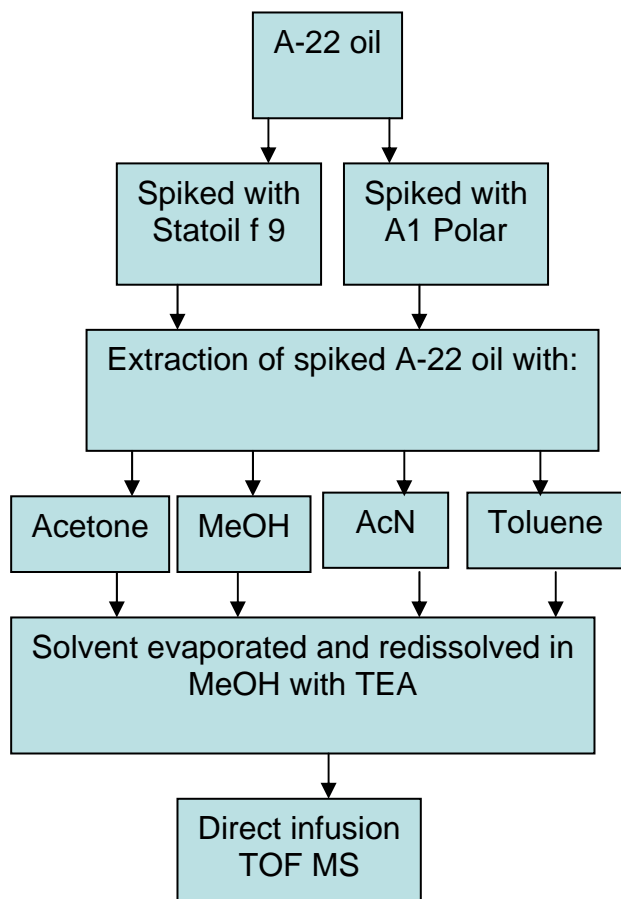


Figure 8: Flow chart of the work done with the extraction of ARN from A-22 oil.

## 2.4 Spiking and extraction of A-22 oil

A-22 oil was weighted and added certain amounts of A1 polar, to obtain the desired concentrations of ARN (see Table 4, only the MeOH extraction is shown as this was the solvent used in the further work), then 5 ml of the spiked oil and 20.0 ml MeOH, AcN, acetone or toluene (with and without 0.1 % TEA) was transferred to a 25 ml glass vial with lid. This solution was treated ultrasonically with heating for one hour. After one hour the glass vial contained two phases; one black crude oil phase, and one yellow translucent solvent phase. The solvent phase was filtered through a 0.20  $\mu\text{m}$  pore size filter, and determined with direct infusion TOF MS. When spiking with the smallest amounts of ARN, 20.00 ml A-22 oil was used to get an amount of ARN which could be weighed with sufficient certainty. Figure 7 illustrates a flow chart of the work done with the A1 polar, and Figure 8 illustrates a flow chart of the work done with the extraction of ARN from A-22 oil.

As the ARN acids precipitates in water, and the MeOH used contains 0.005 % water, the extraction procedure was also done with dried MeOH, no difference was observed, so the extraction procedure was continued without dry MeOH.

Table 4: The spiked samples used for MeOH extraction.

Figure name	Weight of A-22 oil for spiking with ARN (g)	Amount of A1 Polar used for the spiking (g) of A-22 oil	Calculated amount of (ARN/naphthenes) in the measured amount of A1 Polar used in spiking (g)	Concentration of ARN in A-22 oil after spiking (ppm/ $\mu$ g/g)	Amount of MeOH used in the extraction (ml)	ARN cons. in MeOH after extraction (g/ml)	Calculated amount of ARN injected on the column (ng), if 100 % recovery
34	16.9283	0.00	0.00	0.00	20.00	0.00	0.00
36	4.2744	0.8121	0.0214	5006	20.00	1.0734exp-3	536.7
38	4.0745	0.3513	9.3081exp-3	2284	20.00	4.6540exp-4	232.7
40	4.1653	0.0375	9.9360exp-4	238.5	20.00	4.9680exp-5	24.8
42	4.2661	0.0201	5.3138exp-4	124.5	20.00	2.6569exp-5	13.3
44	17.0995	0.0120	3.0443exp-4	17.80	20.00	1.5221exp-5	7.6
46	16.9643	0.0028	7.4023exp-5	4.36	20.00	3.7011exp-6	1.9

## 2.5 Column packing

The columns packed in-house were made of fused silica capillaries from Polymicro Technologies (Phoenix, AZ, USA) the Kromasil material was obtained from Eka Nobel (Bohus Sweden). The column was slurry packed using AcN/H<sub>2</sub>O (grade 1), (70/30 v/v) as packing fluid. Around 30 mg packing material was dispersed in 200  $\mu$ l carbon tetrachloride (Rathburn) and put in an ultrasonic bath for 10 min to get a suitable suspension. The suspension was put into a packing chamber connected via a Valco (Valco Instruments Co) ZU1C union to a fused silica capillary with a length of 10 cm. The other end of the capillary was connected to a union with a frit (Valco 2SR1) to keep the packing material in the capillary. The top of the packing chamber was connected to a downward pressure pump. The pump was programmed to start at 100 bar and increase the pressure at a rate of 200 bar/min to 650 bar. The column was conditioned for 20 min at 650 bar. The pump was disconnected by the use of a valve after the conditioning step. Then the column was depressurized for another 20 min before using another program, which decreased the pressure in the system, starting at 650 bar, down to 1 bar with a rate of -100

bar/min. After this the column was disconnected and a union with a frit inside was connected to the nut and ferrule.

## 2.6 Accurate mass determination of Statoil f 9

Accurate mass determination of the ARN acids in Statoils f 9 was done by John Vedde on an Apex 47e (Bruker Instruments, Inc., Billerica), FTICR MS, with Xmass software, and a Micromass QTOF 2 W, with Masslynx software, the results are shown in Table A2 in Appendix.

### 3. Results and discussion

#### 3.1 Fractionating the A1 polar

By analyses of the NA residue, it was found that it mainly consisted of specific acids called the ARN acid family [43]. If isolated from the A1 polar sample, the presence of ARN could be established using a TOF MS. GPC is an easy method to separate one specific molecular size group (ARN) from a mixture of molecules with different molecular sizes (the other carboxylic acids in A1 polar). This would make it easier to qualitatively and quantitatively determine ARN in A1 polar from the ion exchange extraction (the Acid IER-Method).

A GPC HPLC system with an evaporative light scattering detector (ELSD) was used, and two different columns were tested.

##### 3.1.1 Comparing Waters Styragel HR2 and Ultrastyrigel columns

The repeatability of retention on the GPC system was tested frequently by injection of a standard solution consisting of one polystyrene standard (with an average molecular weight at 1000 g/mol) and one triphenyl standard (with a molecular weight at 228.30 g/mol).

The resolution ( $R_s$ ) between the two polystyrene standards (760 g/mol and 4000 g/mol) when the Waters Styragel HR2 column was used, was found to be  $\sim 0.24$ . This resolution was insufficient to fractionate the ARN from the A1 polar, given that base line separation is defined as a resolution  $R_s = 1.5$  [71].

The resolution between the two standards (760 g/mol and 2000 g/mol) when the Ultrastyrigel column was used, was found to be  $\sim 0.6$ , which was better than for the Styragel HR2 column, and it was decided to be sufficient since the separation was a sample cleanup fractionation. The effective molecular weight area fractionation of this column is 50-1500 g/mol, and further testing with a mixture consisting of three polystyrene standards (with average molecular weights of respectively 2000g/mol, 1000g/mol and 760g/mol) and one polystyrene standard (( $C_6H_4$ )<sub>3</sub> with a molecular weight of 228.30g/mol) was performed. It was confirmed that the column provided sufficient separation in the relevant molecular weight area, (results not shown).

### 3.1.2 GPC fractionating and identification of ARN in A1 polar

The evaporative light scattering detector (ELSD) was chosen because the ARN acids do not have any UV absorbance, and toluene was used as mobile phase because of its ability to solve the carboxylic acid fraction.

The ELSD is a destructive detector, so the GPC HPLC system in Figure 5 was used for the collection of the fractions. The fractions were taken from the aperture for fractionation which is placed in front of the detector. It was corrected for the time difference between detector and fractionation aperture.

As the mobile phase flow was precise and repeatable, the fraction accumulation could be executed on time, compared with a previous fraction done with the detector connected to the system.

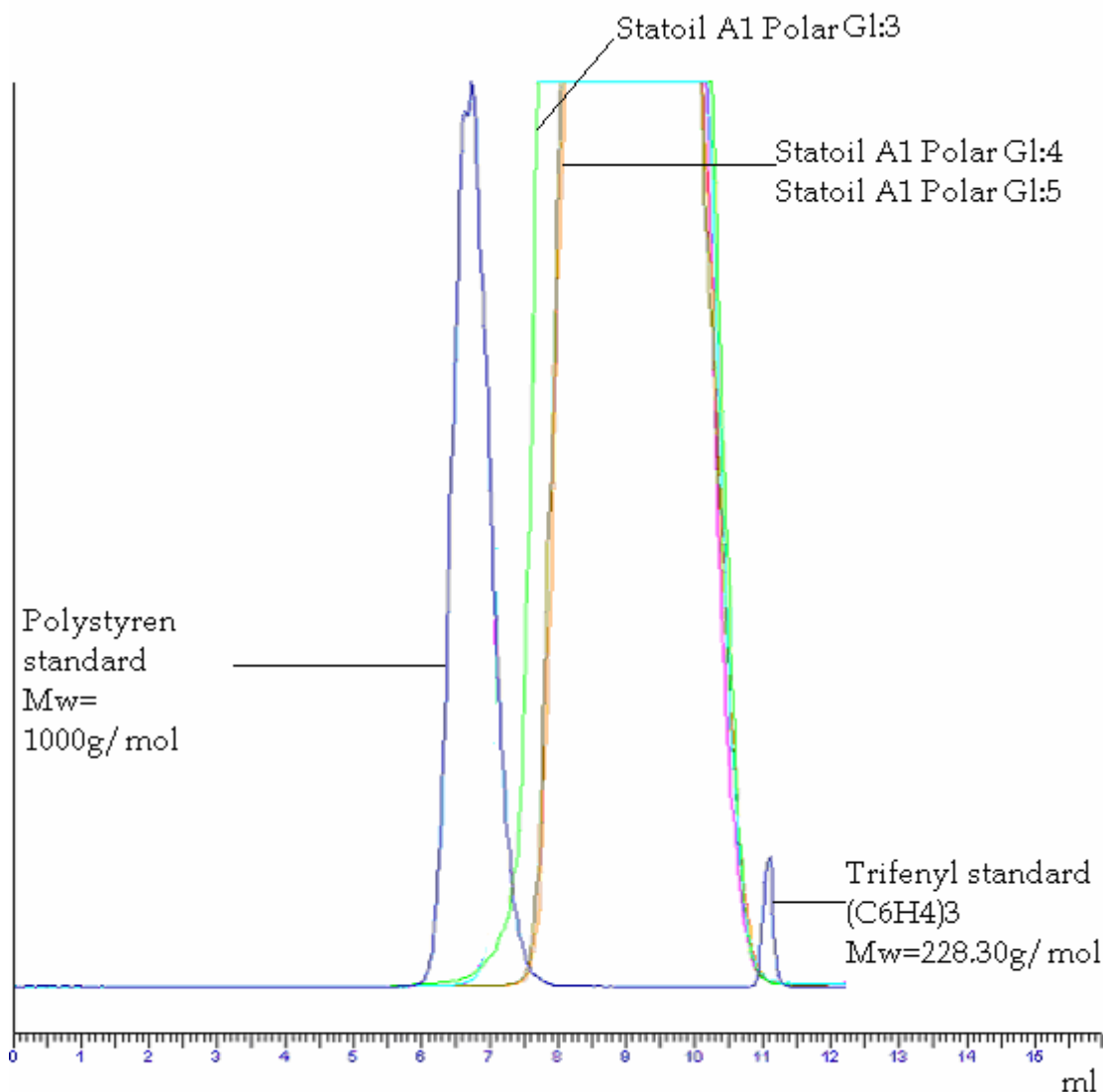


Figure 9: Chromatograms of three of the A1 polar samples given from Statoil, and a standard solution consisting of one polystyrene standard (1000 g/mol) and one triphenyl standard (228.3 g/mol), superimposed to compare retention times.

(A1 polar, Gl: 3, Gl: 4 and Gl: 5, were supposed to contain the same, the only difference were that it were put into three different glass vials.

### 3.1.3 GPC fractionation of A1 polar

The GPC analysis of the A1 polar from Statoil showed that there was no detectable amount of material with the molecular weight similar to ARN. That is, the fraction with a retention of 5.7-6.7 min (see Figure 9), according to the polystyrene standard calibration of the Ultrastyrigel column. This can come from differences in the hydrodynamic volumes between the polystyrene standards and the carboxylic acids in A1 polar. GPC separation is based on size, which has poor correlation to molecular weight, so if the polystyrene standards were linear and the carboxylic acids in A1 polar are spherical, the calibration would have been incorrect [72]. Statoil has confirmed that the A1 polar samples contain considerable amounts of the ARN acid family, so

the A1 polar peak were split into four different fractions, as showed in Table 5, to find the retention of ARN on this column.

Table 5: Fractions taken from Statoils A1 polar sample.

Fraction name	
Statoil A1 polar f. 7	Fraction from 7 ml to 8 ml
Statoil A1 polar f. 8	Fraction from 8 ml to 9 ml
Statoil A1 polar f. 9	Fraction from 9 ml to 10 ml
Statoil A1 polar f. 10	Fraction from 10 ml to 11 ml

### 3.2 Identification of ARN with negative ESI TOF MS

The four GPC fractions from Statoils A1 polar were called Statoil f. 7-10 (see Table 5) and analyzed with direct infusion negative electrospray TOF MS both with and without TEA (0.1 % triethylamine) added to the sample solution. This was done to see if ARN was present in these fractions.

The mass spectra of Statoil f. 7, 8, 9 and 10 are displayed in Figure 10- Figure 13. There was unfortunately no calibration solution for negative ion electrospray ionization with mass over 1000 available. This is why the mass accuracy for the highest masses can be poor. But it can be assumed that it is good in the lower  $m/z$ -range and as ARN has four acid groups, the multiple charged ions can be used with more precision. In Statoil f 9 and 10 (see Figure 12 and Figure13), the ion with highest intensity was the triple charged ion with a value of  $m/z= 409.77$ . This corresponds with a  $M= 1232.3$  if the  $m/z= 409.77$  is  $[M-3H]^{3-}$ . The double charged ion with the highest intensity has  $m/z= 614.79$  which corresponds to  $M = 1231.6$  if it is  $[M-2H]^{2-}$ .

Triple charged  $m/z= 417.1$  can be  $[M-4H+Na]^{3-}$ , while triple charged  $m/z= 409.11$  can be  $[M-3H-H_2]^{3-}$ . Triple charged  $m/z= 403.79$  can be  $[M-3H-H_2O]^{3-}$  while triple charged  $m/z= 389.13$  can be  $[M-3H-H_2O-CO_2]^{3-}$ .

From these results, it can be assumed that one of the main components in the A1polar fraction has a monoisotopic weight mass of 1231 and a molecular weight of 1232, which corresponds with the ARN acid family. Components from the ARN acid family can be seen in fraction 7 and 8 too, but there are obviously a lot of other, lightweight components in these



fractions, that indicates that these fractions are not as clean as Statoil f 9 and 10. These lightweight components can additionally induce ion suppression.

The mass spectra from the analysis of the fractions without TEA in the sample solutions were similar to those in Figure 10- Figure 13, except for the ion intensity, which was a lot lower. The assumption can be made that at this time, TEA does not participate in any adduct formation, but it enhances the MS signal by ionization of the ARN acid groups.

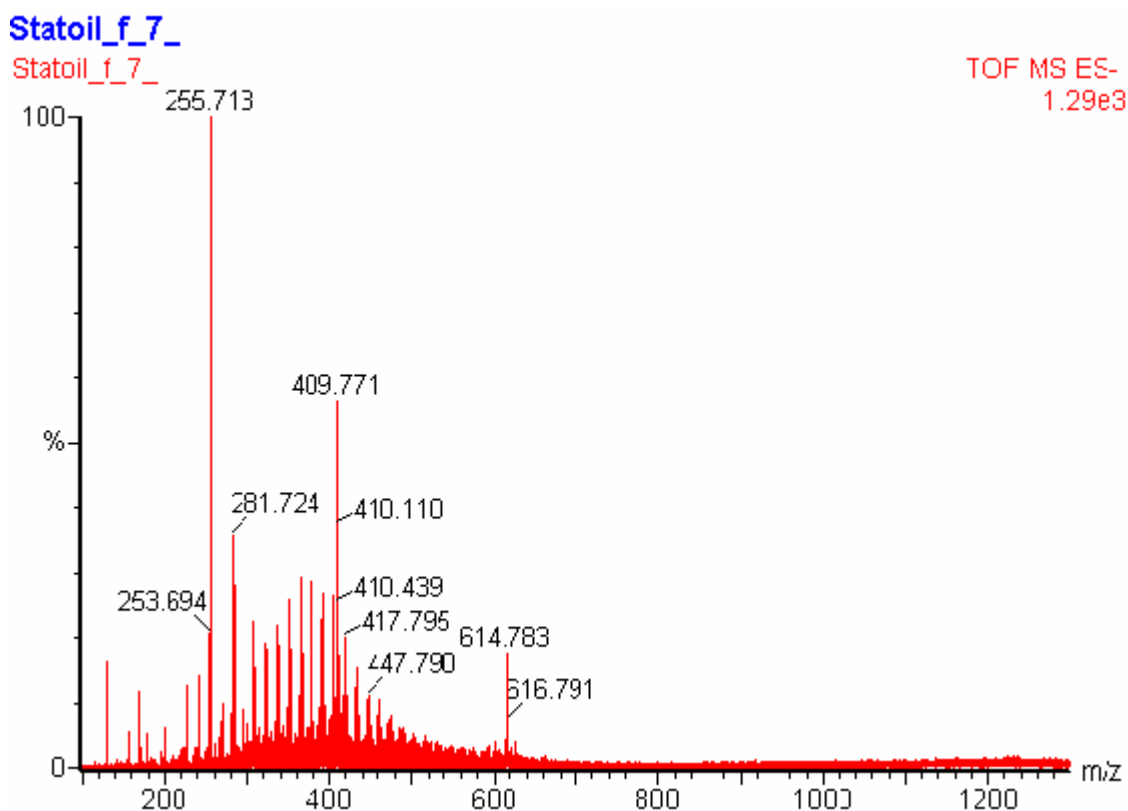


Figure 10: Mass spectrum of Statoil f.7. Direct infusion TOF MS ES-

Statoil\_f\_8\_

Statoil\_f\_8\_

TOF MS ES-  
1.50e4

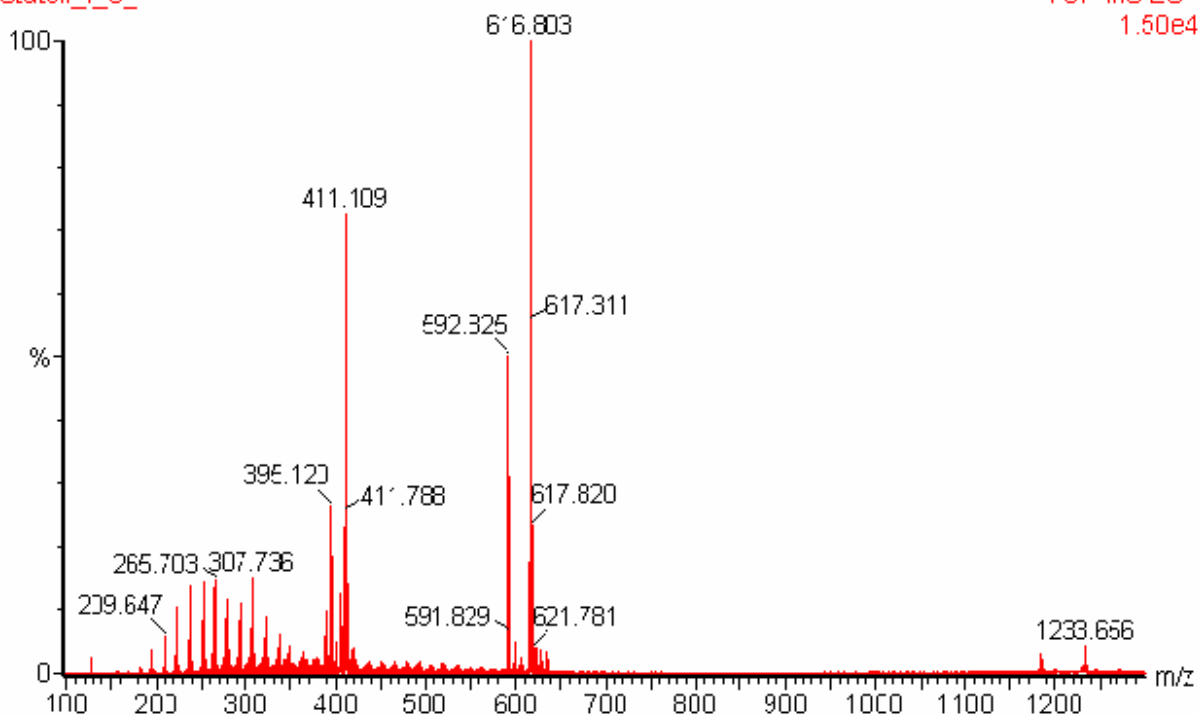


Figure 11: Mass spectrum of Statoil f.8. Direct infusion TOF MS ES-

Statoil\_f\_9\_

Statoil\_f\_9\_

TOF MS ES-  
5.08e4

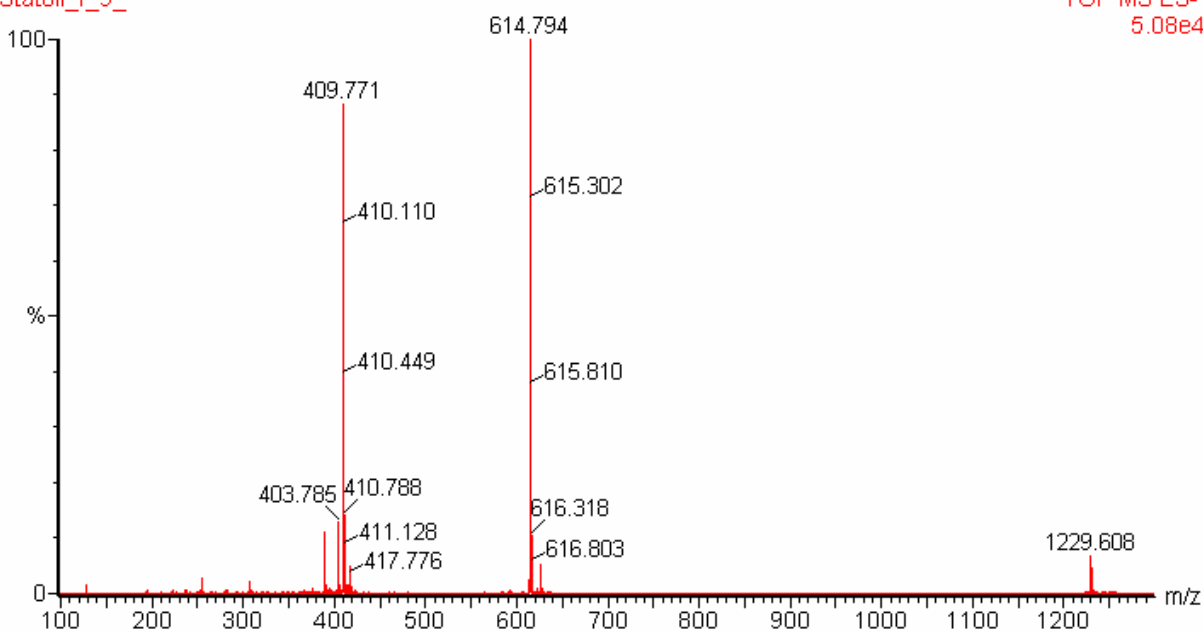


Figure 12: Mass spectrum of Statoil f.9. Direct infusion TOF MS ES-

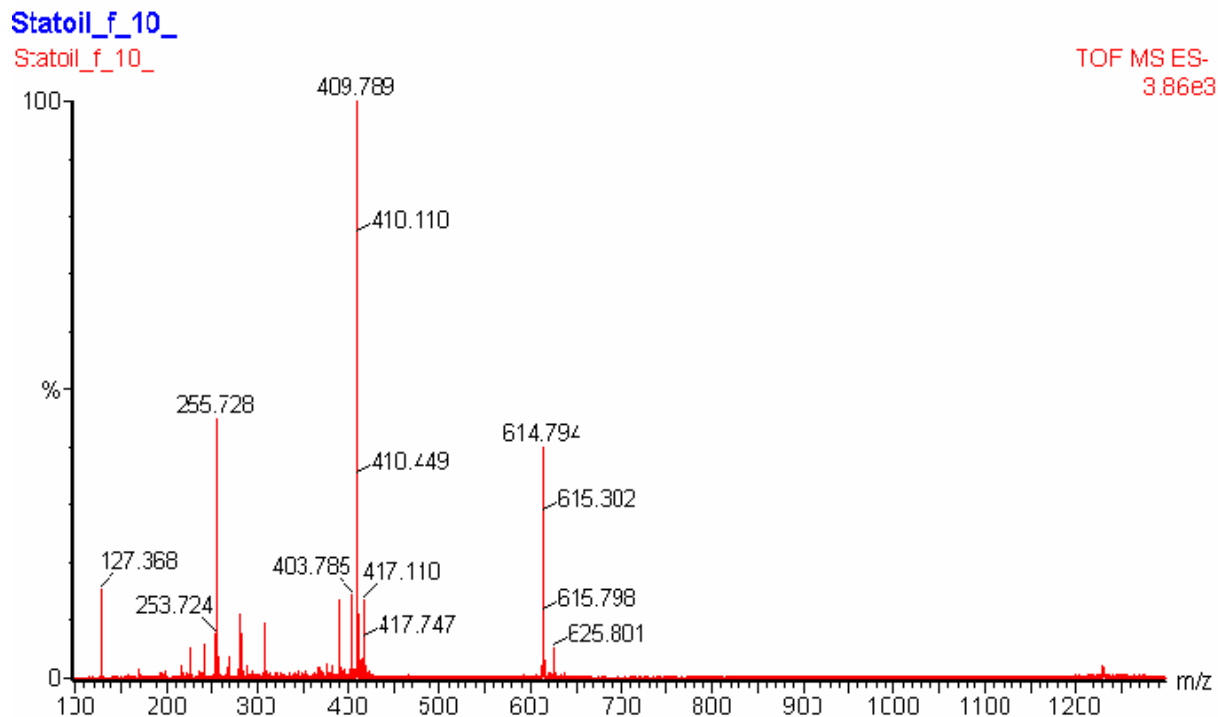


Figure 13: Mass spectrum of Statoil f.10. Direct infusion TOF MS ES-.

### 3.3 Accurate mass determination of Statoil f 9

The Statoil f 9 was sent to further MS analysis to verify the purity of the fraction. The verification of purity was performed on a Bruker Apex 47e FTICR MS, with Xmass software, only one peak was present at the exact  $m/z=614.6$ , see Figure 14. Electrospray attached to a Micromass QTOF 2 W, with Masslynx software, with a resolution of 225000 was used for the exact mass determination. The mass of the neutral molecule was measured to be 1231.0629. The numeral results are shown in Table A2 in the Appendix.

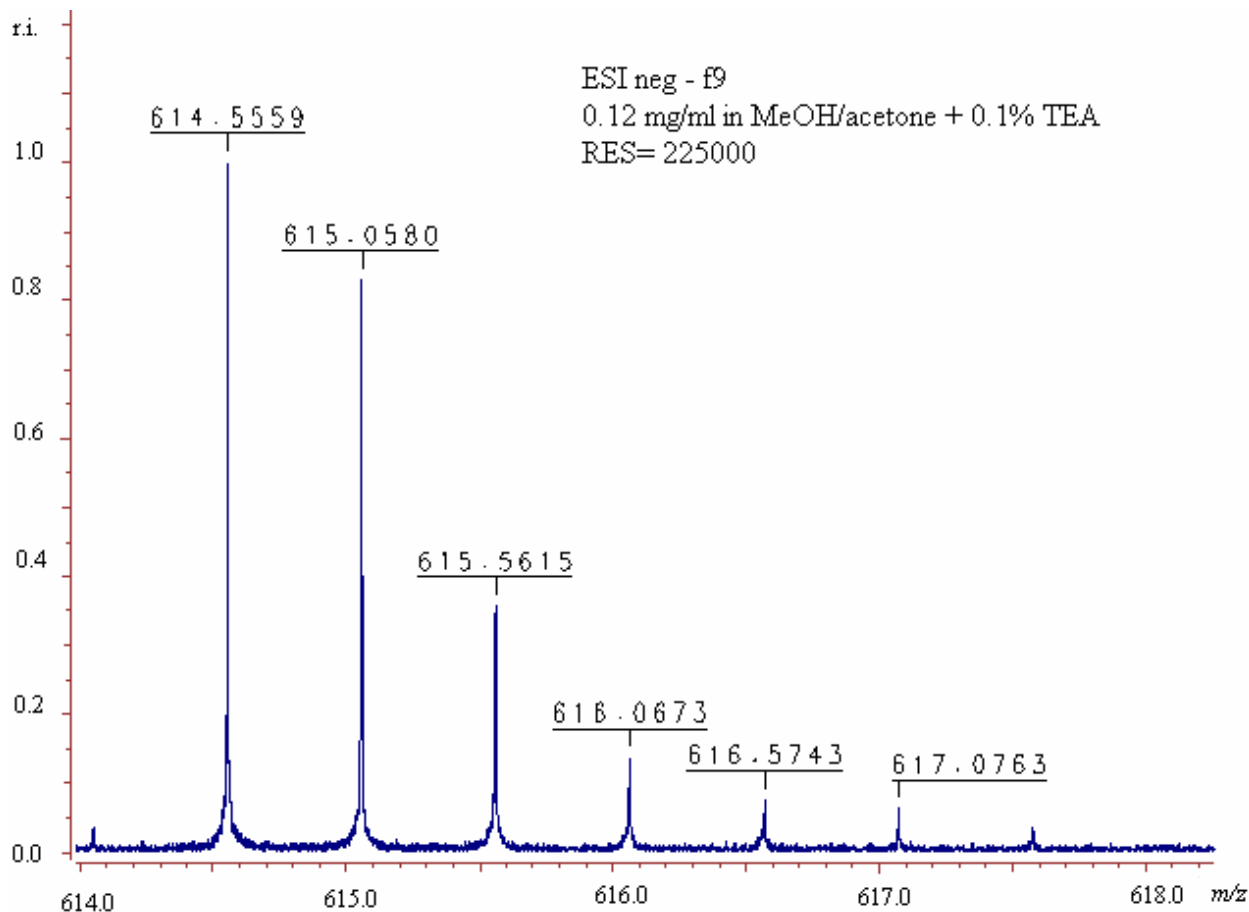


Figure 14: FTICR MS determination of the exact  $m/z$  value of ARN in Statoil f 9. There is only one peak at  $m/z= 614.6$ . The numeral results are shown in Table A2 in the Appendix.

### 3.4 Development of the mobile phase gradient used in the $\mu$ LC MS analysis

Since MeOH with TEA can solvate the ARN acids, and gave the best result in the extraction of ARN from A-22 oil, MeOH was considered used as mobile phase in the  $\mu$ LC MS analysis. A gradient system consisting of mobile phase reservoir A which contained MeOH/H<sub>2</sub>O (50/50; v/v) and 0.1 % TEA and mobile phase reservoir B which contained 99.9 % MeOH and 0.1 % TEA was constructed. To find the mobile phase composition that eluted the ARN acids, a test gradient from 100 % A to 100 % B in 30 min was set. The ARN peaks eluted between 85-90 % MeOH. The ARN acids had to be separated from the pressure peaks that emerged in the beginning of each chromatogram, this made it necessary to stretch the beginning of each gradient. The different ARN acids in the ARN acid family also had to be separated from each other, this meant that the ARN peak had to be stretched as well. Then the question of which other crude oil components that could be extracted from the A-22 oil in the MeOH extraction step came up. It was decided to run the gradient to 90 % B (95 % MeOH), to get rid of the

possibility of other eventual crude oil components. At this point the gradient was finished, but the ARN retention time was unstable. This last problem was solved by elongating the columns recondition time at the end of the gradient. The final gradient used is given in Table 6. The injection volume was 500 nl and the mobile phase flow was 5 µl/min.

Table 6: Gradient “230204”: Gradient used during µLC MS analysis.

Step nr.	Time (min)	MP % B	MeOH /H <sub>2</sub> O, (v/v)
1	0.00	50	75 / 25 (with 0.1 % TEA)
2	0.10	50	75 / 25 (with 0.1 % TEA)
3	15.10	90	95 / 5 (with 0.1 % TEA)
4	20.10	90	95 / 5 (with 0.1 % TEA)
5	20.11	50	75 / 25 (with 0.1 % TEA)
6	35.00	50	75 / 25 (with 0.1 % TEA)

### 3.5 µLC MS detection

Since the GPC fractionation did not give a sufficient separation of A1 polar, a reversed phase system was tested for its suitability to separate the components present in A1 polar. It is also a need for Statoil to have a method that can separate, detect and quantify ARN in a crude oil which also will contain light NAs.

As there are several isomers of NAs with the same molecular mass, further separation of the acids, e.g. with respect to the hydrophobicity of the various isomers, is required to obtain reliable structural determination. It was thus decided to use reversed phased chromatography, with a gradient of MeOH and water as mobile phase, to see if the components in the fractions could be separated. Several reversed phase materials such as C18 materials, C30, polystyrene divinylbenzene and Hypercarb (porous carbon) can provide reversed phase separation with different type of selectivity.

The main aim was to develop a method where ARN can be detected and quantified in a crude oil without tedious prefractionation steps. The concentration of ARN is however, only about 2 ppm (2 µg/g) in Heidrun oil, thus a prefractionation step may be necessary. In this case, a MeOH extraction may be utilized instead of the time consuming ACID IER method previously used.

Negative ESI TOF MS was used for detection of the NAs in the reversed phase µLC system. According to Statoil, the ARN acids in the ARN acid family has similar molecular mass,

and further separation of the acids, with respect to the hydrophobicity of the various isomers, is desirable to obtain reliable determination. Due to good experience with this column material, a Kromasil C18 column was the first choice. Three Kromasil C 18 columns have been used in this thesis, one made in house (see section 2.5) and two purchased from G&T Septeck. All three of the columns gave the same retentions considering the samples analyzed in this thesis. The mobile phase gradient developed in this thesis is described in section 3.4. The injection volume of 500 nl was chosen because Statoil got problems with precipitation of crude oil components in the injector and column entrance when they injected too large sample volumes [67]. Besides, when a sample containing 4.36 ppm ARN was injected on the column, a sufficient signal to noise ratio was observed to get a clear and positive identification of ARN (see Figure 46), hence a 500 nl injector volume was considered enough for this work.

Figure 15 show the total ion current (TIC) chromatogram of Statoil f 9. The fractions obtained from the GPC fractionation of A1 polar were dissolved in MeOH with 0.1 % TEA. Three peaks of ARN were observed in the chromatogram. The gradient in Table 6 was used in all of the analyses.

Figure 16 shows the extracted ion current (EIC) chromatograms of  $m/z$  613-618 from an injection of Statoil f 9, this area was chosen because triple charged ARN with  $m/z$  at 613-618 has better selectivity with regard to the ARN acids and relatively high peak intensities. Double charged ARN with  $m/z$  at 407-412 has higher peak intensities than triple charged ARN, but the selectivity is poorer. The peaks from the three ARN isomers were easily detectable, and the baseline noise was insignificant small. Figure 17 shows the mass spectra of the three ARN peaks from Figure 15 in chronological order. For the first peak, the triple charged ARN with  $m/z=$  409.7, and double charged ARN with  $m/z=$  614.7 dominated. There were almost no single charged ARN with  $m/z=$  1230.45, when 0.1 % TEA was added in the mobile phase. For the second peak, triple charged ARN with  $m/z=$  410.4, and double charged ARN with  $m/z=$  615.7 dominated. The single charged ARN with  $m/z=$  1231.5 were not detected. For the third peak, triple charged ARN with  $m/z=$  411.4, and double charged ARN with  $m/z=$  617.1 dominated. The single charged ARN with  $m/z=$  1234.5 were not detected.

In Figure 18 and Figure 19, the EIC chromatograms from  $m/z=$  1200-1300, 1100-1200, 1000-1100, 900-1000, 800-900, 700-800, 600-700, 500-600, 400-500, 300-400, 200-300 and 100-200, from Figure 15 are shown. No light acids ( $m/z=$  100-300) were observed in the three ARN peaks in the retention window of the chromatograms of Statoil f 9.

Gradient\_230204

28\_inj\_av\_Stat\_f\_9\_m\_z\_100\_1300

TOF MS ES-  
TIC  
2.44e4

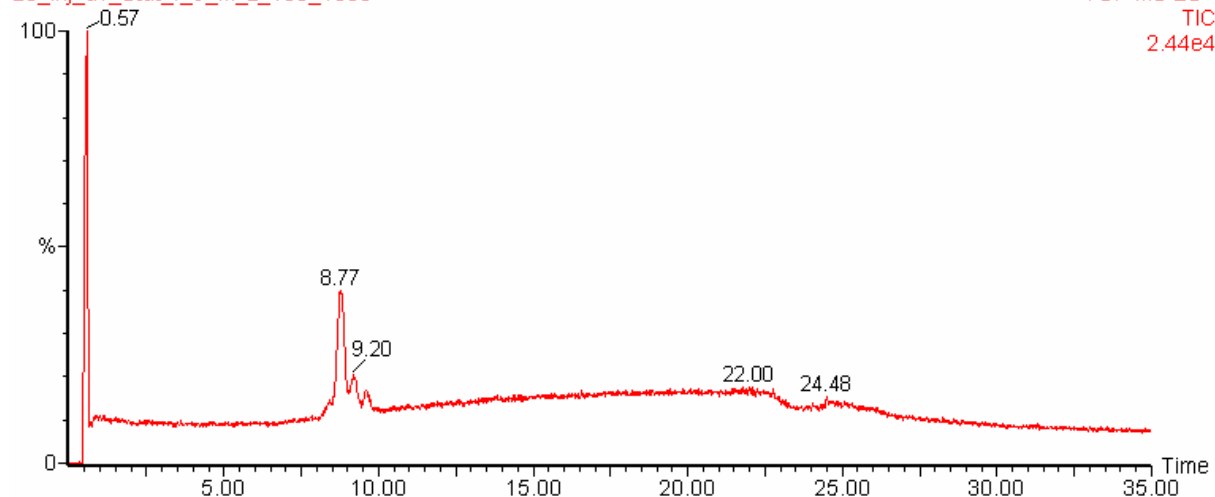


Figure 15: TIC chromatogram of Statoil f 9, dissolved in MeOH with 0.1 % TEA from the GPC fraction of A1 polar, using the 0.32x100mm Kromasil C18 column, with negative electrospray MS detection. The injection volume was 500 nl. The MeOH/H<sub>2</sub>O gradient as described in Table 6 was used with a flow rate of 5 µl/min.

Gradient\_230204

28\_inj\_av\_Stat\_f\_9\_m\_z\_100\_1300

TOF MS ES-  
613\_618  
1.09e3



Figure 16: *m/z* range 613-618 EIC chromatogram, other conditions as in Figure 15.

### Gradient\_230204

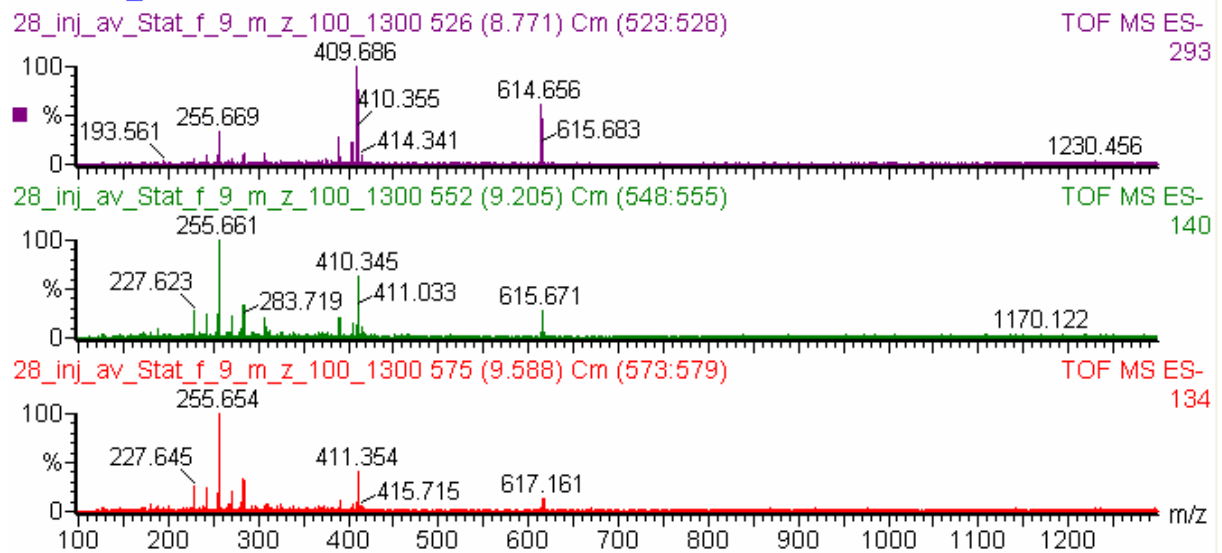


Figure 17: Mass spectra of the three peaks (in chronological order) from Figure 15.

### Gradient\_230204

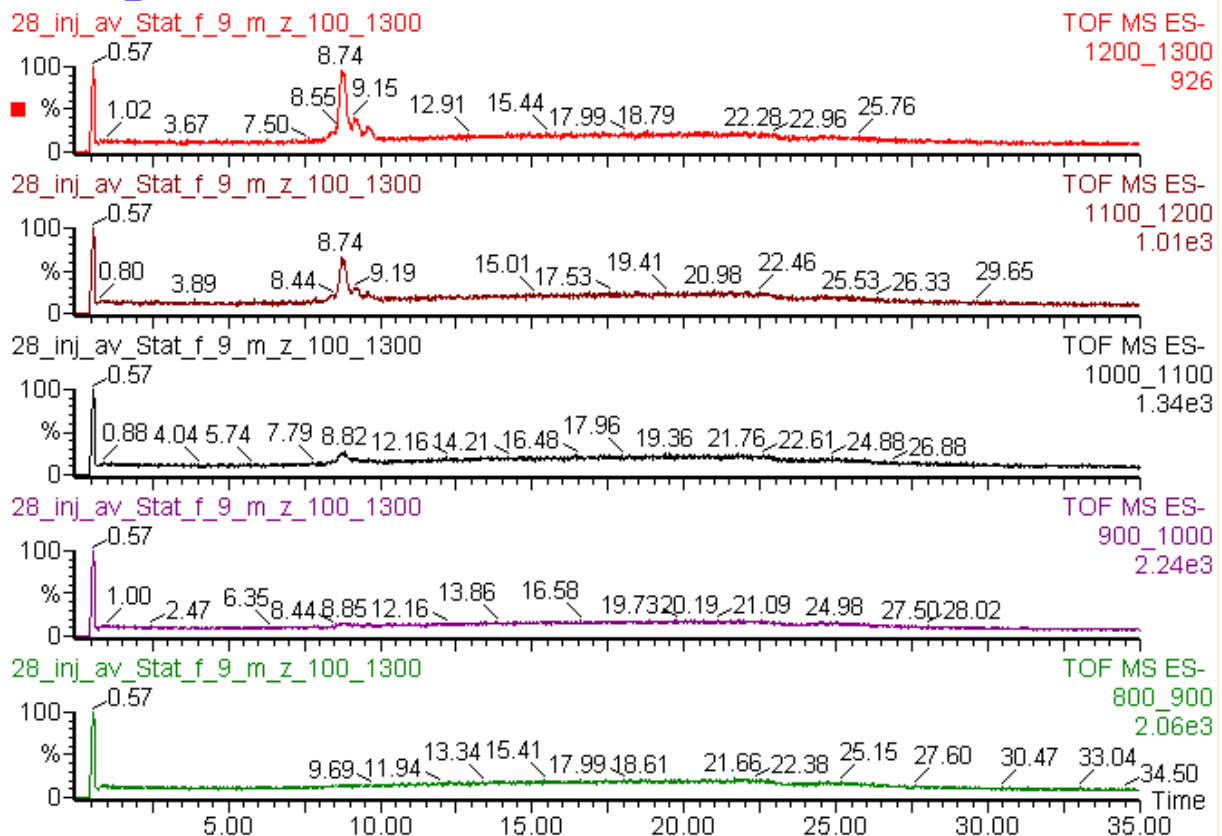


Figure 18:  $m/z$  range 1200-1300, 1100-1200, 1000-1100, 900-1000 and 800-900 EIC chromatograms, other conditions as in Figure 15.



## Gradient\_230204

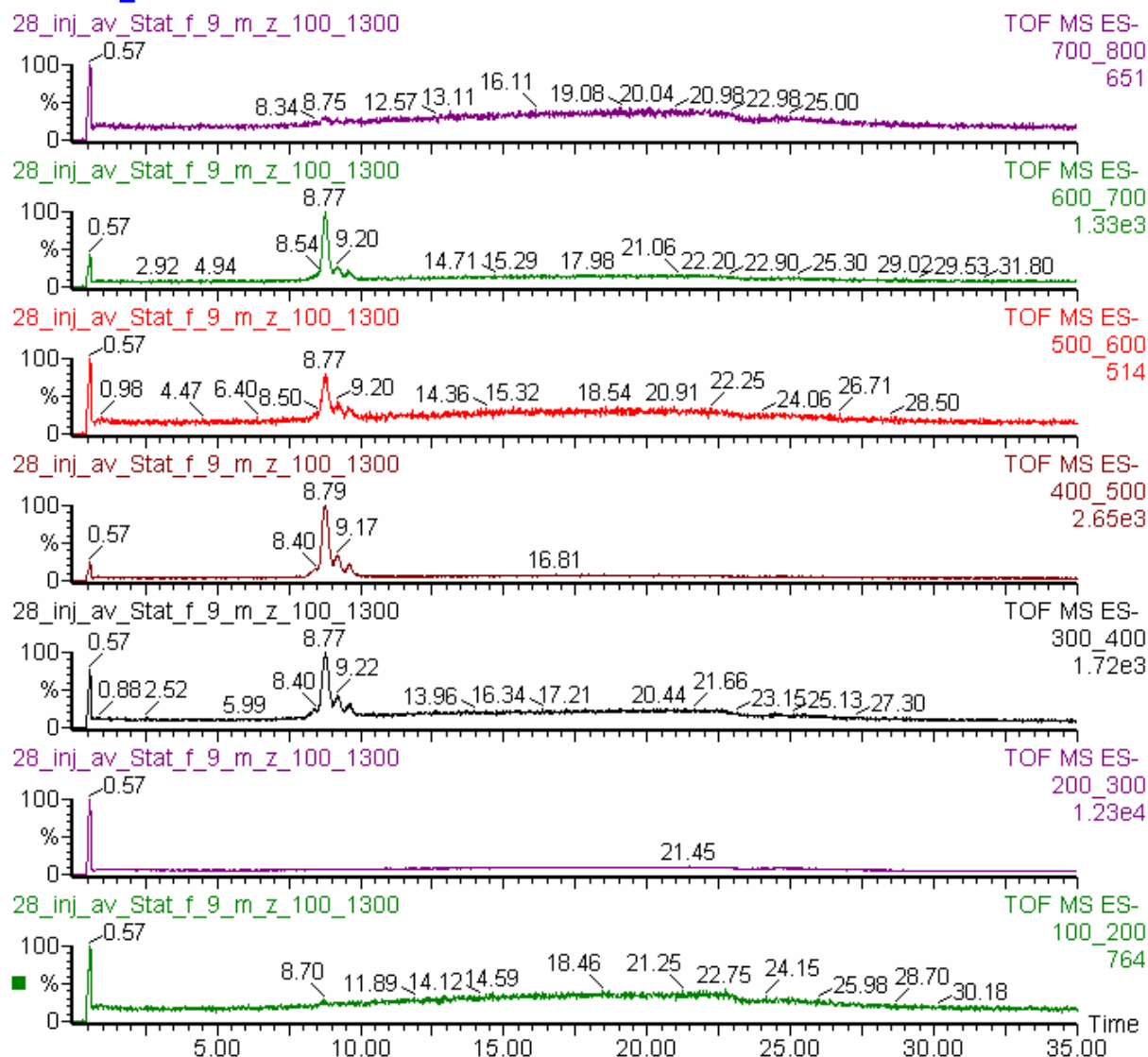


Figure 19:  $m/z$  range 700-800, 600-700, 500-600, 400-500, 300-400, 200-300 and 100-200 EIC chromatograms, other conditions as in Figure 15.

Figure 20 shows the TIC chromatogram of A1 polar. A1 polar was injected to see if the GPC fractionation was a necessary step in the ARN determination. A1 polar was completely dissolved in MeOH added 0.1 % TEA at the same concentration as before the removal of the toluene and isopropanol that Statoil had used to dissolve the A1 polar. As expected there are only small differences between Statoil f 9 from the GPC system and A1 Polar, since Statoil f 9 constitute the larger part of A1 polars heavier acids (ARN), in addition to the solvent. Figure 21 shows the  $m/z$  613-618 EIC chromatograms. The peaks from the three ARN isomers were easily detected, and the baseline noise was small. Figure 22 shows the mass spectra of the three ARN peaks in Figure 20 in chronological order. For the first peak, the triple charged ARN with  $m/z=$  409.7, and double charged ARN with  $m/z=$  614.7 dominated. There were almost no single charged ARN with  $m/z=$  1229.5. For the second peak, triple charged ARN with  $m/z=$  410.4, and

double charged ARN with  $m/z= 615.7$  dominated. The single charged ARN with  $m/z= 1231.5$  were not detected. For the third peak, triple charged ARN with  $m/z= 411.4$ , and double charged ARN with  $m/z= 616.7$  dominated. The single charged ARN with  $m/z= 1234.5$  were not detected.

In Figure 23 and Figure 24, the EIC chromatograms of the mass ranges  $m/z= 1200-1300$ , 1100-1200, 1000-1100, 900-1000, 800-900, 700-800, 600-700, 500-600, 400-500, 300-400, 200-300 and 100-200, from Figure 20 are shown. Light acids with  $m/z= 100-300$  are not found in the retention window of the three ARN peaks, nor with shorter retention time.

These results indicate that the MeOH extraction technique developed in this thesis are quite selective with regard to the ARN acid family, as there are no other hydrocarbons with the same retention as ARN, and there are no other ionic species in the chromatogram that causes ion suppression of the ARN acid family. These results also indicates that the analytical system with the Kromasil C 18 column and the mobile phase gradient as in Table 6 are able to separate the ARN acids from the pressure peak at the beginning of the chromatogram, it partially separates the ARN acids from each other and it is a stable system. A positive detection of ARN has also been made.

There are too many hydrocarbon constituents in a crude oil sample to inject it directly without any sample preparation. The detection limit of the ARN acids would not be as good as they are with sample preparation, as other components may elute at the same retention time as them. Ion suppression can also make detection of the ARN acids difficult, and precipitation in the analytical system of hydrocarbon constituents which are unsolvable in the mobile phase would cause flow problems.

Gradient\_230204\_etter\_onske\_fra\_Statoil

22\_inj\_Stat\_A\_1\_Polar\_m\_z\_100\_1300

TOF MS ES-  
TIC  
2.37e4

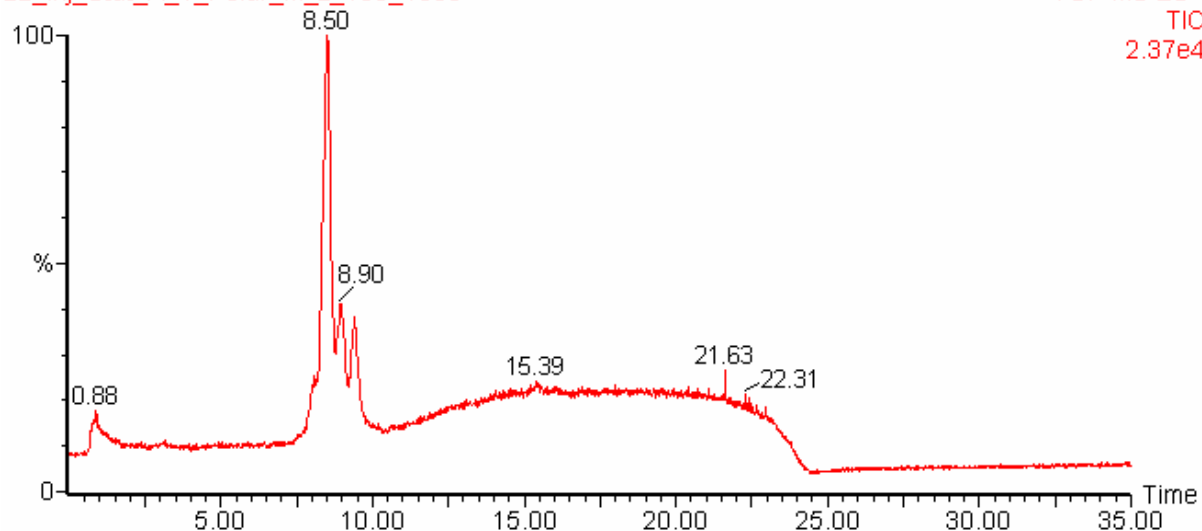


Figure 20: TIC chromatogram of A1 polar from Statoil, dissolved in MeOH with 0.1 % TEA, using the 0.32x100mm kromasil C18 column, with negative electrospray MS detection. The injection volume was 500 nl. The MeOH/H<sub>2</sub>O gradient as described in Table 6 was used with a flow rate of 5 µl/min.

Gradient\_230204\_etter\_onske\_fra\_Statoil

22\_inj\_Stat\_A\_1\_Polar\_m\_z\_100\_1300

TOF MS ES-  
613\_618  
6.14e3

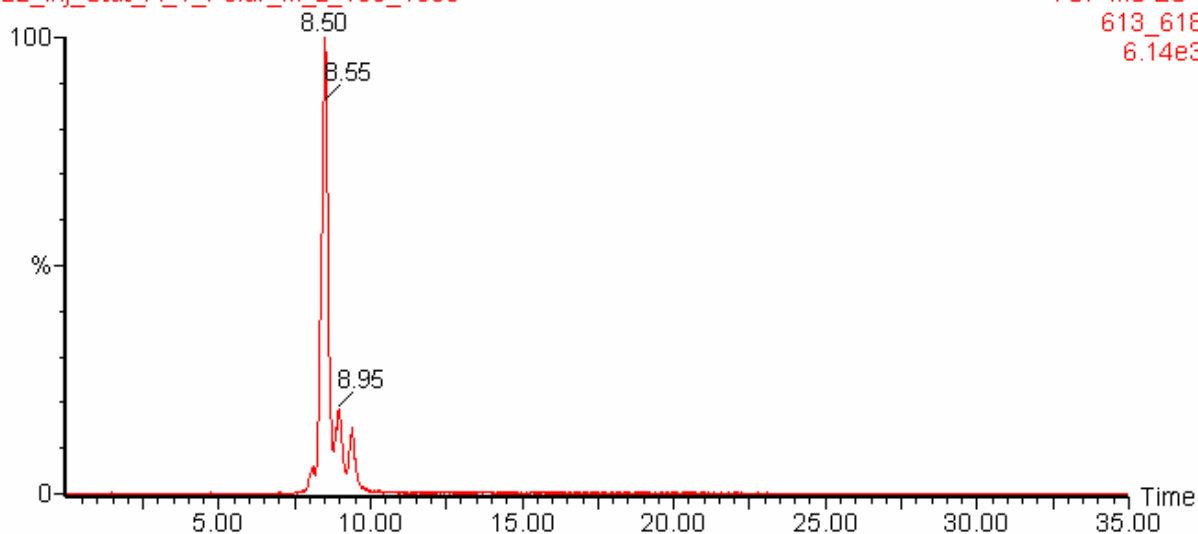


Figure 21: *m/z* range 613-618 EIC chromatogram, other conditions as in Figure 20.

### Gradient\_230204\_etter\_onske\_fra\_Statoil

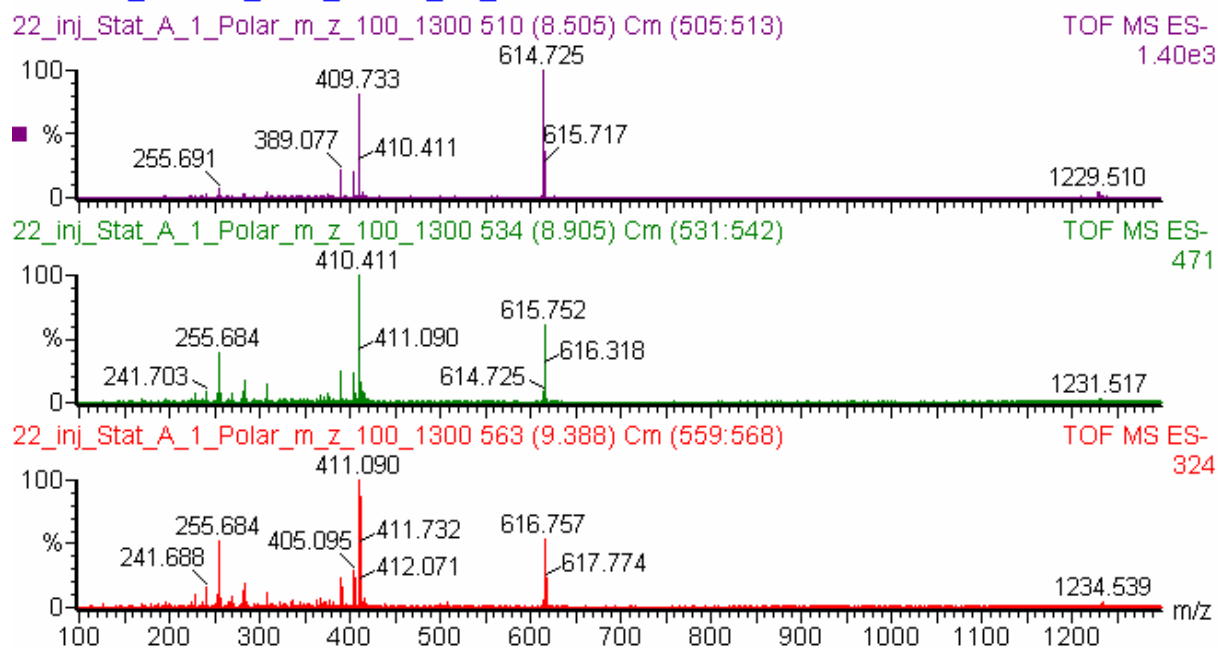


Figure 22: Spectrum from the three peaks (in chronological order) from Figure 20.

# Gradient\_230204\_etter\_onske\_fra\_Statoil

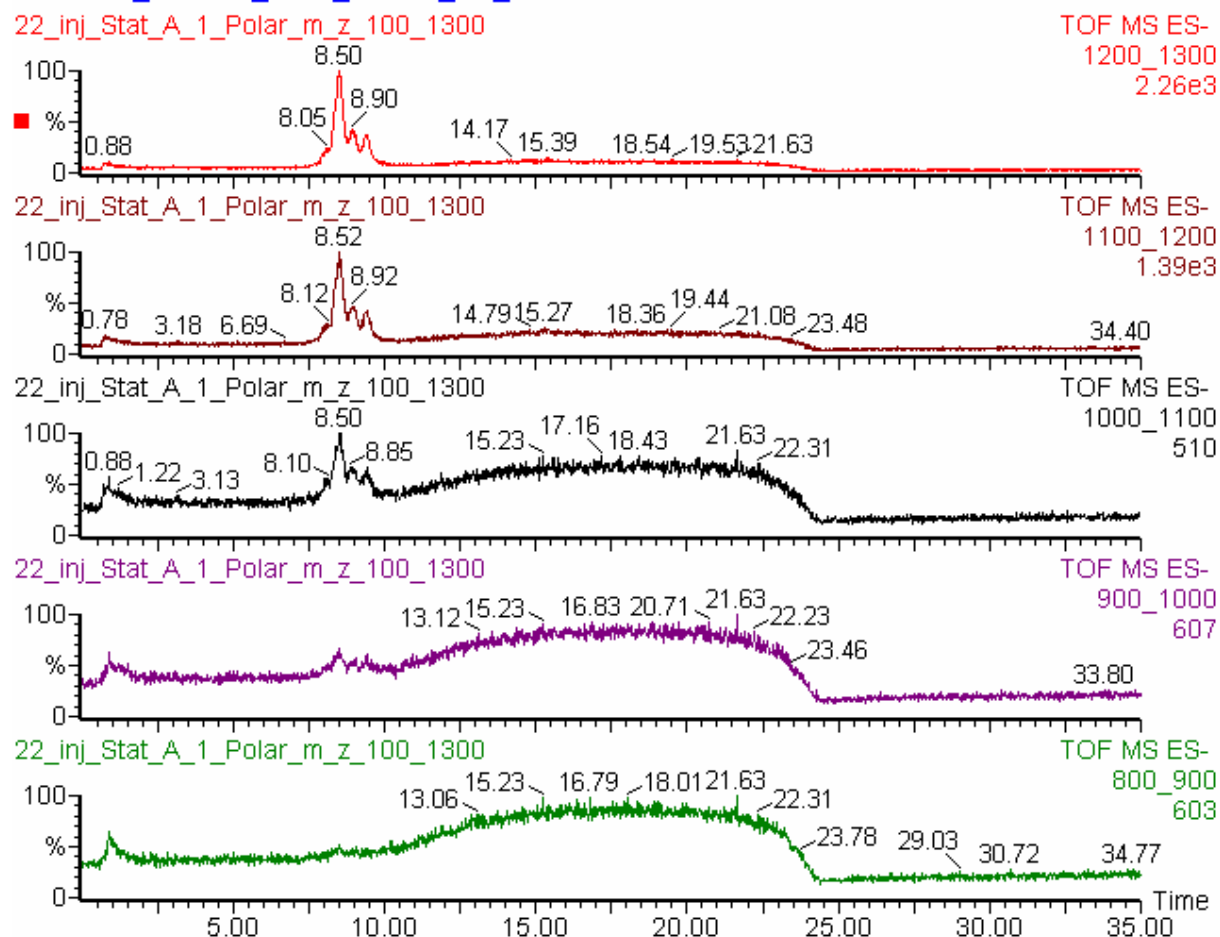


Figure 23:  $m/z$  range 1200-1300, 1100-1200, 1000-1100, 900-1000 and 800-900 EIC chromatograms, other conditions as in Figure 20.

## Gradient\_230204\_etter\_onske\_fra\_Statoil

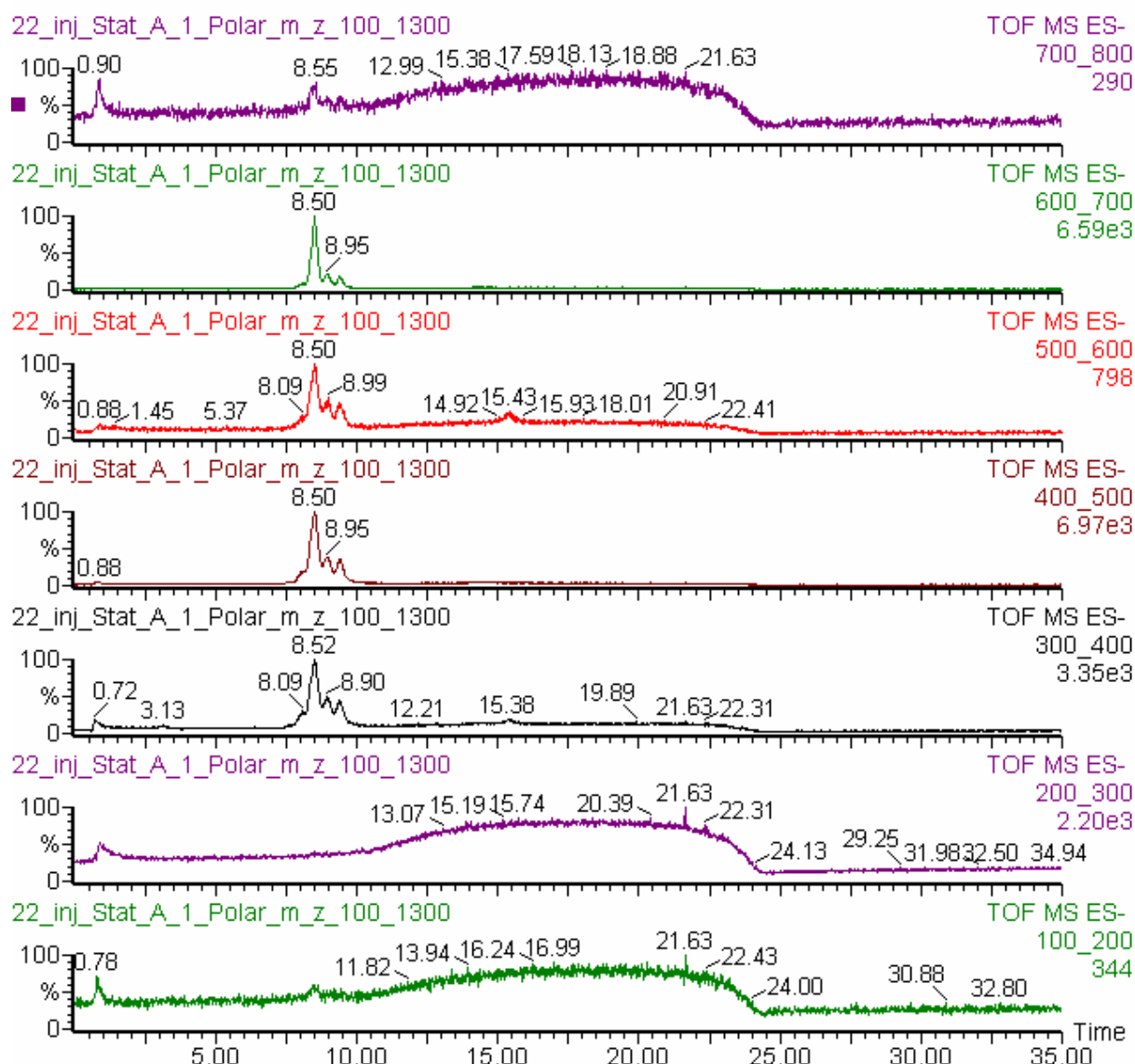


Figure 24:  $m/z$  range 700-800, 600-700, 500-600, 400-500, 300-400, 200-300 and 100-200 EIC chromatograms, other conditions as in Figure 20.

### 3.6 Extraction of ARN from A1 polar spiked crude oil

Four different solvents were tested for use in the extraction of ARN from spiked crude oil, these were MeOH, AcN, acetone and toluene, and all of these were tested both with and without TEA (0.1 %). The MeOH with 0.1 % TEA was also tested both with and without a drying agent (molecularsieb), this was done because the ARN acids precipitates in water, and the MeOH used contained 0.005 % water. No difference was detected between the ordinary MeOH and the dried MeOH, so the ordinary MeOH was used in the further work. The solvent phase was determined with direct infusion TOF MS, and the MeOH with 0.1 % TEA gave the best spectra with regard to the ARN acid family. The other solvents extracted out too many other hydrocarbon

components which again gave ion suppression of the ARN acids, or gave poorer intensities in the MS spectra, even with TEA.

To make sure that all of the ARN acids detected in the  $\mu$ LC MS system comes from the A1 polar used in the spiking procedure, 20 ml of A-22 oil was extracted using MeOH with 0.1 % TEA, to see if any ARN was present in this oil before spiking. No ARN was observed, which confirms that when 5 (or 10) ml A-22 oil is spiked and extracted (see Table 4), all of the ARN acids found in the MS spectra come from the A1 polar, and not from the A-22 oil.

Statoil f 9 was considered used instead of A1 polar in the spiking of A-22 oil, because this was a cleaner sample with a higher percentage of the ARN acid family compared to the other carboxylic acids in A1 polar. But as there is some dilution of the sample in the GPC column, quantitative determination would be difficult to obtain.

### 3.7 Determination of ARN in spiked crude oil

Figure 25 shows the TIC chromatogram from a MeOH extract of spiked crude oil (Heidrun-oil, 030109007.01., spiked with A1 polar). This MeOH extraction was performed because ARN was found to be easily dissolved in MeOH with 0.1 % TEA, (A1 polar and Statoil f 9 were also soluble in MeOH, with 0.1 % TEA).

Figure 26, shows the  $m/z$  613-618 EIC chromatograms of the MeOH extract. The peaks from the three ARN isomers were easily detectable, and the baseline noise was small. There is a difference in relative intensity between the three ARN peaks, compared to A1 polar and Statoil f 9 (Figure 16 and Figure 21). The reason for this most probably was differences made from the methanol extraction procedure.

Figure 27 shows the mass spectra of the three ARN peaks in Figure 25 in chronological order. For the first peak, the triple charged ARN with  $m/z= 409.7$ , and double charged ARN with  $m/z= 614.7$  dominated. There were almost no single charged ARN with  $m/z= 1230.4$ . For the second peak, triple charged ARN with  $m/z= 410.4$ , and double charged ARN with  $m/z= 616.2$  dominated. The single charged ARN with  $m/z= 1231.5$  were not detected. For the third peak, triple charged ARN with  $m/z= 411.4$ , and double charged ARN with  $m/z= 616.7$  dominated. The single charged ARN with  $m/z= 1234.5$  were not detected.

In Figure 28 and Figure 29, the EIC chromatograms of the mass ranges  $m/z=1200-1300$ , 1100-1200, 1000-1100, 900-1000, 800-900, 700-800, 600-700, 500-600, 400-500, 300-400, 200-300 and 100-200, from Figure 25 are shown. Light acids with  $m/z= 100-300$  were neither observed within the retention time window of the three ARN acids, nor at shorter retention time.

There were no indications of other hydrocarbons in the MeOH phase either, which indicates that other hydrocarbons are not well soluble in MeOH. This indicates that ARN can be extracted from crude oils using MeOH with 0.1 % TEA. However, more work is needed to be able to determine whether this extraction method can be used quantitatively.

The MeOH extraction step was performed on the A-22-oil (030123002 A-22-oil Heidrun). When 20 ml A-22-oil in 20 ml MeOH with 0.1 % TEA was used, no indication of ARN in the MeOH extract was found. There were no indications of carryover of ARN from previous injections either (see Figure 30 to Figure 33).

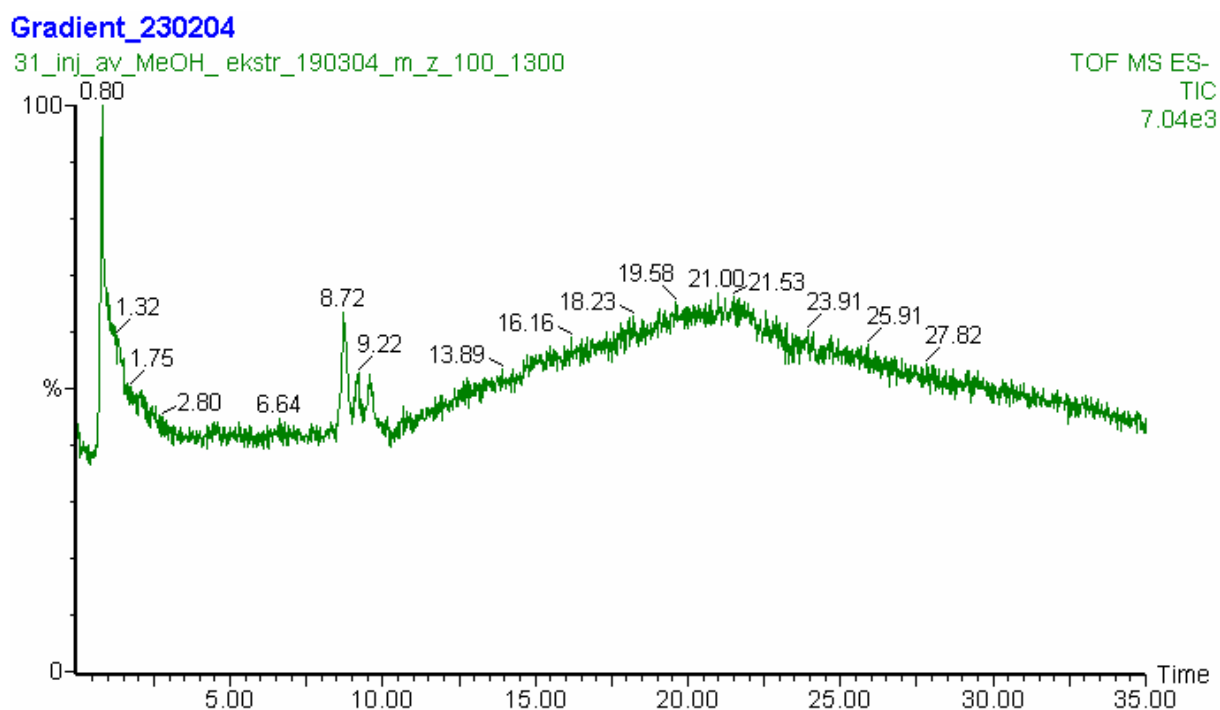


Figure 25: TIC chromatogram of the MeOH (with 0.1 % TEA) extract of A1 polar spiked crude oil, using the 0.32x100mm Kromasil C18 column, with negative electrospray MS detection. The injection volume was 500 nl. MeOH/H<sub>2</sub>O gradient as described in Table 6 was used with a flow rate of 5 µl/min.



### Gradient\_230204

31\_inj\_av\_MeOH\_ekstr\_190304\_m\_z\_100\_1300

TOF MS ES-  
613\_618  
175

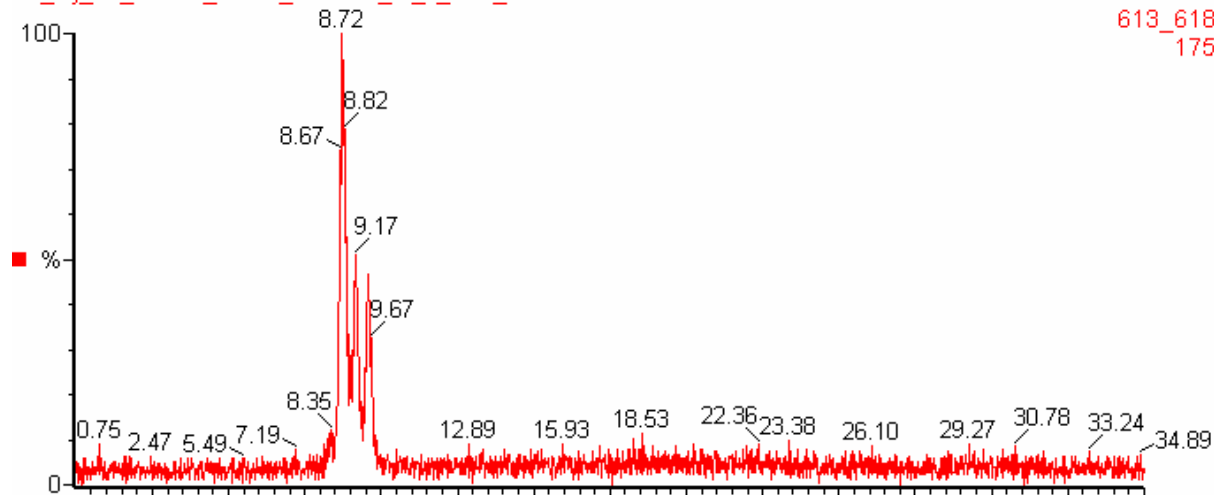


Figure 26:  $m/z$  range 613-618 EIC chromatogram, other conditions as in Figure 25.

### Gradient\_230204

31\_inj\_av\_MeOH\_ekstr\_190304\_m\_z\_100\_1300 523 (8.721) Cm (518:531)

TOF MS ES-  
207



31\_inj\_av\_MeOH\_ekstr\_190304\_m\_z\_100\_1300 553 (9.222) Cm (543:555)

TOF MS ES-  
216



31\_inj\_av\_MeOH\_ekstr\_190304\_m\_z\_100\_1300 574 (9.572) Cm (570:581)

TOF MS ES-  
200

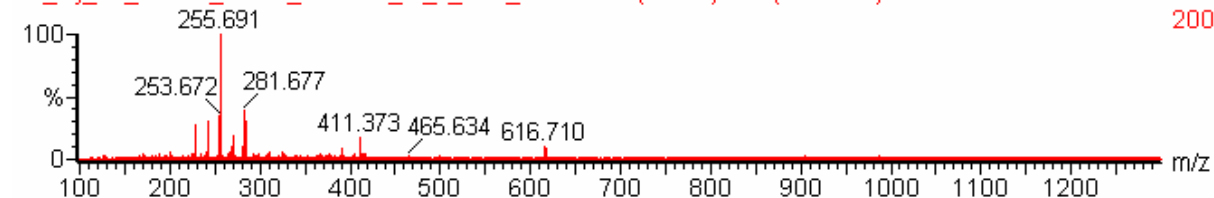


Figure 27: Mass spectra from the three peaks (in chronological order) from Figure 25.

## Gradient\_230204

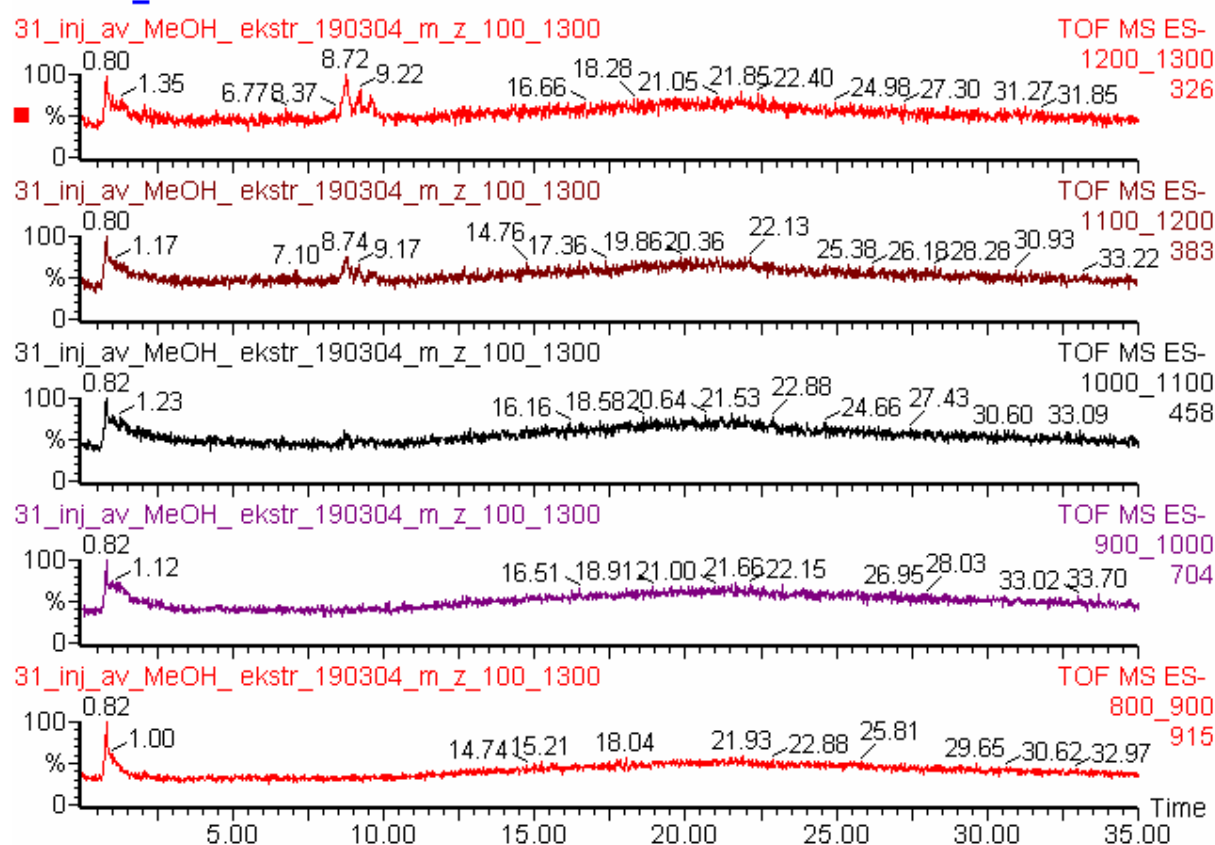


Figure 28:  $m/z$  range 1200-1300, 1100-1200, 1000-1100, 900-1000 and 800-900 EIC chromatograms, other conditions as in Figure 25.

Gradient\_230204

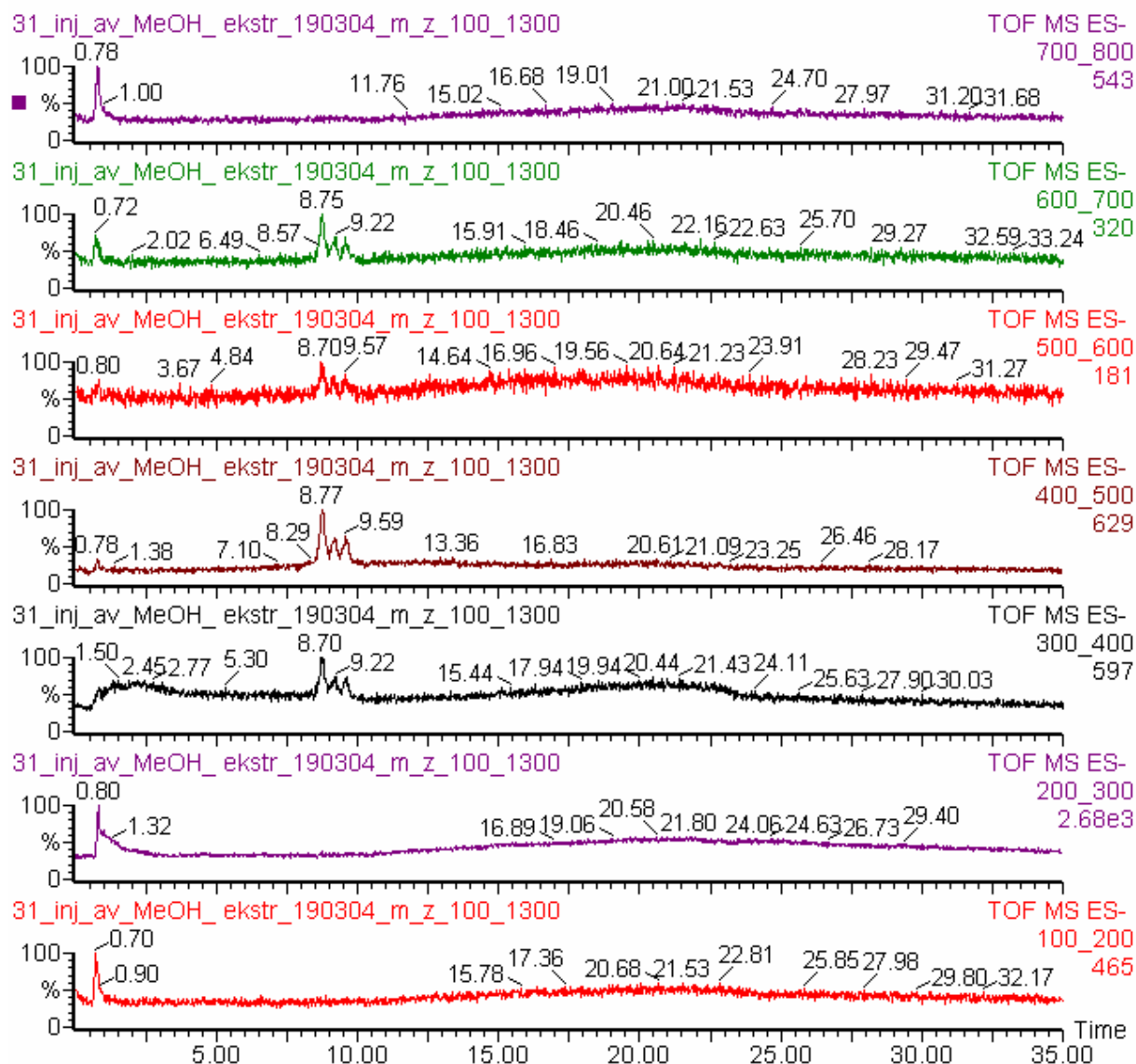


Figure 29: *m/z* range 700-800, 600-700, 500-600, 400-500, 300-400, 200-300 and 100-200 EIC chromatograms, other conditions as in Figure 25.

### Gradient\_230204

34\_inj\_av\_A22\_MeOH\_ekstr\_190304\_m\_z\_100\_1300

TOF MS ES-  
TIC  
7.24e3

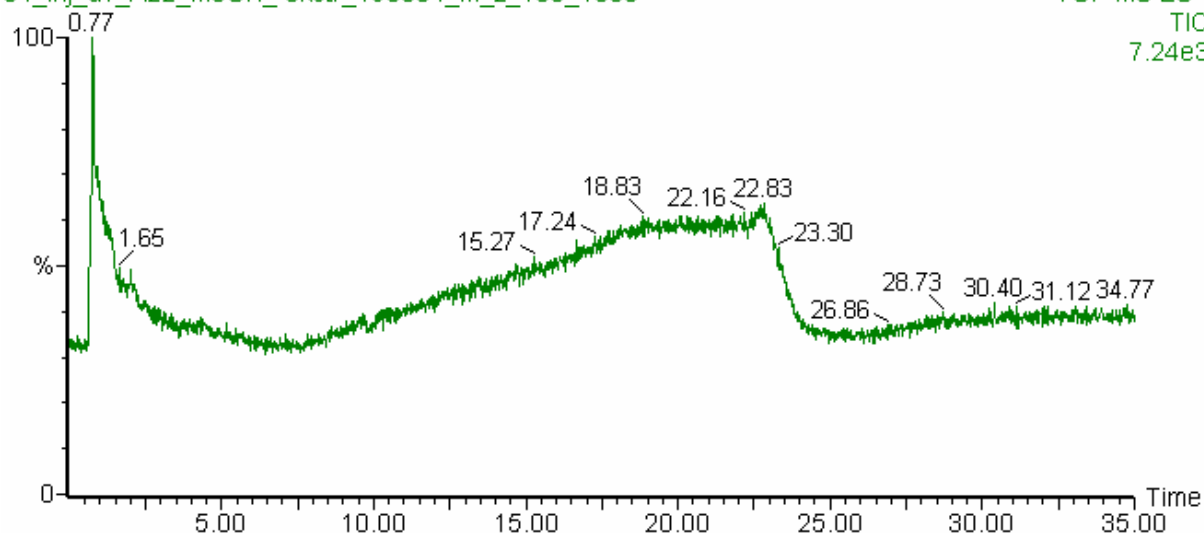


Figure 30: TIC chromatogram of the MeOH extract of unspiked A22 oil, using the 0.32x100mm Kromasil C18 column, with negative electrospray MS detection. The injection volume was 500 nl. The MeOH/H<sub>2</sub>O gradient as described in Table 6 was used with a flow rate of 5 µl/min.

### Gradient\_230204

34\_inj\_av\_A22\_MeOH\_ekstr\_190304\_m\_z\_100\_1300

TOF MS ES-  
613\_61  
1

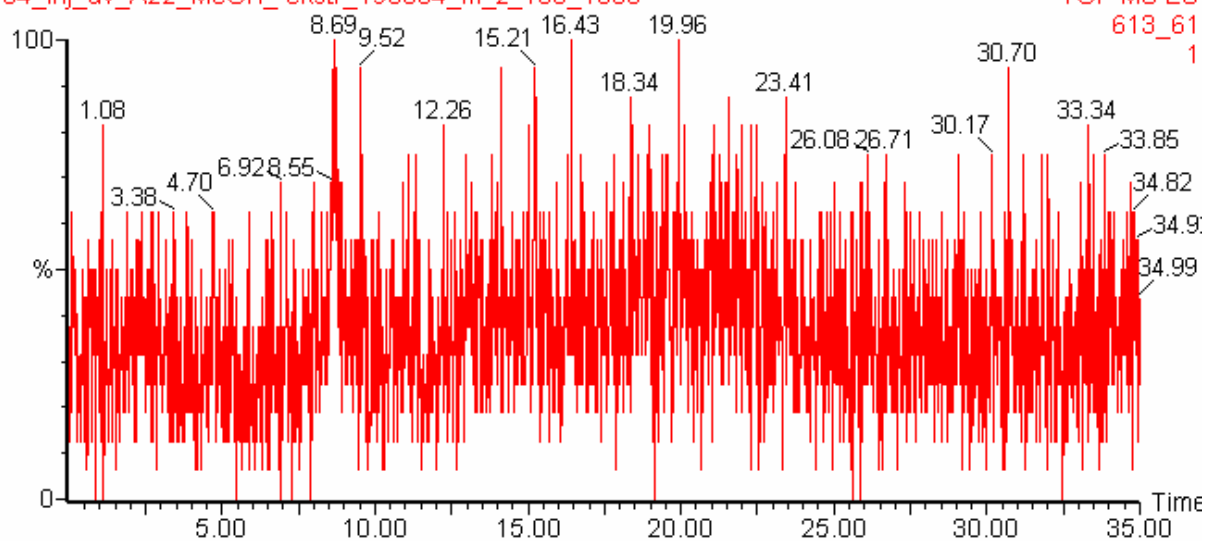


Figure 31: *m/z* range 613-618 EIC chromatogram, other conditions as in Figure 30.

Gradient\_230204

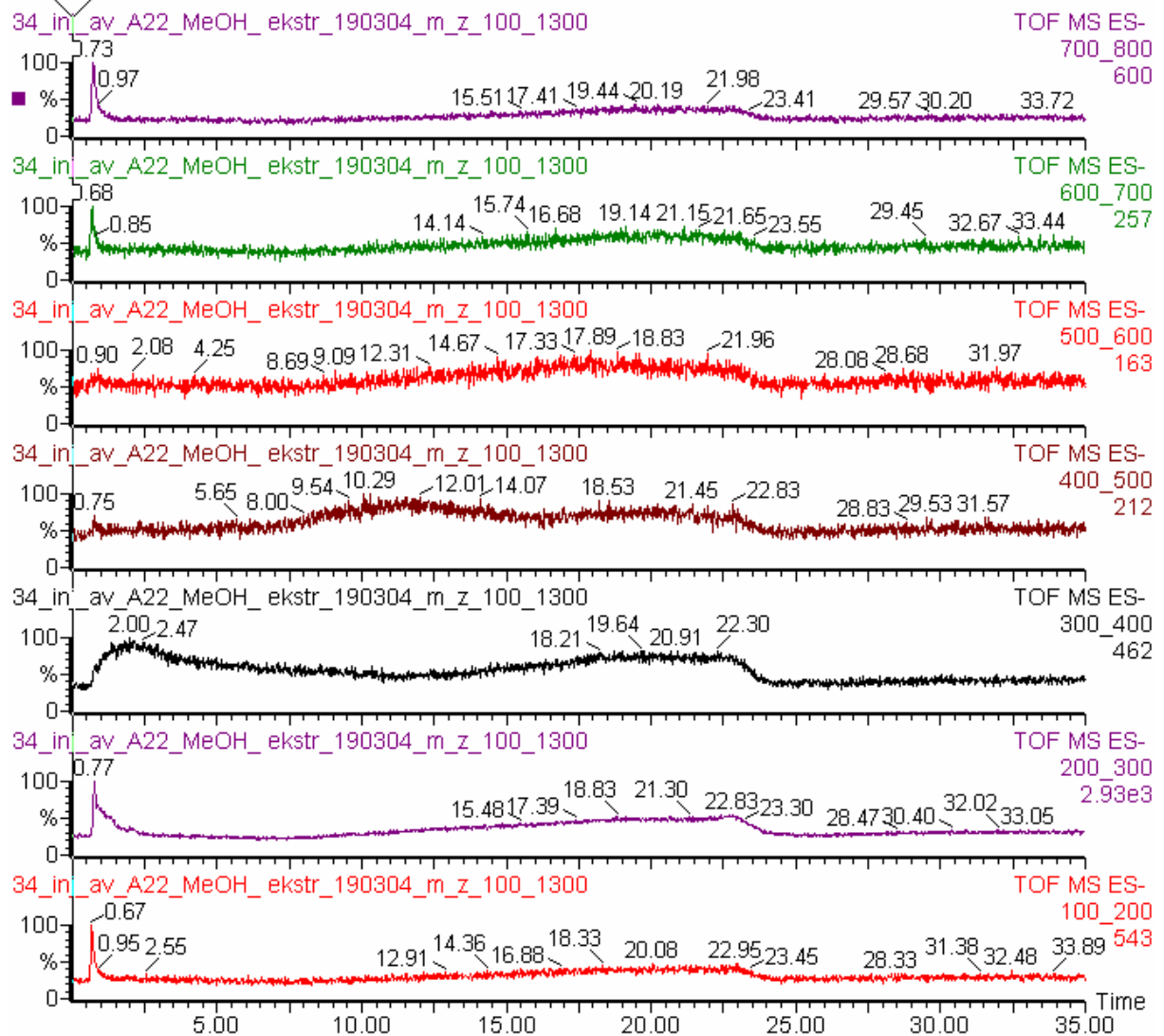


Figure 32: *m/z* range 700-800, 600-700, 500-600, 400-500, 300-400, 200-300 and 100-200 EIC chromatograms, other conditions as in Figure 30.

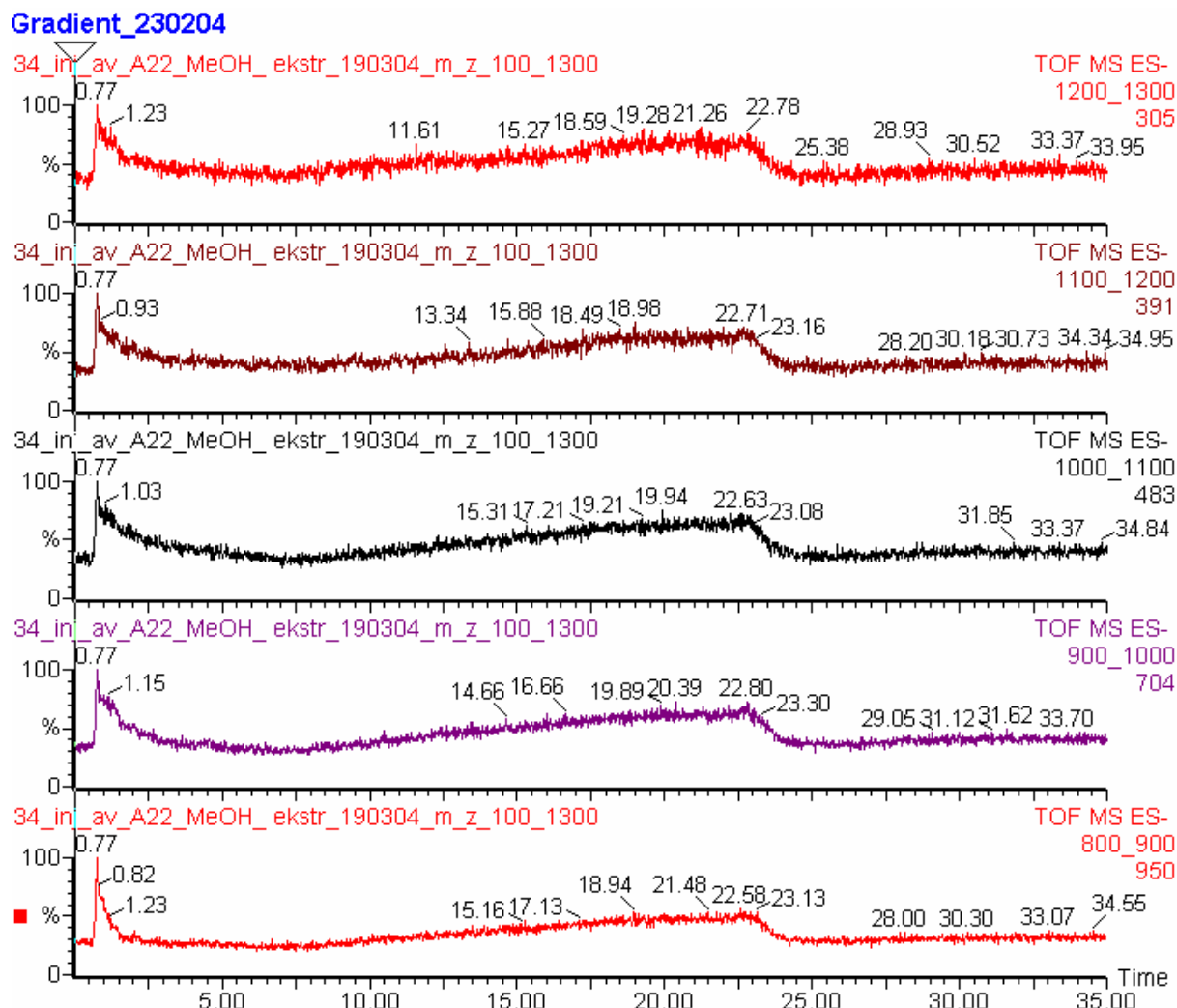


Figure 33:  $m/z$  1200-1300, 1100-1200, 1000-1100, 900-1000 and 800-900 EIC chromatograms, other conditions as in Figure 30.

### 3.8 Quantitative determination of ARN using MeOH extraction and $\mu$ LC MS

The concentration of ARN in the Heidrun field has been measured to be 2 ppm [67]. Since ARN has qualitatively been found in spiked crude oil using  $\mu$ LC MS in combination with MeOH extraction, the possibility for using this method for quantitative determination of ARN in crude oil was explored. The detection limit of the method was investigated by spiking ARN free A22 oil with the A1 polar which was received from Statoil.

The A-22 oil was analyzed to see if it was completely free of ARN before spiking was performed. This was done by extracting and analyzing 20 ml of the A-22 oil using the same method as for the spiked samples. No ARN signal significantly different from the noise was

found in these analyses, as seen in Figure 34 and Figure 35. Blank injections were also made to assure no carryover was observed.

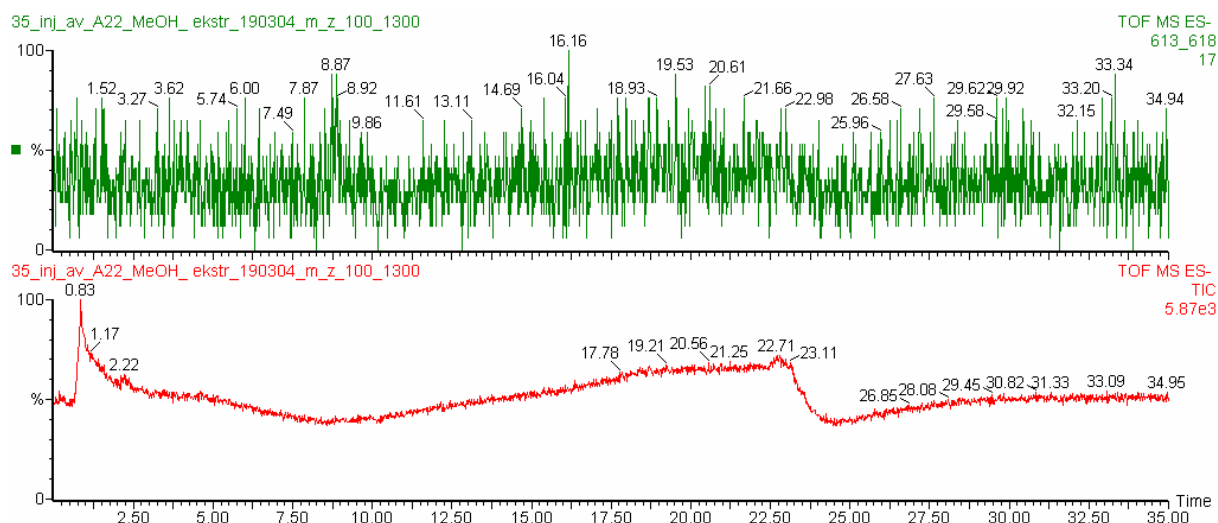


Figure 34: One  $m/z$  range 613-618 EIC chromatogram and one TIC chromatogram of MeOH extracted A-22 oil (20 ml) analyzed by the  $\mu$ LC MS system, using the 0.32x100mm Kromasil C18 column, with negative electrospray MS detection. The injection volume was 500 nl. The MeOH/H<sub>2</sub>O gradient as described in Table 6 was used with a flow rate of 5  $\mu$ l/min.

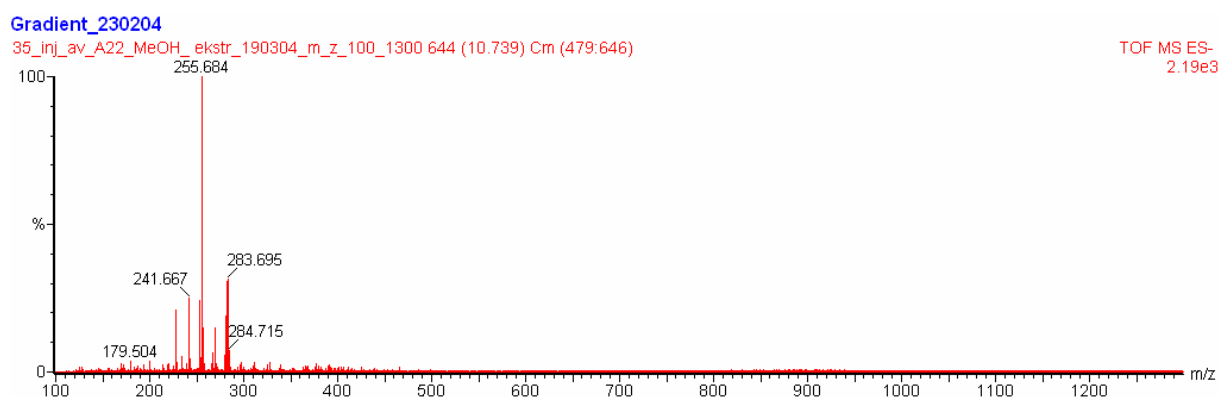


Figure 35: Mass spectrum of the retention time window (7.5-8.3 min) where an ARN peak (in Figure 34) would have been if it was present in the A-22 oil, no ARN is detected.

Six samples of A-22 oil were spiked with a decreasing amount of A1 Polar, containing the ARN concentrations shown in Table 4, and the spiked A-22 oils were MeOH extracted. Figure 36 shows the  $m/z$  613-618 EIC chromatogram and the TIC chromatogram of spiked and MeOH extracted A-22 oil analyzed by the  $\mu$ LC MS system. This oil sample was spiked with 5006 ppm ARN. The peaks from the three ARN isomers were easily detectable, and the baseline noise was insignificant small.

Figure 37 shows the mass spectra of the retention time window in which the three ARN peaks eluted (Figure 36). The triply charged ARN at  $m/z= 409.7$ , at  $m/z= 410.4$ , and at  $m/z= 411.1$ , and double charged ARN with  $m/z= 614.6$ , at  $m/z= 615.6$ , and with  $m/z= 617.2$  were easily detectable. There were observed some single charged ARN with  $m/z$  in the range of 1230 - 1234.

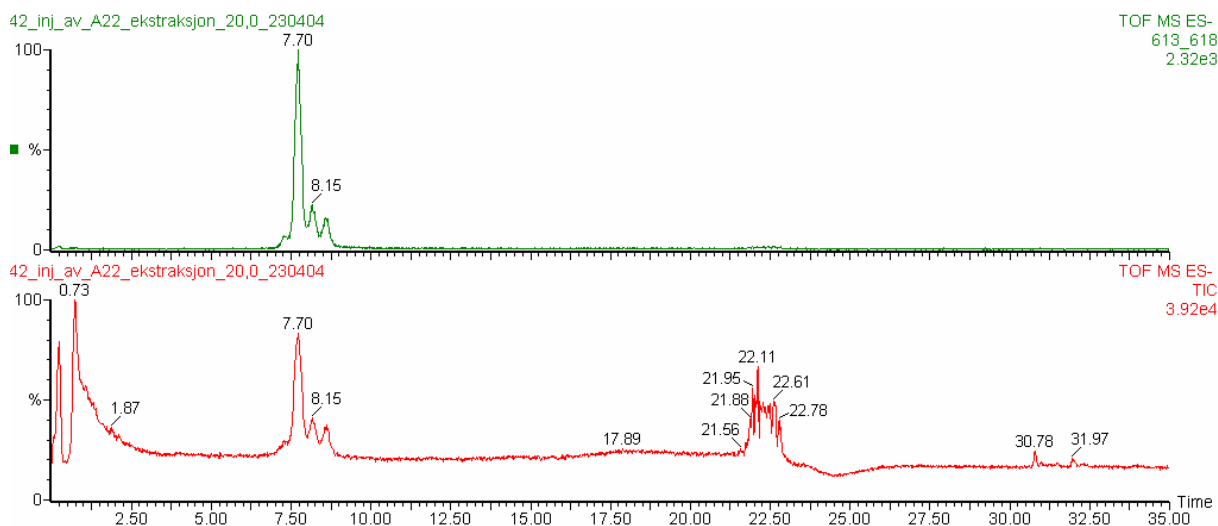


Figure 36: One  $m/z$  range 613-618 EIC chromatogram and one TIC chromatogram of A-22 oil spiked with 5006 ppm ARN, MeOH extracted and analyzed by the  $\mu$ LC MS system, using the 0.32x100mm Kromasil C18 column, with negative electrospray MS detection. The injection volume was 500 nl. The MeOH/H<sub>2</sub>O gradient as described in Table 6 was used with a flow rate of 5  $\mu$ l/min.

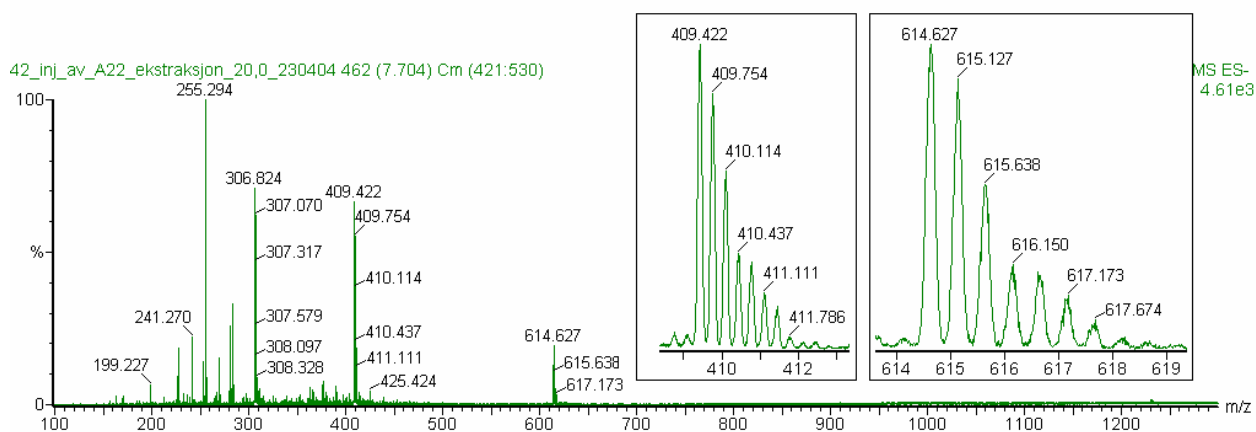


Figure 37: Mass spectrum of the retention time window where the three ARN peaks are in the chromatogram in Figure 36.

Figure 38 shows the  $m/z$  613-618 EIC chromatogram and the TIC chromatogram of 2284 ppm spiked and MeOH fractionated A-22 oil in the  $\mu$ LC MS system. The peaks from the three



ARN isomers were easily detectable, and the baseline noise was insignificant small. Figure 39 shows the mass spectra of the retention time window in which the three ARN peaks eluted (Figure 38).

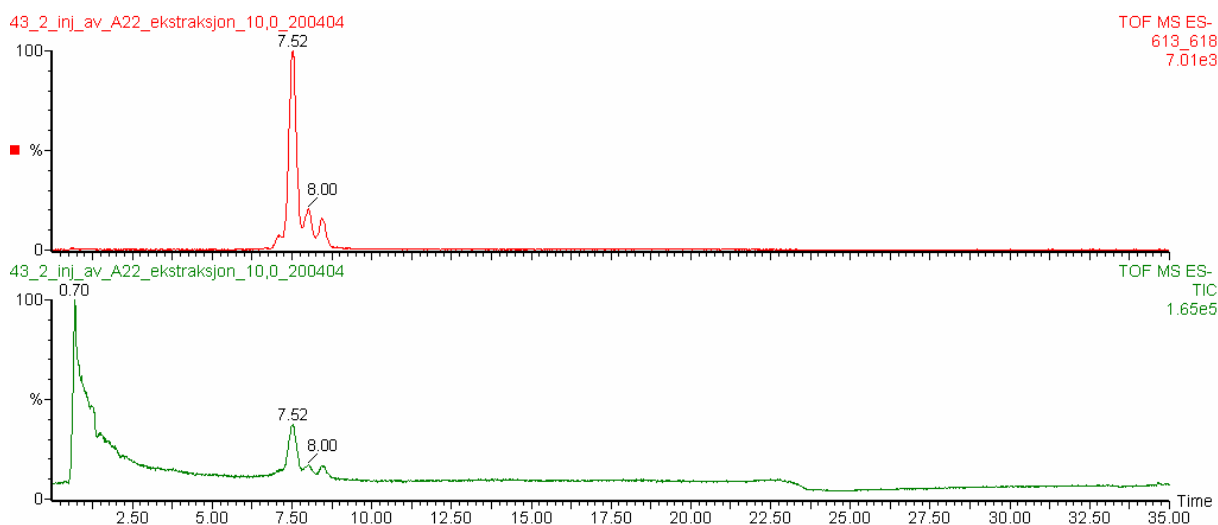


Figure 38: One  $m/z$  range 613-618 EIC chromatogram and one TIC chromatogram of A-22 oil spiked with 2284 ppm ARN, MeOH extracted and analyzed by the  $\mu$ LC MS system, using the 0.32x100mm Kromasil C18 column, with negative electrospray MS detection. The injection volume was 500 nl. The MeOH/H<sub>2</sub>O gradient as described in Table 6 was used with a flow rate of 5  $\mu$ l/min.

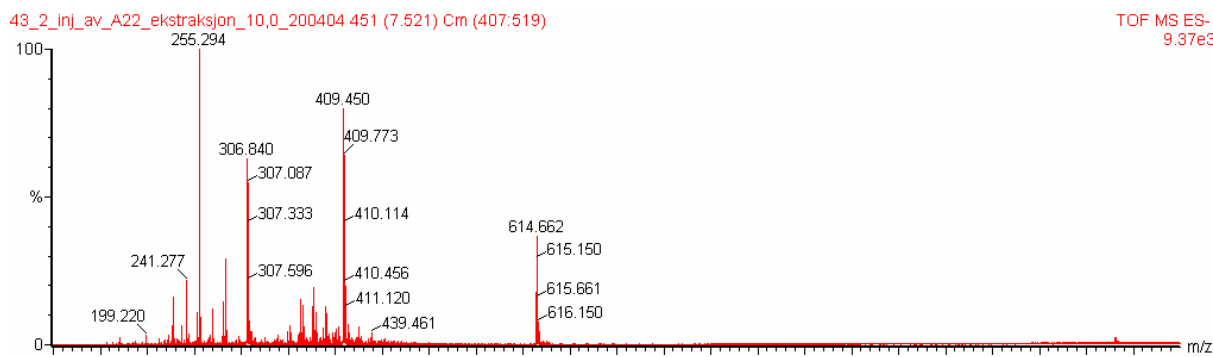


Figure 39: Mass spectrum of the retention time window where the three ARN peaks are in the chromatogram in Figure 38.

Figure 40 shows the  $m/z$  613-618 EIC chromatogram and the TIC chromatogram of 238.5 ppm spiked and MeOH fractionated A-22 oil in the  $\mu$ LC MS system. The peaks from the three ARN isomers were easily detectable in the  $m/z$  613-618 EIC chromatogram, the baseline noise was small.

Figure 41 shows the mass spectra of the retention time window in which the three ARN peaks eluted (Figure 40). The triple charged ARN with  $m/z= 409-411$  range and some double charged ARN with  $m/z= 614-615$  range were observed.

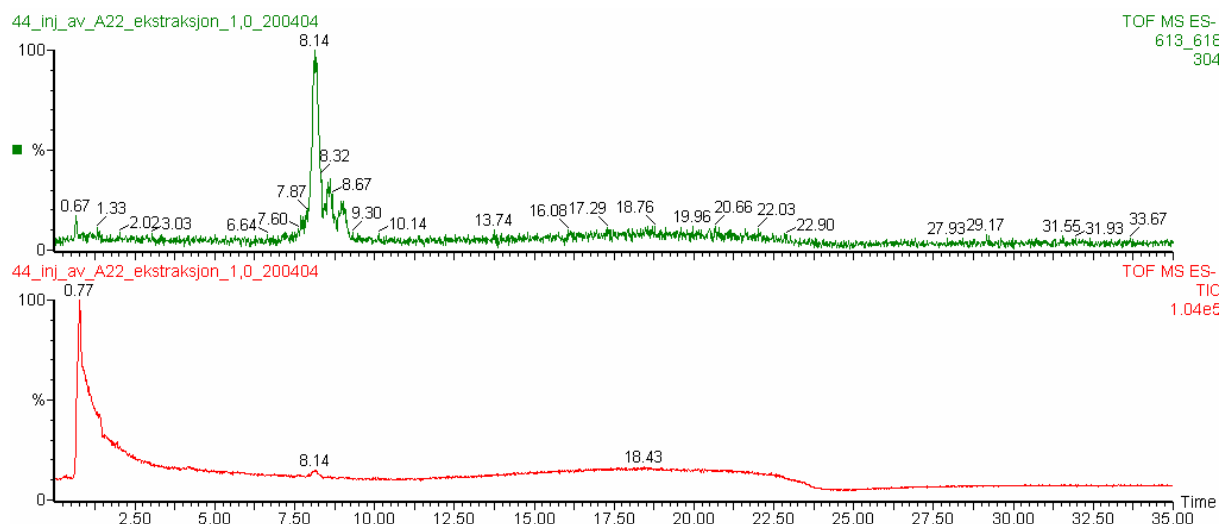


Figure 40: One  $m/z$  range 613-618 EIC chromatogram and one TIC chromatogram of A-22 oil spiked with 238.5 ppm ARN, MeOH extracted and analyzed by the  $\mu$ LC MS system, using the 0.32x100mm Kromasil C18 column, with negative electrospray MS detection. The injection volume was 500 nl. The MeOH/H<sub>2</sub>O gradient as described in Table 6 was used with a flow rate of 5  $\mu$ l/min.

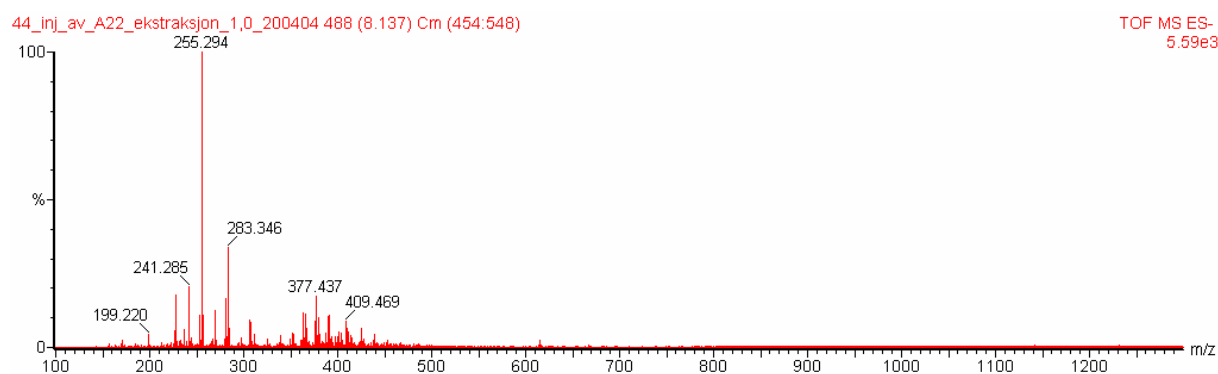


Figure 41: Mass spectrum of the retention time window where the three ARN peaks are in the chromatogram in Figure 40.

Figure 42 shows the  $m/z$  613-618 EIC chromatogram and the TIC chromatogram of 124.5 ppm spiked and MeOH fractionated A-22 oil in the  $\mu$ LC MS system. The peaks from the three ARN isomers were easily detectable in the  $m/z$  613-618 EIC chromatogram, the baseline noise was relatively small.

Figure 43 shows the mass spectra of the retention time window in which the three ARN peaks eluted (Figure 42).

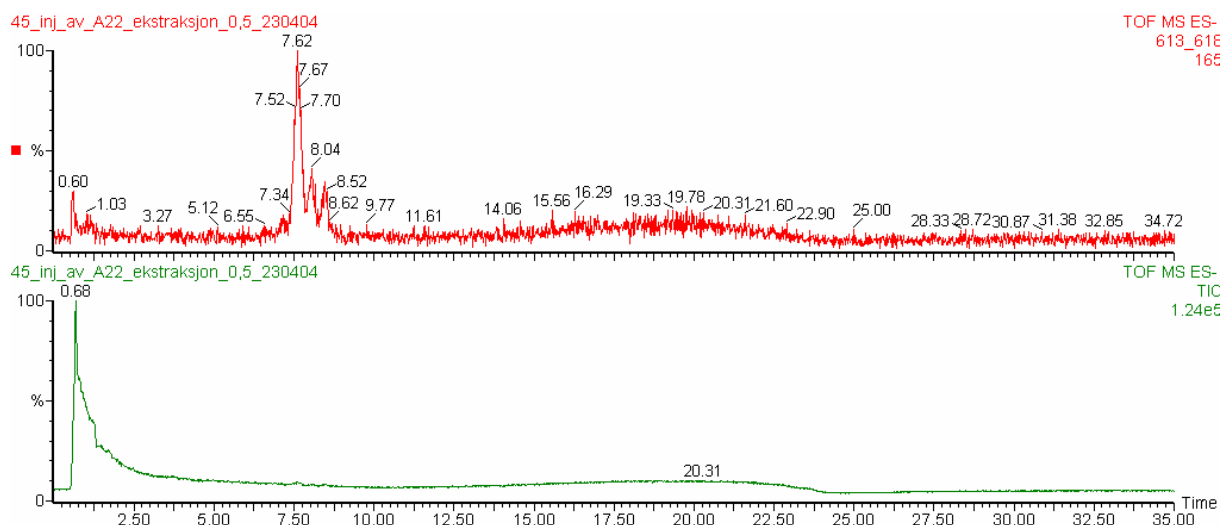


Figure 42: One  $m/z$  range 613-618 EIC chromatogram and one TIC chromatogram of A-22 oil spiked with 124.5 ppm ARN, MeOH extracted and analyzed by the  $\mu$ LC MS system, using the 0.32x100mm Kromasil C18 column, with negative electrospray MS detection. The injection volume was 500 nl. The MeOH/H<sub>2</sub>O gradient as described in Table 6 was used with a flow rate of 5  $\mu$ l/min.

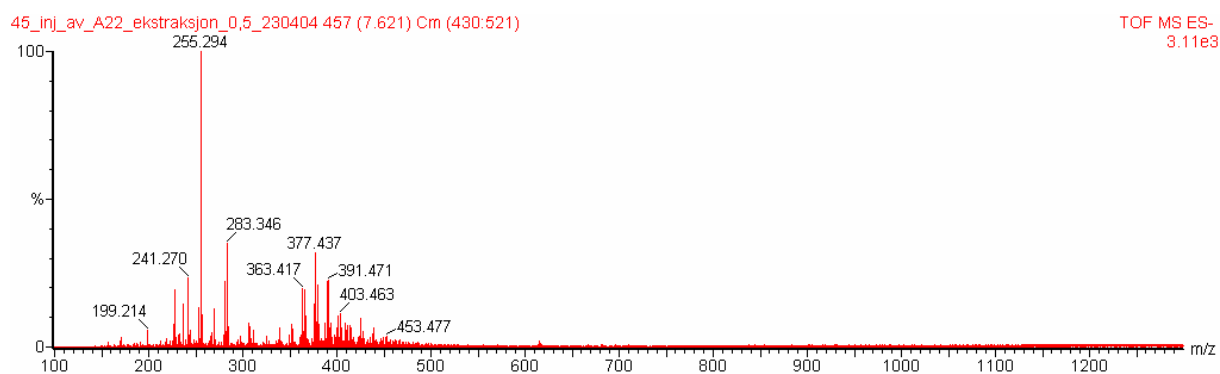


Figure 43: Mass spectrum of the retention time window where the three ARN peaks are in the chromatogram in Figure 42.

Figure 44 shows the  $m/z$  613-618 EIC chromatogram and the TIC chromatogram of 17.80 ppm spiked and MeOH fractionated A-22 oil in the  $\mu$ LC MS system. The peaks from the three ARN isomers were easily detectable in the  $m/z$  613-618 EIC chromatogram, the baseline noise was noticeable.

Figure 45 shows the mass spectra of the retention time window in which the three ARN peaks eluted (Figure 44).

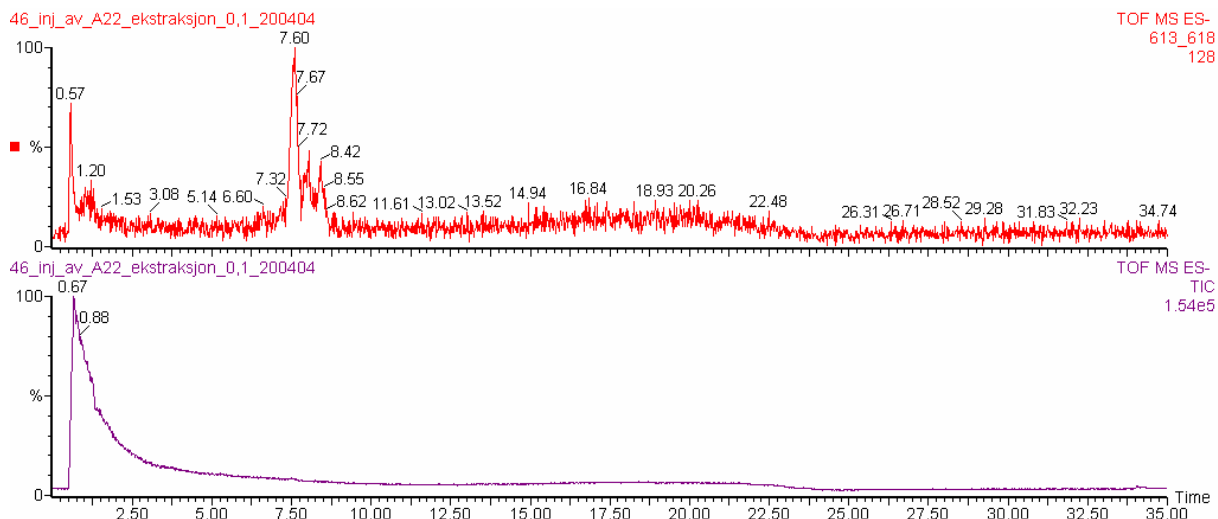


Figure 44: One  $m/z$  range 613-618 EIC chromatogram and one TIC chromatogram of A-22 oil spiked with 17.80 ppm ARN, MeOH extracted and analyzed by the  $\mu$ LC MS system, using the 0.32x100mm Kromasil C18 column, with negative electrospray MS detection. The injection volume was 500 nl. The MeOH/H<sub>2</sub>O gradient as described in Table 6 was used with a flow rate of 5  $\mu$ l/min.

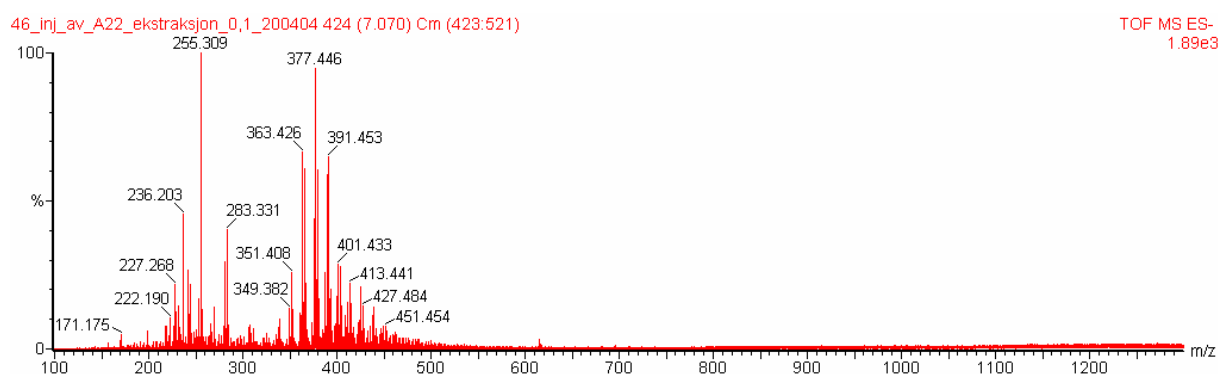


Figure 45: Mass spectrum of the retention time window where the three ARN peaks are in the chromatogram in Figure 44.

Figure 46 shows the  $m/z$  613-618 EIC chromatogram and the TIC chromatogram of 4.36 ppm spiked and MeOH fractionated A-22 oil in the  $\mu$ LC MS system. The peaks from the three ARN isomers were easily detectable in the  $m/z$  613-618 EIC chromatogram, there was some baseline noise.

Figure 47 shows the mass spectra of the retention time window in which the three ARN peaks eluted (Figure 46).

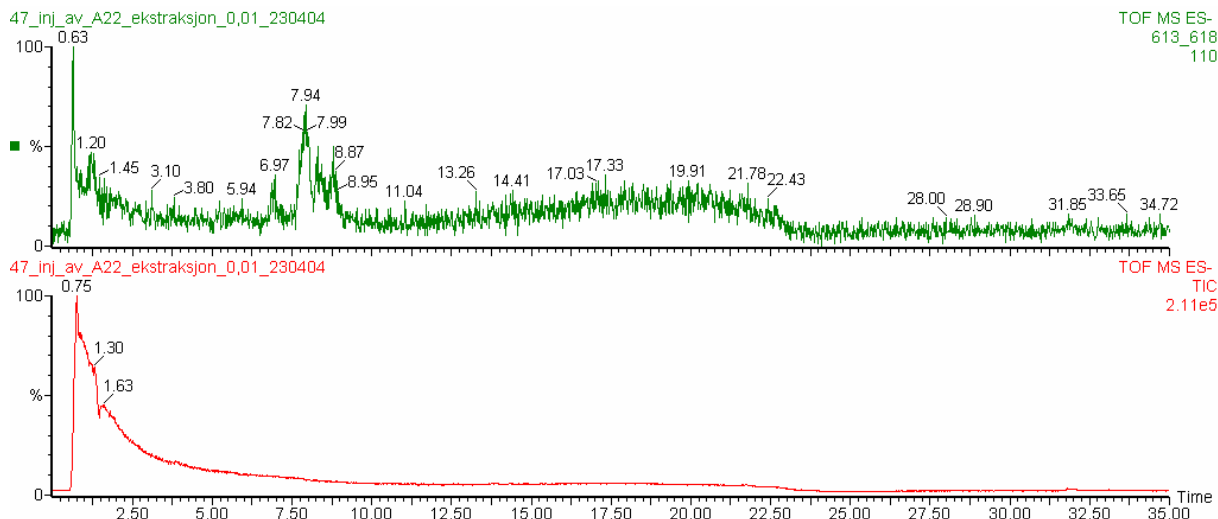


Figure 46: One  $m/z$  range 613-618 EIC chromatogram and one TIC chromatogram of A-22 oil spiked with 4.36 ppm ARN, MeOH extracted and analyzed by the  $\mu$ LC MS system, using the 0.32x100mm Kromasil C18 column, with negative electrospray MS detection. The injection volume was 500 nl. The MeOH/H<sub>2</sub>O gradient as described in Table 6 was used with a flow rate of 5  $\mu$ l/min.

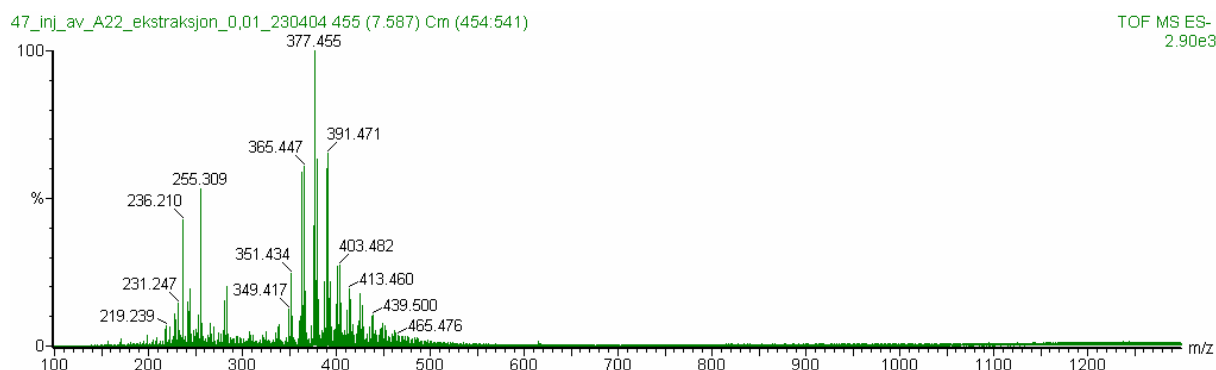


Figure 47: Mass spectrum of the retention time window where the ARN peak is in the chromatogram in Figure 46.

Figure 36 to Figure 47 show an increases of the peak area of  $m/z$  613-618 with increasing ARN concentration (see also Figure 48 and Figure 49,) and Table A3, in Appendix. However, the linear fit was not good, especially when the two highest concentrations were included which gave a  $R^2 = 0.8516$  (Figure 48). When only concentrations up to 238.5 ppm were included, a better linear fit was obtained with  $R^2 = 0.9365$ . However the linear fit was not satisfying, and this shows that the extraction or the MS conditions was not yet under control. The latter was investigated using an internal standard to see if a good enough result in the quantitative analysis of ARN could be obtained.

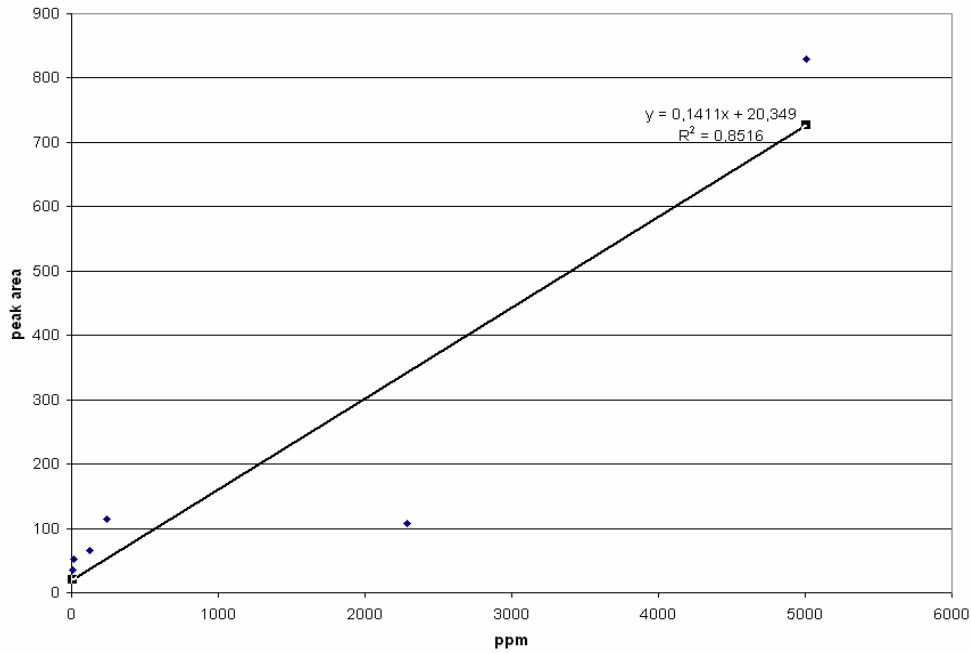


Figure 48: Plot showing peak area vs. ARN concentration (ppm) in the range 4.36 ppm to 5006 ppm, chromatograms are shown in Figure 36- Figure 46 (raw data in Table A3 in Appendix). (Peak areas are integrated from the ARN peak at  $m/z= 613-618$ ).

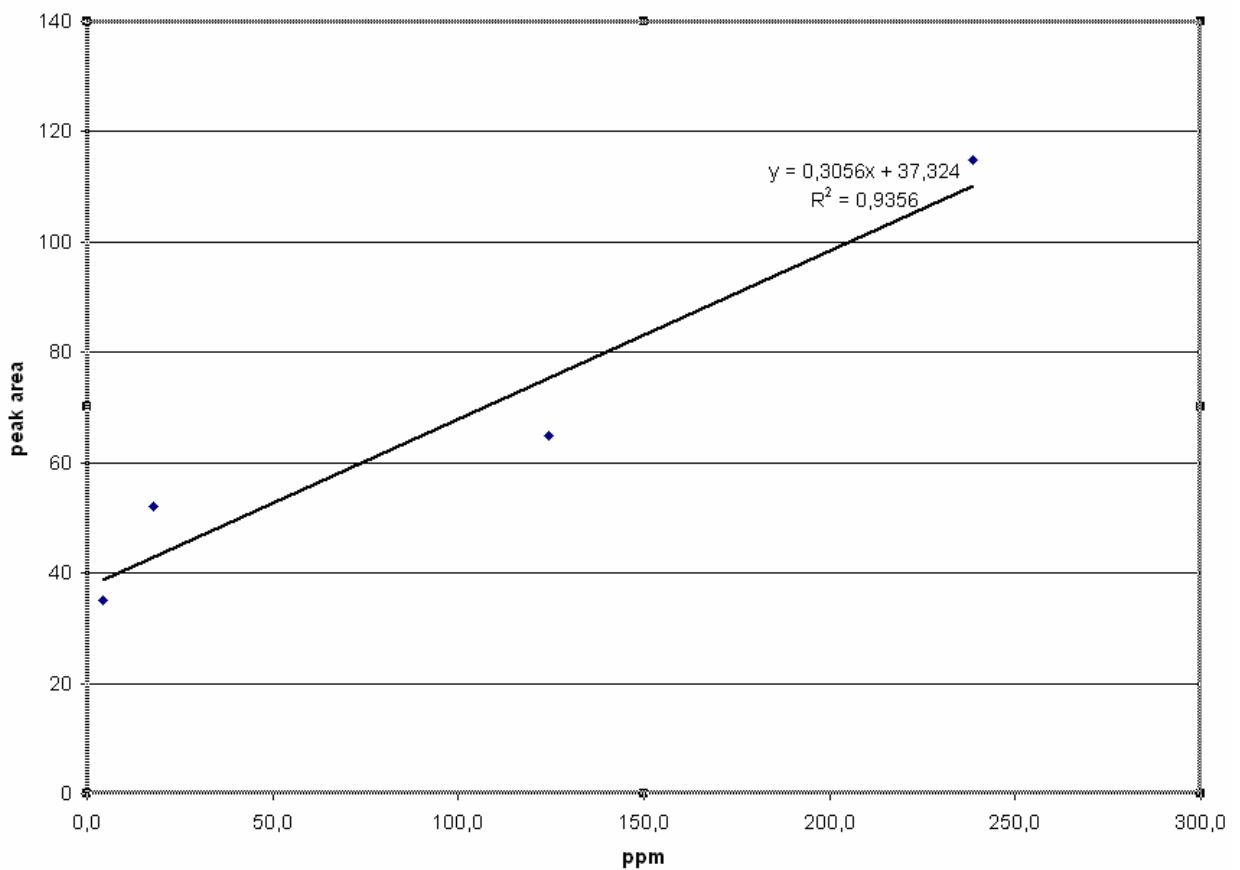


Figure 49: Plot showing peak area vs. ARN concentration (ppm) in the range 4.36 ppm to 238.5 ppm, chromatograms are shown in Figure 36 to Figure 46 (raw data in Table A3 in Appendix). (Peak areas are integrated from the ARN peak at  $m/z= 613-618$ ).

With negative ion ESI it is possible to determine molecular distribution of acids, but ESI MS is only a semi concentration sensitive technique when micro flow is used. If the standard addition method was used, the absolute concentrations could be obtained, and a better control of the method could be obtained, when it comes to quantitative determination of ARN. The internal standard pentadecafluorooctanoic acid was used, and the X and Y values in Figure 52 and Figure 54, and Table A6 and 14 (in Appendix) were obtained using equation 4 and 5:

$$X = (\text{cons. analyte}) / (\text{cons. int.st.}) \quad (4)$$

$$Y = (\text{area analyte}) / (\text{area int.st.}) \quad (5)$$

Standard solutions with three different ARN concentrations with an internal standard added were made to see if the  $\mu$ LC MS method could be controlled in a better way than without internal standard. A better regression line was obtained both with and without taking the internal standard into consideration (Figure 50 and Figure 51) with  $R^2 = 0.9999$ , but it was decided to continue the analysis with the internal standard.

It is unrealistic to find as high concentrations as the two largest, (5006 and 2284 ppm) of ARN in a crude oil. It was therefore decided that the concentration range tested ranged from 4 ppm at the highest to 0.5 ppm at the lowest. For the lowest concentrations, a concentration step (evaporation with  $N_2$ ) was performed prior to the  $\mu$ LC MS analysis.

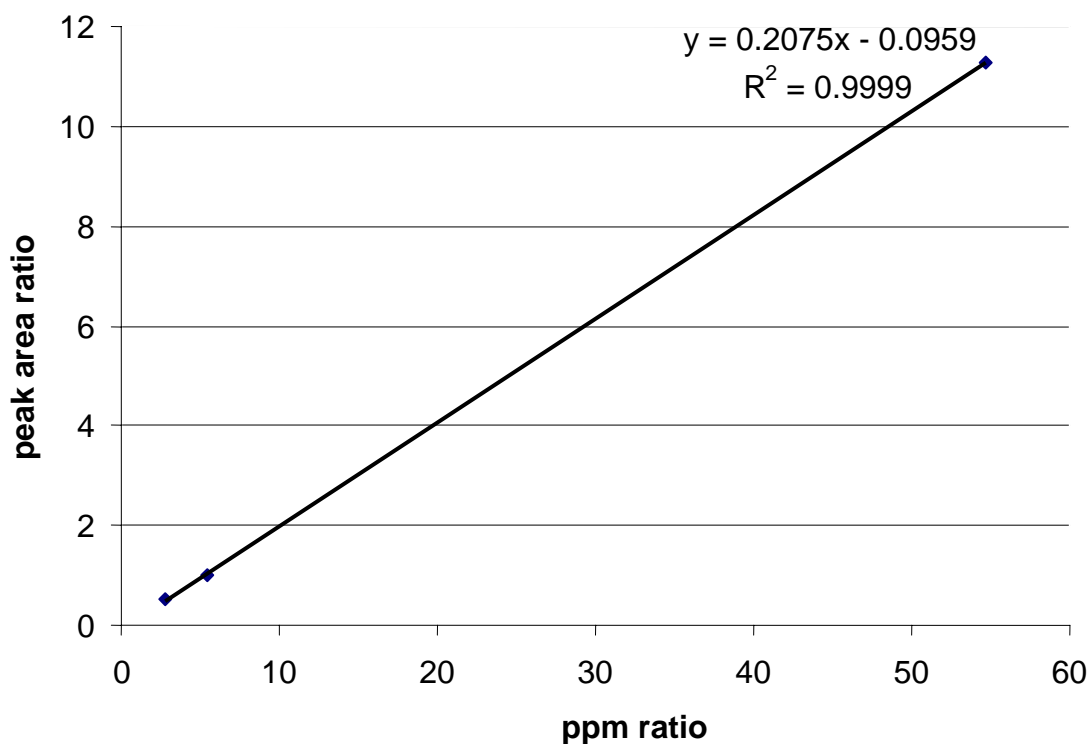


Figure 50: Plot of peak area ratio vs. ARN concentration ratio (ppm) for standard solutions in the range of 27.36 ppm, 54.72 ppm and 547.2 ppm ARN, using an internal standard (10 ppm) and the  $\mu$ LC MS method, numeral values are shown in Table A4 in Appendix.

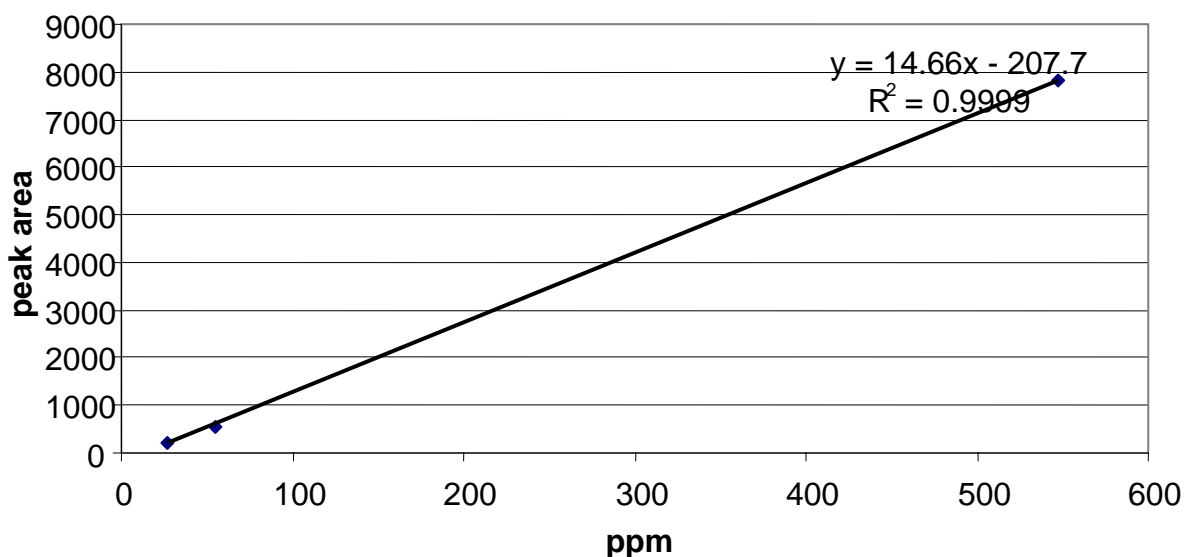


Figure 51: Plot of peak area vs. ARN concentration (ppm) for standard solutions in the range of 27.36 ppm, 54.72 ppm and 547.2 ppm ARN, without taking the internal standard into consideration, the  $\mu$ LC MS method was used. Numeral values are shown in Table A5 in Appendix.



### 3.9 Attempts on quantitative determination of ARN using an internal standard

In this stage of the method development there was a pause for six months. After the break, no ARN peaks were found in the chromatograms even when 5006 ppm of ARN was injected. A new column was purchased from G&T Septeck and the ESI interface as well as the injection valve was thoroughly washed. The pump gradient was extended to 100 % MeOH : TEA (99.99 : 0.01, v/v). Finally the ARN peak could be identified in the chromatogram again.

MeOH extracted spiked A1 polar samples were prepared (with internal standard) in the ARN concentrations of 0.1455 ppm to 2.9006 ppm, and for some of the lowest concentrations, a concentration step (evaporation with N<sub>2</sub>) was performed prior to the  $\mu$ LC MS analysis. This concentration step was possible since there had been no problems with precipitation of analyte or sample matrix components in the injector or column entrance, as experienced at Statoil [67]. As shown in Figure 52 and Figure 54 the method was really out of control. It was clear that the sensitivity and the repeatability were not as good as obtained before, even though an internal standard had been used. Even without taking the internal standard into consideration, the results were really bad as shown in Figure 53 and Figure 55. The integrated peak area of the internal standard was not the same in any of the calculations done to make Figure 52 and Figure 54, (Table A6 and Table A8 in Appendix), which is the reason why Figure 53 and Figure 55 (Table A7 and Table A9 in Appendix) were made. As the internal standard was added before the MeOH extraction, the assumption can be made that the absolute recovery of the internal standard was poor. However, as Figures and Tables both with and without making consideration for the internal standard were made, this can not explain why the results were so poor. To make matters worse, carryover was observed in all of the blank injections, examples of this are shown in Figure 56 and Figure 57, this also enhances the poor results.

To solve the carryover problem all the capillary tubing in the entire analytical system were changed, and all the ferrules in the injector were also changed. The injection valve and ESI interface were thoroughly washed, the mobile phase reservoirs were washed, and the mobile phase as well as the gradient pump was changed. Still carryover was observed, and a new injection valve was purchased. All of the tubing and all of the ferrules in the entire analytical system was changed again and the ESI interface was thoroughly washed again. The new column was backflushed and conditioned with 100 % MeOH : TEA (99.99 : 0.01, v/v) for hours, but nothing helped to prevent the carryover problem.

Because of these problems and the time issue, the project was terminated before the main aim of qualitative and quantitative determination of ARN in the concentrations of 4 ppm to 0.5 ppm was achieved.

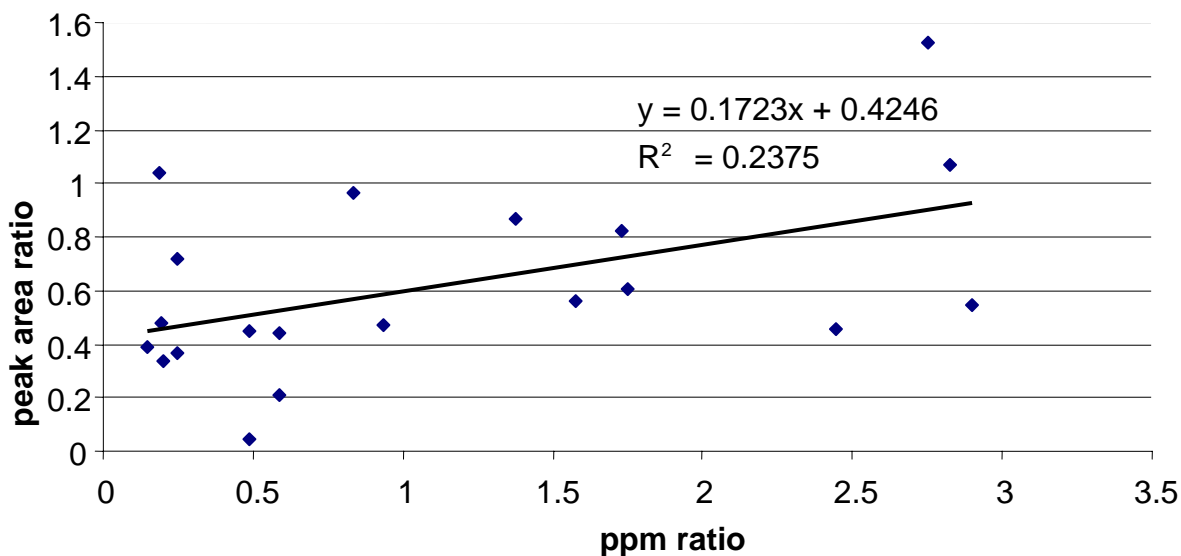


Figure 52: Plot showing peak area ratio vs. ARN concentration ratio (ppm) in the range of 0.1455 ppm to 2.9006 ppm, numeral values are shown in Table A6 in Appendix.

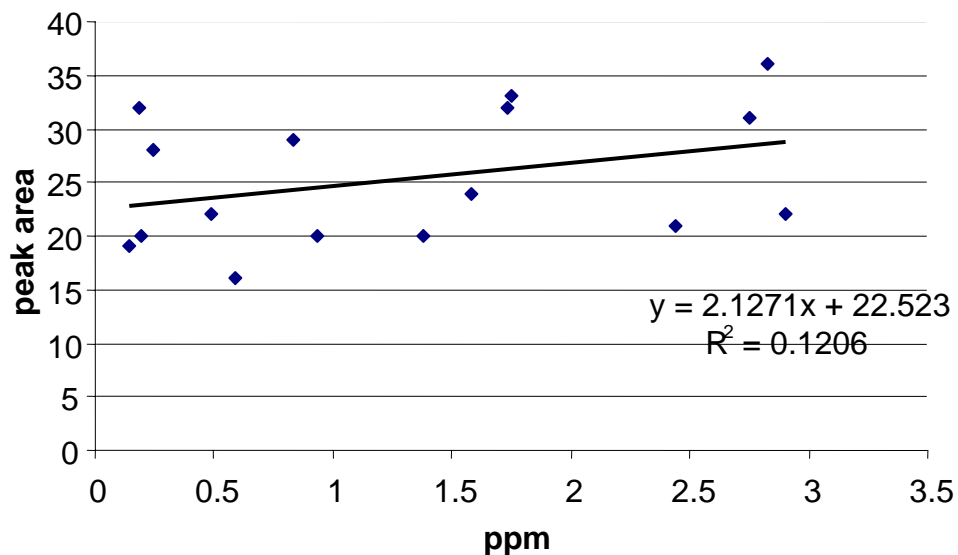


Figure 53: Plot showing peak area vs. ARN concentration (ppm) in the range of 0.1455 ppm to 2.9006 ppm, without taking the internal standard into consideration. Numeral values are shown in Table A7 in Appendix.

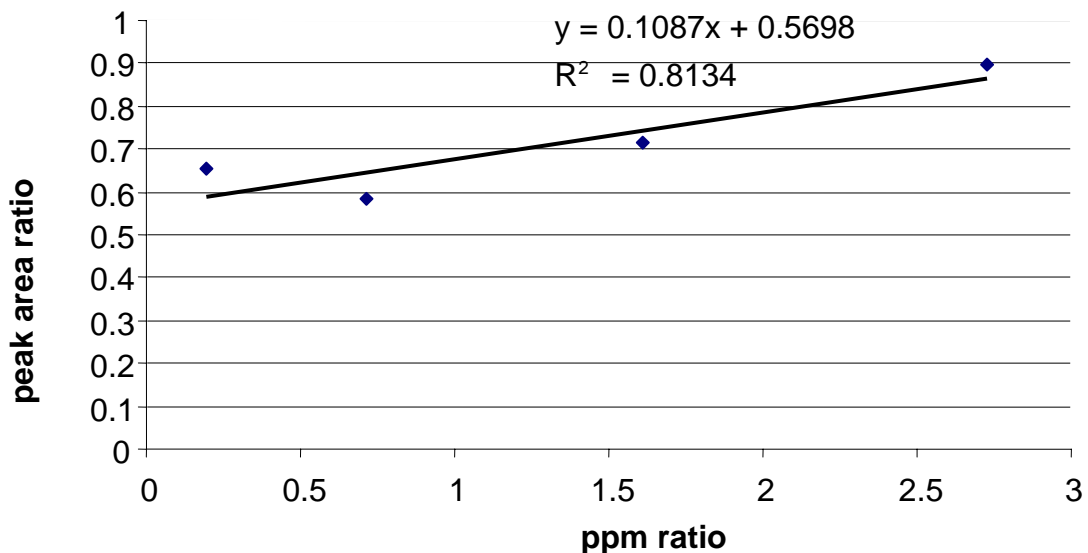


Figure 54: Plot showing mean values of the peak area ratio vs. ARN concentration ratio (ppm) in the range of 0.1932 ppm to 2.7289 ppm, data obtained from Figure 52 and Table A8 in Appendix.

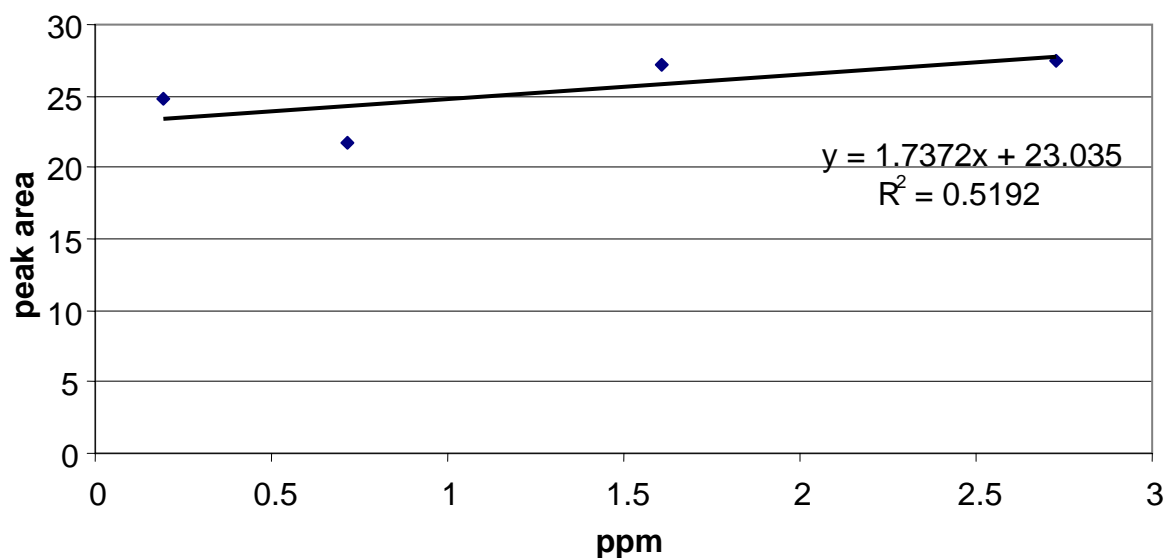


Figure 55: : Plot showing mean values of the peak area vs. ARN concentration (ppm) in the range of 0.1932 ppm to 2.7289 ppm, without taking the internal standard into consideration. Data obtained from Figure 53 and Table A9 in Appendix.

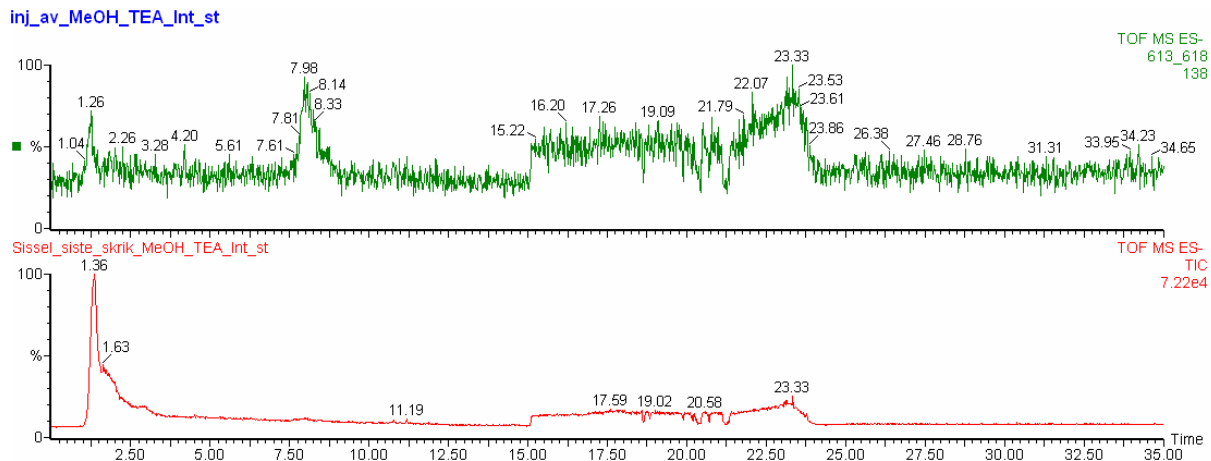


Figure 56: One  $m/z$  range 613-618 EIC chromatogram and one TIC chromatogram of MeOH (HPLC grade) : TEA (99.99 : 0.01 v/v), and 1.0 ppm internal standard, analyzed by the  $\mu$ LC MS system, using the 0.32x100mm Kromasil C18 column, with negative electrospray MS detection. The injection volume was 500 nl. The MeOH/H<sub>2</sub>O gradient as described in Table 6 was used with a flow rate of 5  $\mu$ l/min.

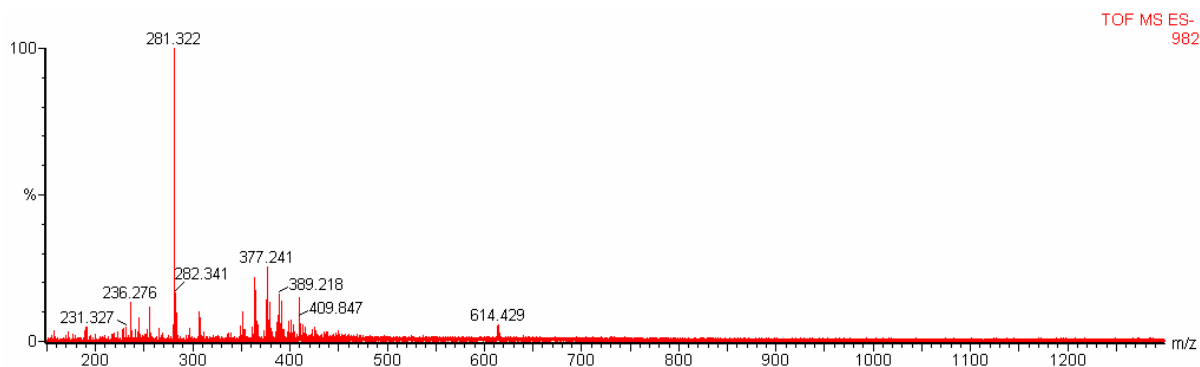


Figure 57: Mass spectrum of the retention area where the ARN peak is in the chromatogram in Figure 56.

## 4. Conclusion

A  $\mu$ LC MS method for separation of three homologues of ARN acids in Heidrun oil has been developed. A C18 column packed with 3.5  $\mu$ m particles was used, with a MeOH / water (0.1 % TEA added) mobile phase gradient. Detection was performed with negative ESI TOF MS. A MeOH extraction step, which can replace the tedious Acid IER method, was used as sample preparation, but the repeatability and efficiency of the MeOH extraction step could not be verified in the time course of this thesis. To be able to determine the low expected concentrations of the ARN acids in crude oil, this MeOH extraction step, which separates the ARN acids from the crude oil, was considered necessary. The bad repeatability could also be caused by the  $\mu$ LC MS method even though an internal standard was used. The ARN acid family was qualitatively determined in the  $\mu$ LC MS analysis down to a concentration of 4 ppm in crude oil. However, further method development is needed to achieve a method which can be used for quantification of ARN in crude oil since the expected concentrations is below 3 ppm.

## 5. References

1. <http://www.epa.gov/region6/6en/xp/lppapp6a.pdf>  
Aug 2006.
2. <http://www.newton.dep.anl.gov/askasci/chem00/chem00937.htm>. Aug 2006.
3. Kane, R.D. and M.S. Cayard, *Understanding critical factors that influence refinery crude corrosiveness*. Materials Performance 1999. **38**(7): p. 48-54.
4. Moulijn, J., A., M. Makkee, and A. Van Diepen, *Chemical process technology*. 2001: John Wiley & Sons, Ltd.
5. <http://science.howstuffworks.com/oil-refining1.htm>. Aug 2006.
6. [http://www.kcpc.usyd.edu.au/discovery/9.2.1/9.2.1\\_CrudeOil.html](http://www.kcpc.usyd.edu.au/discovery/9.2.1/9.2.1_CrudeOil.html). Jan 2006.
7. <http://www.schoolscience.co.uk/content/4/chemistry/fossils/p8.html>. Aug 2006.
8. Clemente, J.S. and P.M. Fedorak, *A review of the occurrence, analyses, toxicity, and biodegradation of naphthenic acids*. Chemosphere, 2005. **60**(5): p. 585-600.
9. Meredith, W., S.-J. Kelland, and D.M. Jones, *Influence of biodegradation on crude oil acidity and carboxylic acid composition*. Organic Geochemistry, 2000. **31**(11): p. 1059-1073.
10. Havre, T.E., *Formation of calcium naphthenate in water /oil systems, naphthenic acid chemistry and emulsion stability in Department of Chemical Engineering 2002*, Norwegian University of Science and Technology: Trondheim.
11. Brient, J.A., P.J. Wessner, and M.N. Doyle, *Naphthenic acids*. 4th ed. Kirk-Othmer encyclopedia of chemical technology, ed. J.I. Kroschwitz. Vol. 16. 1995, New York: John Wiley and Sons. 1017-1029.
12. Rudzinski, W.E., L. Oehlers, and Y. Zhang, *Tandem mass spectrometric characterization of commercial naphthenic acids and a maya crude oil*. Energy and Fuels, 2002. **16**(5): p. 1178-1185.
13. Clemente, J.S., N.G.N. Prasad, M.D. MacKinnon, and P.M. Fedorak, *A statistical comparison of naphthenic acids characterized by gas chromatography mass spectrometry*. Chemosphere, 2003. **50**(10): p. 1265-1274.
14. Hsu, C.S., G.J. Dechert, W.K. Robbins, and E.K. Fukuda, *Naphthenic acids in crude oils characterized by mass spectrometry*. Energy and Fuels, 2000 **14**(1): p. 217-223.
15. Hao, C., J.V. Headly, K.M. Peru, R. Frank, P. Yang, and K.R. Solomon, *Characterization and pattern recognition of oil-sand naphthenic acids using comprehensive two-dimensional gas chromatography/ time-of-flight mass spectrometry*. Journal of Chromatography A, 2005. **1067**(1-2): p. 277-284.
16. Laredo, G.C., C.R. López, R.E. Álvarez, J.J. Castillo, and J.L. Cano, *Identification of naphthenic acids and other corrosivity-related characteristics in crude oil and vacuum gas oils from a mexican refinery*. Energy and Fuels, 2004. **18**(6): p. 1687-1694.
17. Herman, D.C., P.M. Fedorak, M.D. McKinnon, and J.W. Costerton, *Biodegradation of naphthenic acids by microbial populations indigenous to oil sand tailings*. Canadian Journal of Microbiology, 1994. **40**(6): p. 467-477.
18. Havre, T.E., J. Sjöblom, and J.E. Vinstad, *Oil/water partitioning and interfacial behavior of naphthenic acids*. Journal of Dispersion Science and Technology 2003. **24**(6): p. 789-801.
19. Rogers, V.V., M. Wickstrom, K. Liber, and M.D. MacKinnon, *Acute and subchronic mammalian toxicity of naphthenic acids from oil sands tailings*. Toxicological Sciences, 2002. **66**(2): p. 347-355.
20. Slavcheva, E., B. Shone, and A. Turnbull, *Review of naphthenic acid corrosion in oil refining*. British Corrosion Journal, 1999. **34**(2): p. 125-131.

21. <http://www.energy.gov.ab.ca/1967.asp>. Jan 2006.
22. Tomczyk, N.A., R.E. Winans, J.H. Shinn, and R.C. Robinson, *On the nature and origin of acidic species in petroleum. 1. Detailed acidic type distribution in a California crude oil*. Energy and Fuels, 2001. **15**(6): p. 1498-1504.
23. St. John, W.P., J. Rughani, S.A. Green, and G.D. McGinnis, *Analysis and characterizations of naphthenic acids by gas chromatography-electron impact mass spectrometry of tert.-butyldimethylsilyl derivatives*. Journal of Chromatography A, 1998. **807**(2): p. 214-251.
24. Turnbull, A., E. Slavcheva, and B. Shone, *Factors controlling naphthenic acid corrosion*. Corrosion, 1998. **54**(11): p. 922-930.
25. Laredo, G.C., C.R. López, R.E. Álvarez, and J.L. Cano, *Naphthenic acids, total acid number and sulfur content profile characterization in Isthmus and Maya crude oils*. Fuel, 2004. **83**(11-12): p. 1689-1695.
26. Wu, X., H. Jing, Y. Zheng, Z. Yao, and W. Ke, *Erosion-corrosion of various oil-refining materials in naphthenic acid*. Wear, 2004. **256**(1-2): p. 133-144.
27. Quagraine, E.K., J.V. Headly, and H.G. Peterson, *Is biodegradation of bitumen a source of recalcitrant naphthenic acid mixtures in oil sands tailing pond waters?* Journal of Environmental Science and Health, 2005. **40**(3): p. 617-684.
28. Scott, A.C., M.D. MacKinnon, and P.M. Fedorak, *Naphthenic acids in Athabasca oil sands tailings are less biodegradable than commercial naphthenic acids*. Environmental Science and Technology, 2005. **39**(21): p. 8388-8394.
29. Headly, J.V. and D.W. McMartin, *A review of the occurrence and fate of naphthenic acids in aquatic environments*. Journal of Environmental Science and Health, 2004. **A39**(8): p. 1989-2010.
30. Holowenko, F.M., M.D. MacKinnon, and P.M. Fedorak, *Characterization of naphthenic acids in oil sands wastewaters by gas chromatography mass spectrometry*. Water Research, 2002. **36**(11): p. 2843-2855.
31. Lai, J.W.S., L.J. Pinto, E. Kiehlmann, L.I. Bendell-Young, and M.M. Moore, *Factors that affect the degradation of naphthenic acids in oil sands wastewater by indigenous microbial communities*. Environmental Toxicology and Chemistry, 1996. **15**(9): p. 1482-1491.
32. Herman, D.C., P.M. Fedorak, and J.W. Costerton, *Biodegradation of cycloalkane carboxylic acids in oil sand tailings*. Canadian Journal of Microbiology, 1993. **39**(6): p. 576-580.
33. <http://www.engineering.ualberta.ca/nav02.cfm?nav02=30941&nav01=18430>. Aug 2006.
34. Clemente, J.S., M.D. MacKinnon, and P.M. Fedorak, *Aerobic biodegradation of two commercial naphthenic acids preparations*. Environmental Science and Technology, 2004. **38**(4): p. 1009-1016.
35. MacKinnon, M.D. and H. Boerger, *Description of two treatment methods for detoxifying oil sands tailings pond water*. Water Pollution Research Journal of Canada, 1986. **21**(4): p. 496-512.
36. Atlas, R.M., *Effects of Temperature and Crude Oil Composition on Petroleum Biodegradation*. Applied Microbiology, 1975. **30**(3): p. 396-403.
37. Rogers, V.V., K. Liber, and M.D. MacKinnon, *Isolation and characterization of naphthenic acids from Athabasca oil sands tailings pond water*. Chemosphere, 2002. **48**(5): p. 519-527.
38. Fan, T.P., *Characterization of naphthenic acids in petroleum by fast atom bombardment mass spectrometry*. Energy and Fuels, 1991. **5**(3): p. 371-375.
39. Barrow, M.P., L.A. McDonnell, X. Feng, J. Walker, and P. Derrick, *Determination of the nature of naphthenic acids present in crude oils using nanospray fourier transform ion cyclotron resonance mass spectrometry: The continued battle against corrosion*. Analytical Chemistry, 2003. **75**(4): p. 860-866.

40. Wong, D.C.L., R. van Compernelle, J.G. Nowlin, D.L. O'Neal, and G.M. Johnson, *Use of supercritical fluid extraction and fast ion bombardment mass spectrometry to identify toxic chemicals from refinery effluent adsorbed onto granular activated carbon*. Chemosphere, 1996. **32**(8): p. 1669-1679.
41. Seifert, W.K. and R.M. Teeter, *Preparative thin-layer chromatography and high resolution mass spectrometry of crude oil carboxylic acids*. Analytical Chemistry, 1969. **41**(6): p. 786-795.
42. Baugh, T.D., K.V. Grande, H. Mediaas, J.E. Vinstad, and N.O. Wolf, *The discovery of high molecular weight naphthenic acids (ARN Acid) responsible for calcium naphthenate deposits*. International Symposium on Oilfield Scale held in Aberdeen UK, 2005. **SPE 93011**.
43. Baugh, T.D., N.O. Wolf, H. Mediaas, J.E. Vinstad, and K.V. Grande, *Characterization of a calcium naphthenate deposit - The ARN Acid discovery*. Petroleum Chemistry Division Preprints, 2004.
44. Vinstad, J.E., A.S. Bye, K.V. Grande, B.M. Hustad, E. Hustvedt, and B. Nergård, *Fighting naphthenate deposition at the Statoil-operated Heidrun field*. 5th Int. Oilfield Scale Symposium Aberdeen UK, 2002. **SPE 80375**.
45. Lutnaes, B.F., Ø. Brandal, J. Sjöblom, and J. Krane, *Archaeal C80 isoprenoid tetraacids responsible for naphthenate deposition in crude oil processing*. Organic & Biomolecular Chemistry, 2006. **4**(4): p. 616-620.
46. Brandal, Ø., A.M. Hanneseth, P. Hemmingsen, J. Sjöblom, S. Kim, R. Rodgers, and A.G. Marshall, *Isolation and Characterization of Naphthenic Acids from a Metal Naphthenate Deposit: Molecular Properties at Oil-Water and Air-Water Interfaces*. Journal of Dispersion Science and Technology, 2006. **27**(3): p. 295-305.
47. <http://www.sweb.cz/VPrelog/>. Aug 2006.
48. Lo, C.C., B.G. Brownlee, and N.J. Bunce, *Electrospray-mass spectrometric analysis of reference carboxylic acids and Athabasca oil sands naphthenic acids*. Analytical Chemistry, 2003. **75**(23): p. 6394-6400.
49. Headly, J.V., K.M. Peru, D.W. McMartin, and M. Winkler, *Determination of dissolved naphthenic acids in natural waters by using negative ion electrospray mass spectrometry*. Journal of AOAC International, 2002. **85**(1): p. 182-187.
50. Jones, D.M., J.S. Watson, W. Meredith, M. Chen, and B. Bennett, *Determination of naphthenic acids in crude oils using nonaqueous ion exchange solid-phase extraction*. Analytical Chemistry, 2001. **73**(3): p. 703-707.
51. Saab, J., I. Mokbel, A.C. Razzouk, N. Ainous, N. Zydowicz, and J. Jose, *Quantitative extraction procedure of naphthenic acids contained in crude oils. Characterization with different spectroscopic methods*. Energy and Fuels, 2005. **19**(2): p. 525-531.
52. Gabryelski, W. and K.L. Froese, *Characterization of naphthenic acids by high-field asymmetric waveform ion mobility spectrometry mass spectrometry*. Analytical Chemistry, 2003. **75**(17): p. 4612-4623.
53. Green, J.B., B.K. Stierwalt, J.S. Thomson, and C.A. Treese, *Rapid isolation of carboxylic acids from petroleum using high-performance liquid chromatography*. Analytical Chemistry, 1985. **57**(12): p. 2207-2211.
54. McDaniel, L.H. and L.T. Taylor, *Esterification of decanoic acid during supercritical fluid extraction employing either methanol-modified carbon dioxide or a methanol trap*. Journal of Chromatography A, 1999. **858**(2): p. 201-207.
55. Ovalles, C., M. del Carmen Garcia, E. Lujano, W. Aular, R. Bermudez, and E. Cotte, *Structure/interfacial activity relationships and thermal stability studies of Cerro Negro crude oil and its acid, basic and neutral fractions*. Fuel, 1998. **77**(3): p. 121-126.
56. Ramljak, Z., A. Solc, P. Arpino, J.-M. Schmitter, and G. Guiochon, *Separation of acids from asphalts*. Analytical Chemistry 1977. **49**(5): p. 1222-1225.



57. Mediaas, H., K.V. Grande, B.M. Hustad, H.G. Rueslåtten, and J.E. Vinstad, *The Acid IER Method – a method for selective isolation of carboxylic acids from crude oils and other organic solvents*. . 5th Int. Oilfield Scale Symposium Aberdeen UK, 2002. **SPE 08404**.
58. Qian, K., W.K. Robbins, C.A. Hughey, H.J. Cooper, R.P. Rodgers, and A.G. Marshall, *Resolution and identification of elemental compositions for more than 3000 crude acids in heavy petroleum by negative-ion microelectrospray high-field Fourier Transform ion cyclotron resonance mass spectrometry*. Energy and Fuels 2001. **15**(6): p. 1505-1511.
59. Yen, T.-W., W.P. Marsh, M.D. MacKinnon, and P.M. Fedorak, *Measuring naphthenic acid concentrations in aqueous environmental samples by liquid chromatography*. Journal of Chromatography A, 2004. **1033**(1): p. 83-90.
60. Clemente, J.S., T.-W. Yen, and P.M. Fedorak, *Development of a high performance liquid chromatography method to monitor the biodegradation of naphthenic acids*. Journal of Environmental Engineering and Science, 2003. **2**(3): p. 177-186.
61. Lo, C.C., B.G. Brownlee, and N.J. Bunce, *Mass spectrometric and toxicological assays of Athabasca oil sands naphthenic acids*. Water Research, 2006. **40**(4): p. 655-664.
62. Cole, R.B., *Electrospray ionization mass spectrometry, fundamentals, instrumentation and applications*. 1997, New York: John Wiley and Sons.
63. Chang, S.H., G.J. Dechert, W.K. Robbins, and E.K. Fukuda, *Naphthenic acids in crude oil characterized by mass spectrometry*. Energy and Fuels, 2000. **14**(1): p. 217-223
64. Dzidic, I., A.C. Somerville, J.C. Raia, and H.V. Hart, *Determination of naphthenic acids in California crudes and refinery waste waters by fluoride ion chemical ionization mass spectrometry*. Analytical Chemistry, 1988. **60**(13): p. 1318-1323.
65. Barnett, D.A., B. Ells, R. Guevremont, and R.W. Purves, *Separation of leucine and isoleucine by electrospray ionization-high field asymmetric waveform ion mobility spectrometry-mass spectrometry*. Journal of the American Society for Mass Spectrometry, 1999. **10**(12): p. 1279-1284.
66. Barnett, D.A., R.W. Purves, B. Ells, and R. Guevremont, *Separation of o-, m- and p-phthalic acids by high-field asymmetric waveform ion mobility spectrometry (FAIMS) using mixed carrier gases*. Journal of Mass Spectrometry, 2000. **35**(8): p. 976-980.
67. Mediaas, H., T.V. Løkken, and H. Kummernes, *Personal Communication*. 2004, Statoil: Trondheim.
68. Vissers, J.P.C., *Recent developments in microcolumn liquid chromatography*. Journal of Chromatography A, 1999. **856**(1-2): p. 117-143.
69. Vissers, J.P.C., H.A. Claessens, and C.A. Cramers, *Microcolumn liquid chromatography: instrumentation, detection and applications*. Journal of Chromatography A, 1997. **779**(1-2): p. 1-28.
70. Alltech Associates, I. and U. Deerfield, *Evaporative light scattering detector (ELSD) MKIII operating manual*. 1995.
71. Greibrokk, T., E. Lundanes, and K. Rasmussen, E., *Kromatografi Separasjon og deteksjon*. 3 ed. 1994, Oslo: Universitetsforlaget.
72. Poole, C.F., *The essence of chromatography*. First ed. 2003: Elsevier, Amsterdam.

## 6. Appendix

In the following, Tables containing raw data for the results presented in the main text are shown.

Table A1: Samples obtained from Statoil, isolated NAs, sent to UiO: Samples 020103003.03 A1 polar (isol: 08.04.02) are determined with LC MS, they contain much of the heavy acids (MW: 1232), but also some of the lighter acids.

Sample 020103003.03 A (isol: 14.01.02) may contain more of the lighter acids than A1 polar.

Reference number to sample data base at Statoil	Date for isolating the naphthenic acid	Empty glass container with label but without cover (g)	Naphthenic acid in the container (g)
020103003.03 Bunn midts. TSA A1 polar Gl: 3	08.04.02	10.0454	0.2414
020103003.03 Bunn midts. TSA A1 polar Gl: 4	08.04.02	9.9327	0.2489
020103003.03 Bunn midts. TSA A1 polar Gl: 5	08.04.02	9.2420	0.2537
020103003.03 Bunn midts. A Gl: 3	14.01.02	9.8835	0.4010
020103003.03 Bunn midts. A Gl: 4	14.01.02	10.0131	0.3711

Table A2: Accurate mass determination was accomplished with electrospray connected to a QTOF MS. The mass of the neutral molecule was measured to 1231.0629. Verification of purity was completed with electrospray connected to a FTICR MS. The MS was tuned to resolution equal to 225000. It was only one peak present at  $m/z=614.6$ , (see Figure 14).

MS-recording	Negative ions, deprotonation						
	Observed mass	Charge	Corr. mass obs.	Electron	Corr. mass neutral	Protons	Corrected mass
<b>QTOF</b>							
#2103							neutral
	614,5218	2	1229,0436	0,000549	1229,0425	2	1231,0582
	614,5197	2	1229,0394	0,000549	1229,0383	2	1231,0540
	614,5200	2	1229,0400	0,000549	1229,0389	2	1231,0546
<b>QTOF</b>							
#2077 -2079							
	614,5269	2	1229,0538	0,000549	1229,0527	2	1231,0684
	614,5276	2	1229,0552	0,000549	1229,0541	2	1231,0698
	614,5289	2	1229,0578	0,000549	1229,0567	2	1231,0724
					Mass of neutral molecule:		
Average	614,5242				Average:		1231,0629
St. deviation	0,0041				St. deviation:		0,0082

Table A3: Numeral values for the data points in Figure 48 and Figure 49, chromatograms are shown in Figure 36- Figure 46, and peak areas are integrated from the ARN peak at  $m/z= 613-618$ .

Figure nr:	ppm	peak area
36	5006	830
38	2284	108
40	238,5	115
42	124,5	65
44	17,80	52
46	4,363	35

Table A4: Numeral values for the data points in Figure 50.

Cons. ARN (ppm)	X	Y
27.36	2.736	0.517
54.72	5.472	0.9928
547.2	54.72	11.262

Table A5: Numeral values for the data points in Figure 51.

cons ARN (ppm)	X	Y
27.36	27.36	227
54.72	54.72	559
547.2	547.2	7816

Table A6: Numeral values for the data points in Figure 52.

inj. Name	X	Y
Blank	0	
Blank conc	0	
MeOH + +	0	
0.5_1	0.2443	0.7142
0.5_2	0.1947	0.4761
0.5_3	0.1455	0.3888
0.5_4	0.1885	1.0416
0.5_1 conc	0.2443	0.3636
0.5_2 conc	0.1974	0.3387
1_1	0.4903	0.4516
1_2	0.5903	0.4444
1_3	0.9377	0.4687
1_4	0.834	0.9666
1_1 conc	0.4903	0.0478
1_2 conc	0.5903	0.2121
2_1	1.3762	0.8709
2_2	1.7319	0.8235
2_3	1.5786	0.5625
2_4	1.7524	0.6046
4_1	2.9006	0.5476
4_2	2.7486	1.5217
4_3	2.4429	0.4545
4_4	2.8236	1.0697

Table A7: Numeral values for the data points in Figure 53.

inj. Name	X	Y
Blank	0	
Blank conc	0	
MeOH + +	0	
0.5_1	0.2443	28
0.5_2	0.1947	20
0.5_3	0.1455	19
0.5_4	0.1885	32
1_1	0.4903	22
1_2	0.5903	16
1_3	0.9377	20
1_4	0.834	29
2_1	1.3762	20
2_2	1.7319	32
2_3	1.5786	24
2_4	1.7524	33
4_1	2.9006	22
4_2	2.7486	31
4_3	2.4429	21
4_4	2.8236	36

Table A8: Numeral values for the data points in Figure 54, which display the mean values from Figure 52 and Table 12.

Mean value: inj name.	X	Y
0.5	0.1932	0.6551
1	0.713	0.5828
2	1.6097	0.7153
4	2.7289	0.89611

Table A9: Numeral values for the data points in Figure 55, which display the mean values from Figure 52 and Table 13.

mean value: inj name	X	Y
0.5	0.1932	24.75
1	0.7131	21.75
2	1.6097	27.25
4	2.7289	27.5